[redacted]

#2

FUNCTIONAL ANALYSIS OF SYSTEMS CHARACTERIZED BY NONLINEAR DIFFERENTIAL EQUATIONS

ROBERT BRUCE PARENTE

TECHNICAL REPORT 444

JULY 15, 1966

MASSACHUSETTS INSTITUTE OF TECHNOLOGY
RESEARCH LABORATORY OF ELECTRONICS
CAMBRIDGE, MASSACHUSETTS

The Research Laboratory of Electronics is an interdepartmental laboratory in which faculty members and graduate students from numerous academic departments conduct research.

The research reported in this document was made possible in part by support extended the Massachusetts Institute of Technology, Research Laboratory of Electronics, by the JOINT SERVICES ELECTRONICS PROGRAMS (U.S. Army, U.S. Navy, and U.S. Air Force) under Contract No. DA36-039-AMC-03200(E); additional support was received from the National Science Foundation (Grant GP-2495), the National Institutes of Health (Grant MH-04737-05), and the National Aeronautics and Space Administration (Grant NsG-496).

MASSACHUSETTS INSTITUTE OF TECHNOLOGY

RESEARCH LABORATORY OF ELECTRONICS

Technical Report 444

July 15, 1966

FUNCTIONAL ANALYSIS OF SYSTEMS CHARACTERIZED BY NONLINEAR DIFFERENTIAL EQUATIONS

Robert Bruce Parente

Submitted to the Department of Electrical Engineering, M. I. T., August 23, 1965, in partial fulfillment of the requirements for the degree of Doctor of Philosophy.

(Manuscript received September 1, 1965)

ABSTRACT

An analysis, by functional calculus, of a class of nonlinear systems is presented. The class of nonlinear systems that are analyzed includes all those analytic systems that are characterized by nonlinear differential equations. Applications of this analysis are shown for several actual nonlinear physical systems that are analytic.

The precise definition of an analytic system is given. Loosely speaking, an analytic system is any system with these three properties: (i) It is deterministic. (For a given input signal, the system can have one and only one corresponding output signal.) (ii) It is time-invariant. (iii) It is "smooth." (The system cannot introduce any abrupt or switchlike changes into its output. All such changes in the output must be caused by the input rather than the system.)

Given a nonlinear differential equation, the conditions are shown under which it characterizes an analytic system. Given an analytic system characterized by a nonlinear differential equation, it is shown how that system can be analyzed by an application of functional calculus. Specifically, an inspection technique is developed whereby a Volterra functional power series is obtained for that system's input-output transfer relationship. Applications are given for (i) the demonstration of a pendulum's nonlinear resonance phenomenon; (ii) the computation of a shunt-wound motor's response to white noise excitation; (iii) the computation of a varactor frequency doubler's transient response; and (iv) the determination of the stability of a magnetic suspension device that is now being used in space vehicles. Experimental confirmation of the last stability determination is treated in an appendix.

TABLE OF CONTENTS

I. INTRODUCTION

We shall present an analysis, by functional calculus, of a class of nonlinear systems. The class of nonlinear systems which we shall analyze are all those analytic systems that are characterized by nonlinear differential equations. We shall also give applications of this analysis to several actual nonlinear analytic physical systems.

The precise definition of analytic systems will be given. For the time being, we shall say that analytic systems are all those systems having the three following properties: (i) Analytic systems are deterministic (that is, for a given input they may have one and only one corresponding output). (ii) Analytic systems are time-invarient (that is, the system's inputs and outputs co-translate in time). (iii) Analytic systems are "smooth" (loosely speaking, by smooth we mean that the system cannot introduce an abrupt or switchlike change into the system's output. If such a change is present in the system's output, then it must be due to a similar switchlike change in the system's input or to one of the derivatives of the system's input).

Given an analytic system characterized by a nonlinear differential equation, we shall show how that system can be analyzed by an application of functional calculus. On the other hand, given a nonlinear differential equation, we shall show the conditions under which it characterizes an analytic system. Specifically, we shall show a technique whereby a Volterra functional power series solution for that system's input-output transfer relationship can be obtained from its characterizing equation by inspection. We shall then show some applications of that functional solution of the system's input-output relationship. These applications will include: the demonstration of a pendulum's nonlinear resonance phenomenon, computation of a shunt-wound motor's response to white noise, computation of a varactor frequency doubler's transient response, and the determination of the stability of a magnetic suspension device that is now being used in our nation's space vehicles.

The analysis of nonlinear systems by functional calculus is not new; Wiener introduced it, in 1942.[39] The Volterra series solution of nonlinear differential equations is not new; Volterra did so in the nineteenth century.[32] Barrett gave a solution technique for a certain kind of nonlinear differential equation, in 1957.[1] In 1963, Liou gave a procedure that will often (but not always) yield a solution for another type of differential equation.[24] Van Trees, in 1964, solved the particular differential equation characterizing a phase-locked loop.[31] The technique that he used there parallels many of the essential features of the inspection technique that we present here.

Since many of the laws of physics are most readily stated by a differential equation, it is quite natural to specify a system's behavior by a differential equation. The system is then said to be characterized by that differential equation. For some applications, however, a functional description (the Volterra series solution of the characterizing differential equation) is more useful. For example, if we want an explicit

expression for a system's output or if we wish to calculate the properties of a system's output when its input is stochastic, then the functional description is more desirable than the differential equation description. As an illustration of a method (but not the inspection technique that we shall present later) whereby a functional characterization of a system may be obtained from its differential equation characterization, we now present two examples – a linear lowpass filter and an associated nonlinear lowpass filter.

1.1 LINEAR LOWPASS FILTER

Consider the lowpass filter shown in Fig. 1. If we are primarily interested in the relation of this filter's external variables (the voltages x and y) rather than in its internal variables (such as the current i), then we can express that relation by a differential equation

$$0 = \frac{dy}{dt} + y - x \tag{1}$$

and the boundary condition of initial rest

$$y(t) = 0 \text{ until } x(t) \neq 0. \tag{2}$$

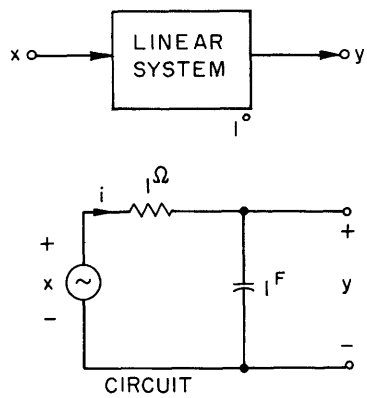

Fig. 1. Linear lowpass filter.

Another way in which we can express that relation is by the convolution of x with h, the filter's impulse response. That is,

$$y(t) = h(t) \,(*)\, x(t)$$

$$= \int_{-\infty}^{\infty} h(\tau)\, x(t - \tau)\, d\tau . \tag{3}$$

Equation 3 shows that the filter's output y is a functional of its input x.

1.2 NONLINEAR LOWPASS FILTER

Consider the lowpass filter, squarer, lowpass filter system shown in Fig. 2. We can express the relation of its input voltage x to its output voltage z by an integro-differential equation

$$0 = \frac{dz}{dt} + z - \left(\int_{-\infty}^{\infty} u_{-1}(\tau) \exp(-\tau)\, x(t-\tau)\, d\tau \right)^2 \tag{4}$$

(where u_{-1} is the unit step function), and the boundary condition of initial rest

$$z(t) = 0 \text{ until } x(t) \neq 0. \tag{5}$$

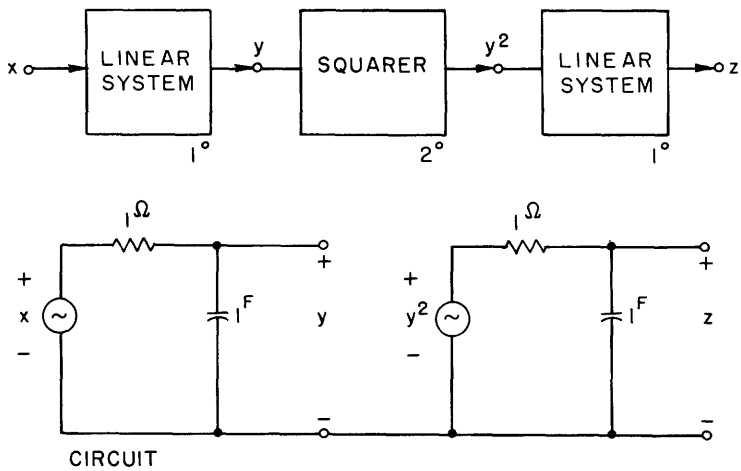

Fig. 2. Nonlinear lowpass filter.

We can also express that relation in a form analogous to Eq. 3. That is,

$$z(t) = h_0 + \int_{-\infty}^{\infty} h_1(\tau_1)\, x(t-\tau_1)\, d\tau_1 + \int_{-\infty}^{\infty} h_2(\tau_1, \tau_2)\, x(t-\tau_1)\, x(t-\tau_2)\, d\tau_1\, d\tau_2 + \cdots \tag{6}$$

Equation 6 is called a Volterra functional power series and the constant h_0, together with the functions h_1, h_2, h_3, . . . , are called its Volterra kernels. Wiener introduced the use of such a Volterra series to express the input-output transfer relation of a nonlinear system in 1942.[39]

Not all nonlinear systems have input-output transfer relations that can be expressed by means of a Volterra series (Eq. 6). We shall deal with the question of which nonlinear systems can and cannot be expressed by Eq. 6. For the time being, we shall merely state that the system shown in Fig. 2 is expressible by Eq. 6 and show how we can solve for its Volterra kernels.

A major topic of this report will be the development of a technique whereby the Volterra series description of a nonlinear system can be found from its differential equation or integro-differential equation description by inspection. In order to illustrate this technique we shall solve for the Volterra series description of the systems shown in Fig. 2, but not by inspection. In order to make this illustration clearer, we shall first use this technique to solve for the convolution integral description of the linear system shown in Fig. 1. In this case, the technique that we shall use will be unorthodox and more tedious than the usual well-known methods, but it will help to illustrate the use of the same technique on the nonlinear system.

Consider Eq. 3, where h is unknown. By differentiating we obtain

$$\frac{dy}{dt} = h^{(1)}(t) \,(*)\, x(t)$$

$$= \int_{-\infty}^{\infty} h^{(1)}(\tau)\; x(t - \tau)\; d\tau, \tag{7}$$

where $h^{(1)}$ is the derivative of h. Any input x is related to itself, through the unit impulse, u_0, in the form

$$x(t) = u_0(t) \,(*)\, x(t)$$

$$= \int_{-\infty}^{\infty} u_0(\tau)\; x(t - \tau)\; d\tau. \tag{8}$$

When Eqs. 3, 7, and 8 are substituted in Eq. 1, the result is

$$0 = \left[h^{(1)}(t) + h(t) - u_0(t) \right] (*)\, x(t)$$

$$= \int_{-\infty}^{\infty} \left[h^{(1)}(\tau) + h(\tau) - u_0(\tau) \right] x(t - \tau)\; d\tau. \tag{9}$$

Equation 9 must be true for any x. This implies that the entire kernel of Eq. 9 is zero. That is,

$$0 = h^{(1)}(\tau) + h(\tau) - u_0(\tau), \quad \text{all } \tau. \tag{10}$$

If we take the bilateral Laplace transform of Eq. 10, we get

$$0 = (s + 1)\, H(s) - 1, \tag{11}$$

where

$$H(s) = \int_{-\infty}^{\infty} h(\tau) \exp(-s\tau)\, d\tau. \tag{12}$$

Solving Eq. 11 for H, we get

$$H(s) = \frac{1}{s + 1}. \tag{13}$$

By taking the inverse transform of Eq. 13 and taking into account the boundary condition (Eq. 2), we find that the system's impulse response is

$$h(t) = u_{-1}(t) \exp(-t). \tag{14}$$

We have thus found the desired function h so that the system shown in Fig. 1 can be expressed by means of Eq. 3, the convolution integral. We shall now show an analogous method by which we shall find the Volterra kernels whereby the system shown in Fig. 2 can be expressed by means of Eq. 6.

Consider Eq. 6. By differentiating, we can obtain

$$\frac{dz}{dt} = \int_{-\infty}^{\infty} h_1^{(1)}(\tau_1)\, x(t - \tau_1)\, d\tau_1 + \int_{-\infty}^{\infty}\int \left[h_2^{(1,0)}(\tau_1,\tau_2) + h_2^{(0,1)}(\tau_1,\tau_2)\right] x(t - \tau_1)\, x(t - \tau_2)\, d\tau_1\, d\tau_2 + \int_{-\infty}^{\infty}\iint \left[h_3^{(1,0,0)}(\tau_1,\tau_2,\tau_3) + h_3^{(0,1,0)}(\tau_1,\tau_2,\tau_3) + h_3^{(0,0,1)}(\tau_1,\tau_2,\tau_3)\right] x(t - \tau_1)\, x(t - \tau_2)\, x(t - \tau_3) \cdot d\tau_1\, d\tau_2\, d\tau_3 + \ldots, \tag{15}$$

where $h_p^{(i,j,k,\ldots)}$ is the i^{th} partial derivative with respect to the first argument, j^{th} partial derivative with respect to the second argument, and so on, of the function h_p.

When Eqs. 6 and 15 are substituted in Eq. 4, the result is

$$0 = h_0 + \int_{-\infty}^{\infty} \left[h_1(\tau_1) + h_1^{(1)}(\tau_1) \right] x(t - \tau_1)\, d\tau_1$$

$$+ \iint_{-\infty}^{\infty} \left[h_2(\tau_1,\tau_2) + h_2^{(1,0)}(\tau_1,\tau_2) + h_2^{(0,1)}(\tau_1,\tau_2) \right.$$

$$\left. - u_{-1}(\tau_1)\, u_{-1}(\tau_2) \exp(-\tau_1 - \tau_2) \right] x(t - \tau_1)\, x(t - \tau_2)\, d\tau_1\, d\tau_2$$

$$+ \iiint_{-\infty}^{\infty} \left[h_3(\tau_1,\tau_2,\tau_3) + h_3^{(1,0,0)}(\tau_1,\tau_2,\tau_3) + \ldots \right]$$

$$\cdot\, x(t - \tau_1)\, x(t - \tau_2)\, x(t - \tau_3)\, d\tau_1\, d\tau_2\, d\tau_3 + \ldots . \qquad (16)$$

Equation 16 must hold for any x. One way in which this can be true is if each kernel in Eq. 16 is zero. That is,

$$0 = h_0 \qquad (17)$$

$$0 = h_1(\tau_1) + h_1^{(1)}(\tau_1) \qquad (18)$$

$$0 = h_2(\tau_1,\tau_2) + h_2^{(1,0)}(\tau_1,\tau_2) + h_2^{(0,1)}(\tau_1,\tau_2)$$

$$- u_{-1}(\tau_1)\, u_{-1}(\tau_2) \exp(-\tau_1 - \tau_2) \qquad (19)$$

$$0 = h_k + h_k^{(1,0,0,\ldots,0)} + h_k^{(0,1,0,\ldots,0)} + h_k^{(0,0,1,\ldots,0)}$$

$$+ \ldots + h_k^{(0,0,0,\ldots,1)};\quad k = 3,4,5, \ldots . \qquad (20)$$

Equations 18 – 20 are analogous to Eq. 10. They are multilinear, rather than nonlinear, and can be solved with the aid of the multivariate bilateral Laplace transform.[2] It is

$$H_k(s_1, \ldots, s_k) = \int_{-\infty}^{\infty} \cdots \int h_k(\tau_1, \ldots, \tau_k) \exp(-s_1 \tau_1 - \ldots - s_k \tau_k)\, d\tau_1 \ldots d\tau_k. \tag{21}$$

The transformation of Eqs. 18 – 20 yields

$$0 = (s_1 + 1)\, H_1(s_1) \tag{22}$$

$$0 = (s_1 + s_2 + 1)\, H_2(s_1, s_2) - \frac{1}{(s_1 + 1)(s_2 + 1)} \tag{23}$$

$$0 = (s_1 + s_2 + \ldots + s_k + 1)\, H_k(s_1, s_2, \ldots, s_k); \quad k = 3,4,5, \ldots \quad . \tag{24}$$

By solving these equations for the kernel transforms, taking the inverse transform, and taking into account the boundary condition (Eq. 5), we find that all of the kernels except h_2 are zero. The transform of h_2 is

$$H_2(s_1, s_2) = \frac{1}{(s_1 + 1)(s_2 + 1)(s_1 + s_2 + 1)} \tag{25}$$

and the second-order kernel is

$$h_2(\tau_1, \tau_2) = u_{-1}(\tau_1)\, u_{-1}(\tau_2) \left[\exp(-\bar{m}(\tau_1, \tau_2)) - \exp(-\tau_1 - \tau_2) \right], \tag{26}$$

where $\bar{m}$ is the max function

$$\bar{m}(\tau_1, \tau_2) = \left\{ \tau_1, \tau_1 \geq \tau_2;\ \tau_2, \tau_1 \leq \tau_2 \right\}. \tag{27}$$

It can now be verified, by direct substitution in Eq. 4, that the input-output relation of the system shown in Fig. 2 is

$$z(t) = \int_{-\infty}^{\infty} \int h_2(\tau_1, \tau_2)\, x(t - \tau_1)\, x(t - \tau_2)\, d\tau_1\, d\tau_2 \ . \tag{28}$$

Equations 4 and 28 both represent the input-output transfer relation of the nonlinear system. Depending upon the application, either representation has some advantages over the other. In the case of stochastic inputs, Eq. 28 is more tractable than Eq. 4.

One would normally write Eq. 11 by inspection of Eq. 1. We shall show a technique whereby Eqs. 17, 22, 23 and 24 could have been written by inspection of Eq. 4.

II. FUNCTIONALS AND SYSTEMS

We shall develop an inspection technique for finding Volterra series solutions to those nonlinear differential equations that characterize analytic systems. We shall now summarize the results of system theory and functional calculus which we shall need to use.

2.1 FUNCTIONALS

Functionals are somewhat like functions. Functions assign points to points but functionals assign points to functions (that is, functionals assign points to the way in which points are assigned to points). Volterra, the father of functionals, puts it that the "definition of a functional recalls especially the ordinary general definition of a function given by Dirichlet".[33] The formal definitions of functions and functionals presuppose set theory.[15] An informal definition[10,33] of a functional is the following.

Definition of a Functional. If F assigns a point F[x] to a function x, then F is a functional, x is the argument of F, and F[x] is the value of F for x.

Figure 3 illustrates the definition of a functional. Each function is a bundle of lines going from its domain to its range. A string is tied around each of these bundles of lines (function) and goes from it to some point in a set of points $\mathscr{R}_F$. The bundle of all these strings is a functional F.

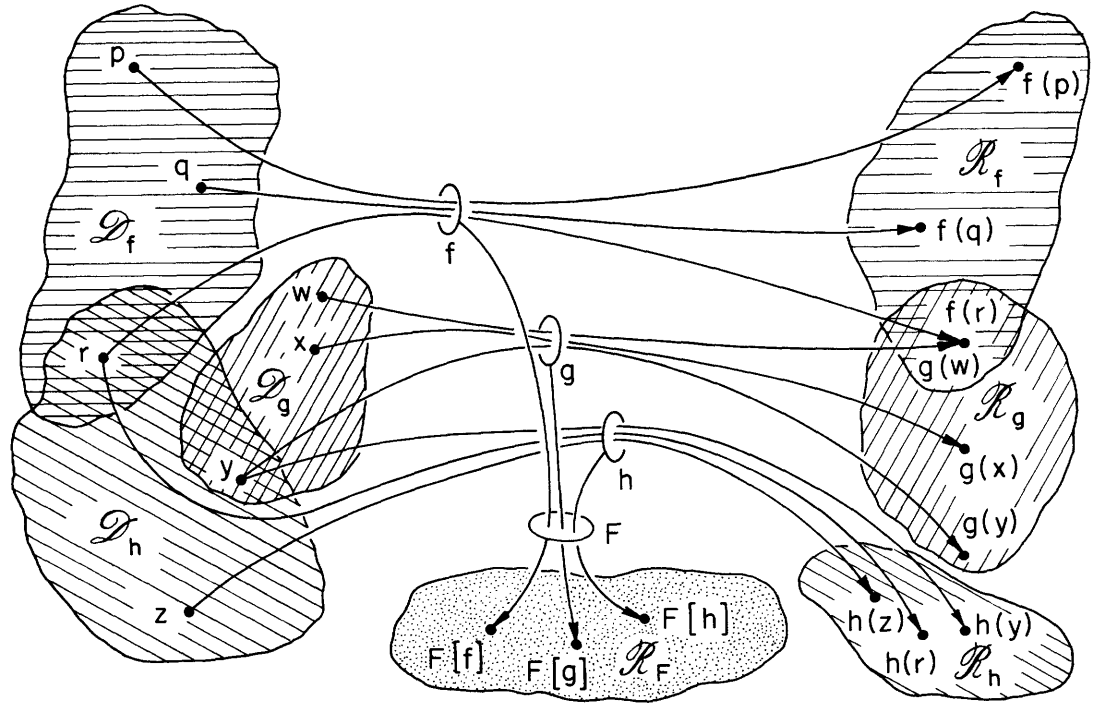

Fig. 3. Illustration of a functional.

2.2 SYSTEMS

A system associates pairs of signals (a signal is a function of time). An informal definition of a deterministic system follows.

Definition of a Deterministic System. If S assigns a signal y to a signal x, then S is a deterministic system, x is the input to S, and y is the system's output for x. The set of inputs to S is called the system's input ensemble. The set of outputs of S is called the system's output ensemble.

Not all systems are deterministic systems. For example, the communication channels that are studied in information theory, which for input x_i can have output y_j with probability $p(y_j|x_i)$, are not deterministic systems.[11] Such systems might be called probabilistic systems. Also, systems with hysteresis may or may not be deterministic systems, depending upon whether or not they are always started from the same state.

The input-output relations of deterministic systems can be expressed by a functional. For example, if a system is linear, deterministic, time-invariant, realizable and stable, then the value of its output y at a time t is the convolution of its input x with its impulse response h. That is,

$$y(t) = \int_0^{\infty} h(\tau)\ x(t-\tau)\ d\tau = \int_{-\infty}^{t} x(\tau)\ h(t-\tau)\ d\tau \tag{29}$$

Equation 29 shows that at any given time t_0 the system's output is the value of some functional L_0 for x. That is,

$$y(t_0) = L_0[x]. \tag{30}$$

On the other hand, Eq. 29 also shows that for any given input signal x_0 the system's output is the value of some function L_{x_0} at t. That is,

$$y(t) = L_{x_0}(t). \tag{31}$$

Equations 30 and 31 together show that there is an L which is both a function and a functional such that the value of the system's output for x at t is

$$y(t) = L[x,(t)]. \tag{32}$$

Equation 29 is more specific than Eq. 32 as to the way in which the system's input influences its output. For example, Eq. 29 shows that only the interval $(-\infty,t)$ of the domain of x pertains to y(t). Whenever we wish to explicitly exhibit the domain of a function which influences the value of a functional, we shall do so by the notation[10,33]

$$y = F\left[x(\tau)\right]_{\tau=a}^{b} . \tag{33}$$

Equation 33 is read as "y is the value of the functional F for the function x from the interval (a,b) of its domain".

With the added notational explicitness of Eq. 33, for the linear system we can now write

$$y(t) = \int_{-\infty}^{t} x(\tau)\ h(t - \tau)\ d\tau = L\left[x(\tau),(t)\right]_{\tau=\infty}^{t} . \tag{34}$$

The input-output relations of nonlinear systems can also be expressed by functionals. Consider any deterministic system S with input signal ensemble $X = \left\{x_n\right\}$ and output signal ensemble $Y = \left\{y_m\right\}$, as is shown in Fig. 4. Since S is deterministic, for any given input signal $x_k \in X$ the system's output can be one and only one signal $y_k \in Y$. Thus the value of any deterministic system's output signal y at a time t is, by definition, a functional of that system's input signal x. That is,

$$y(t) = S\left[x(\tau),(t)\right]_{\tau=\alpha(t)}^{\beta(t)} \tag{35}$$

where the interval $(\alpha(t),\beta(t))$ is any common interval of the domains of all the $x_k \in X$ such that each x_k that assigns a distinct $y_k(t)$ is distinct (in other words, the interval is long enough so that we can tell which input signal it is).

If system S is time-invariant as well as deterministic, then there are input-output pairs of signals, (x,y) and (x_T,y_T), where $x,x_T \in X$ and $y,y_T \in Y$, such that for any T

$$x(\xi) = x_T(\xi - T) \tag{36}$$

$$y(\zeta) = y_T(\zeta - T). \tag{37}$$

Equation 35 shows that the value of the system's output at a time t_0 for the input x_T is

$$y_T(t_0) = S\left[x_T(\tau),(t_0)\right]_{\tau=\alpha(t_0)}^{\beta(t_0)} . \tag{38}$$

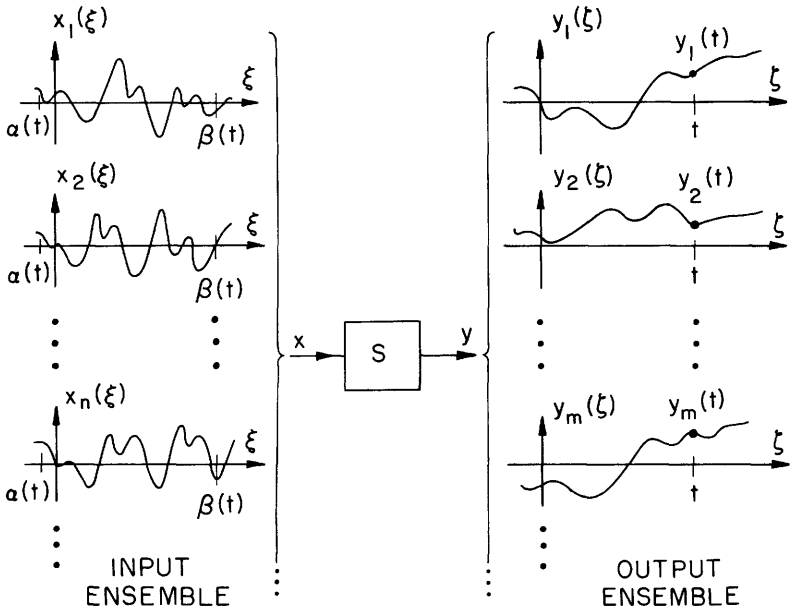

Fig. 4. Deterministic system.

When we substitute Eqs. 36 and 37 in Eq. 38 and choose $T = t - t_0$, then the result* is

$$y(t) = S\left[x(t+\tau),(t_0)\right]_{\tau=a}^{b}, \tag{39}$$

where $a = \alpha(t_0) - t_0$, and $b = \beta(t_0) - t_0$.

That is, if we know a time-invariant deterministic system's functional at some instant of time, then we know that system's output at any time for any input.

Figure 5 illustrates Eq. 39. Referring to Fig. 5, it is clear why (a) the interval (a,b) is called the system's memory; (b) if $b > 0$, then the system is unrealizable; (c) if $b \leq 0$, then the system is realizable; and (d) if $a = b = 0$, then the value of the system's output at time t depends exclusively upon the value of the system's input at time t. That is, the value of the system's output is a function (rather than a functional) of its input. Such a system is called a no-memory system.

*Equation 34 is not a contradiction of Eq. 39. Equation 34 could have been written

$$y(t) = \int_0^\infty h(\tau)\, x(t-\tau)\, d\tau = L\left[x(t+\tau),(0)\right]_{\tau=-\infty}^{0}.$$

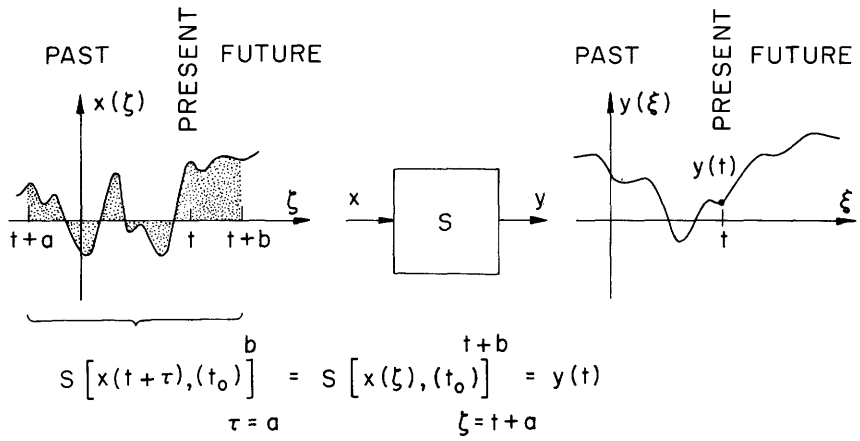

Fig. 5. Time-invariant deterministic system.

There are two results about finite memory, time-invariant, deterministic systems that can be shown from Eq. 39: input signals that are constant in time yield output signals that are also constant in time; and input signals that are periodic in time T yield output signals that are also periodic in time T. Thus oscillators, counters, "divide-by" circuits, etc. are not systems that are deterministic, time-invariant, and finite memoried (the last systems because their outputs can contain frequency components that are subharmonics of their input signals[41]).

2.3 CALCULUS OF FUNCTIONALS

Volterra and others, have developed a calculus of functionals. Continuity for functionals has been defined.[34] The first functional derivative,

$$F^{(1)}\left[x(\tau),(\tau_1)\right]_{\tau,\tau_1=a}^{b},$$

and the n^{th} functional derivative,

$$F^{(n)}\left[x(\tau),(\tau_1),\ \ldots\ ,(\tau_n)\right]_{\tau,\tau_1,\ \ldots\ ,\tau_n=a}^{b}$$

of the functional

$$F\left[x(\tau)\right]_{\tau=a}^{b}$$

have been defined.[35] Volterra has shown a theorem for analytic functionals which is an analog of Taylor's theorem for analytic functions.[36] Volterra's theorem is

$$F\Big[x_0(\tau) + x(\tau)\Big]_{\tau=a}^{b} = F\Big[x_0(\tau)\Big]_{\tau=a}^{b}$$

$$+ \int_a^b F^{(1)}\Big[x_0(\tau),(\tau_1)\Big]_{\tau,\tau_1=a}^{b} x(\tau_1)\, d\tau_1 + \ldots$$

$$+ \frac{1}{n!}\int_a^b \cdots \int F^{(n)}\Big[x_0(\tau),(\tau_1), \ldots, (\tau_n)\Big]\, x(\tau_1) \ldots$$

$$\ldots\, x(\tau_n)\, d\tau_1 \ldots\, d\tau_n + \ldots \quad . \tag{40}$$

For our applications, we are interested in Eq. 40 when the function x_0 is zero. That is,

$$F\Big[x(\tau)\Big]_{\tau=a}^{b} = F\Big[(0)\Big] + \int_a^b F^{(1)}\Big[(0),(\tau_1)\Big]\, x(\tau_1)\, d\tau_1 + \ldots$$

$$+ \frac{1}{n!}\int_a^b \cdots \int F^{(n)}\Big[(0),(\tau_1), \ldots, (\tau_n)\Big]\, x(\tau_1) \ldots$$

$$\ldots\, x(\tau_n)\, d\tau_1 \ldots\, d\tau_n + \ldots \quad . \tag{41}$$

2.4 ANALYTIC SYSTEMS

Definition of an Analytic System. If the functional of a time-invariant deterministic system S (see Eq. 39) is analytic about zero input at some time t_0, then S is an analytic system.

Equations 39 and 41 can be used to show that the value of the output y of an analytic system S for input x is

$$y(t) = S\Big[(0),(t_0)\Big] + \int_a^b S^{(1)}\Big[(0), (t_0), (\tau_1)\Big]\, x(t+\tau_1)\, d\tau_1 + \ldots$$

$$+ \frac{1}{n!}\int_a^b \cdots \int S^{(n)}\Big[(0), (t_0), (\tau_1), \ldots, (\tau_n)\Big]\, x(t+\tau_1) \ldots$$

$$\ldots\, x(t+\tau_n)\, d\tau_1 \ldots\, d\tau_n + \ldots \quad . \tag{42}$$

For our purposes, much of the notation in Eq. 42 is unnecessary. For example, $S\left[(0),(t_0)\right]$ is merely a constant and $S^{(n)}\left[(0),(t_0),(\tau_1), \ldots , (\tau_n)\right]$ is merely a symmetric function on n variables. For notational ease and in order to conform with the works of others, we shall write in place of Eq. 42 that the value of the output y of an analytic system H for input x is

$$y(t) = H[x]$$

$$= h_0 + \int_{-\infty}^{\infty} h_1(\tau_1)\, x(t - \tau_1)\, d\tau_1 + \ldots$$

$$\ldots + \int_{-\infty}^{\infty} \cdots \int h_n(\tau_1, \ldots , \tau_n)\, x(t - \tau_1) \ldots x(t - \tau_n)\, d\tau_1 \ldots d\tau_n$$

$$+ \ldots , \tag{43}$$

where

$$h_0 = S\left[(0),(t)\right]_{\tau=a}^{b} , \quad (h_0 \text{ is a constant}) \tag{44}$$

and

$$\underset{(\tau_1, \ldots , \tau_n)}{\text{Sym}} \left\{ h_n (\tau_1, \ldots , \tau_n) \right\} = \frac{1}{n!}\, S^{(n)}\left[(0),(t_0),(-\tau_1), \ldots , (-\tau_n)\right]_{\tau,\tau_1, \ldots , \tau_n=a}^{b}$$

$$\prod_{k=1}^{n} u_{-1}(-\tau_k - a)\, u_{-1}(\tau_k + b),$$

(h_n is a function of n variables), (45)

with

$$\underset{(\tau_1, \ldots, \tau_n)}{\text{Sym}} f(\tau_1, \ldots, \tau_n)$$

indicating the operation of symmetrization of the function f in its n arguments.[40] This is accomplished by summing the values of f at all n! possible permutations of its n arguments and dividing the sum by n!. This symmetrization operator must be introduced because $S^{(n)}$ is symmetric in its n arguments (this is a property of functional derivatives), but h_n need not be symmetric in its n arguments. Equation 45 is a necessary and sufficient condition such that like order intergrals in Eqs. 42 and 43 have the same values for all signals x. (The symmetrization operator corresponds to permuting the dummy variables of integration.)

We shall refer to Eq. 43 as a Volterra series and call the constant h_0 and the functions h_n the kernels of the Volterra series.* We shall also have need to refer to separate terms within the Volterra series. For this purpose, when we say "the k^{th} order term in the Volterra series", we mean

$$y_0(t) = H_0[x] = h_0, \text{ when } k = 0, \tag{46}$$

and when $k \neq 0$,

$$y_k(t) = H_k[x] = \int_{-\infty}^{\infty} \cdots \int h_k(\tau_1, \ldots, \tau_k)\, x(t - \tau_1) \cdots x(t - \tau_k)\, d\tau_1 \cdots d\tau_k. \tag{47}$$

2.5 COMBINATIONS OF ANALYTIC SYSTEMS

The combinations of analytic systems have been studied extensively.[3,16,42] We shall now summarize those results that we shall use. These results are more easily stated in the frequency domain than in the time domain, hence we shall define the multivariate bilateral Laplace transform of a function of k variables.[2]

$$H_k(s_1, \ldots, s_k) = \int_{-\infty}^{\infty} \cdots \int h_k(\tau_1, \ldots, \tau_k) \exp(-s_1 \tau_1 - \cdots - s_k \tau_k)\, d\tau_1 \cdots d\tau_k, \tag{48}$$

where $s_k = \sigma_k + j\omega_k$.

*Of course, h_0 is not a kernel; however, it would be awkward to forever have to refer to "h_0 and the kernels".

Consider three analytic systems, F, G, and H, whose outputs are p, q, and r. That is, by Eqs. 43, 46, and 47, when the input to these systems is x, their outputs are

$$p(t) = F[x] = \sum_{k=0}^{\infty} F_k[x] \tag{49}$$

$$q(t) = G[x] = \sum_{k=0}^{\infty} G_k[x] \tag{50}$$

$$r(t) = H[x] = \sum_{k=0}^{\infty} H_k[x]. \tag{51}$$

Additive Combination. $F + G = H$ (see Fig. 6).

If the outputs of two analytic systems, F and G, are added, then their sum, $r = p + q$, is the output of an analytic system H and[4]

$$H_k(s_1, \ldots, s_k) = F_k(s_1, \ldots, s_k) + G_k(s_1, \ldots, s_k). \tag{52}$$

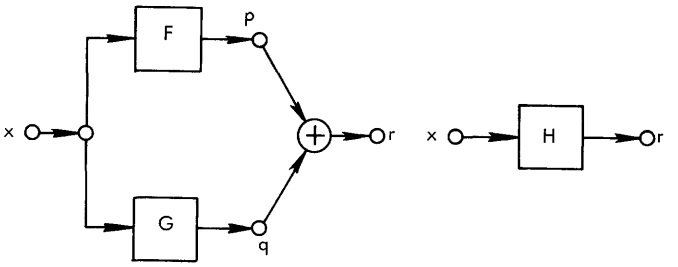

Fig. 6. Additive combination of analytic systems.

Multiplicative Combination. $F \cdot G = H$ (see Fig. 7).

If the outputs of two analytic systems F and G are multiplied, then their product, $r = pq$, is the output of an analytic system H and[5]

$$H_n(s_1, \ldots, s_n) = \sum_{m=0}^{n} F_m(s_1, \ldots, s_m)\, G_{n-m}(s_{m+1}, \ldots, s_n). \tag{53}$$

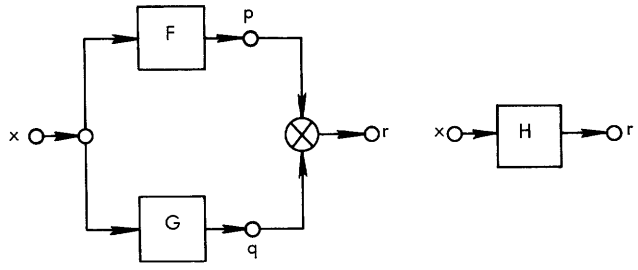

Fig. 7. Multiplicative combination of analytic systems.

Cascade Combination. G(*)F = H (see Fig. 8).

If the input to an analytic system F is x, and its output $p\big(p = F[x]\big)$ is the input to an analytic system G, then its output $q\Big(q = G[p] = G\big[F[x]\big]\Big)$ is the output of an analytic system H and[6]

Case 1: If G is linear, then

$$H_n(s_1, \ldots, s_n) = F_n(s_1, \ldots, s_n)\, G_1(s_1 + \ldots + s_n). \tag{54}$$

Case 2: If F is linear, then

$$H_n(s_1, \ldots, s_n) = F_1(s_1)\, F_1(s_2) \ldots F_1(s_n)\, G_n(s_1, \ldots, s_n). \tag{55}$$

Case 3: If neither F nor G is linear, then see Brilliant for the combination formula.[6]

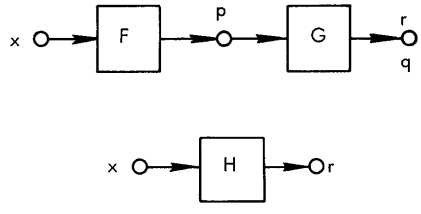

Fig. 8. Cascade combination of analytic systems.

Feedback Combination. (See Fig. 9.)

The feedback combination of analytic systems is an analytic system (except when the feedback makes the system unstable). See Brilliant, George, and Zames.[7,17,43]

2.6 GEORGE'S ASSOCIATION TECHNIQUE

The remaining result of functional calculus that we shall use but have not yet introduced is George's frequency association technique.[19] It is a technique for evaluating, by inspection, the transforms of signals that are the outputs of analytic systems.

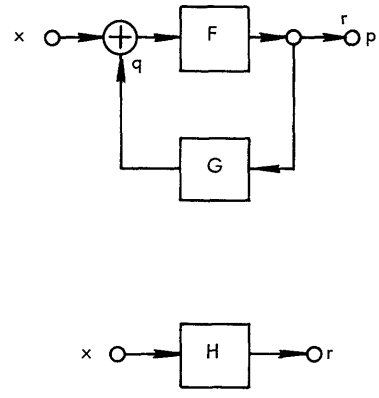

Fig. 9. Feedback combination of analytic systems.

The k^{th}-order term of the system's output (see Eq. 47) has a multilinear correspondent. It is[18]

$$y_{(k)}(t_1, \ldots, t_k) = \int_{-\infty}^{\infty} \cdots \int h_k(\tau_1, \ldots, \tau_k)\, x(t_1 - \tau_1) \ldots x(t_k - \tau_k)\, d\tau_1 \ldots d\tau_k. \tag{56}$$

The transform of the multilinear correspondent is a product.

$$Y_{(k)}(s_1, \ldots, s_k) = H_k(s_1, \ldots, s_k)\, X(s_1) \ldots X(s_k). \tag{57}$$

An example of the application of George's frequency association technique follows. If

$$Y_{(2)}(s_1, s_2) = A(s_1 + s_2)\, \frac{B}{s_1 + b}\, \frac{C}{s_2 + c}, \tag{58}$$

then

$$Y_2(s) = A(s)\, \frac{BC}{s + b + c}. \tag{59}$$

If

$$Y_{(2)}(s_1, s_2) = A(s_1 + s_2)\, \frac{B}{(s_1 + b)^n}\, \frac{C}{(s_2 + c)^m}, \tag{60}$$

then

$$Y_2(s) = A(s) \frac{BC(n + m - 2)!}{(n - 1)!\,(m - 1)!\,(s + b + c)^{n+m-1}} \tag{61}$$

In our applications of George's frequency association technique it will become clear that the evaluation of the transforms of the output signals of analytic systems is straightforward as long as the transforms of the multilinear correspondents have partial fraction expansions.

2.7 MULTI-INPUT SYSTEMS

The extension of these results to multi-input systems is straightforward. The value of the output y of an analytic system whose simultaneous input signals are u, v, w, ... is

$$y(t) = H[u,v,w, \ldots]$$

$$= \sum_{i=0}^{\infty} \sum_{j=0}^{\infty} \sum_{k=0}^{\infty} \ldots H_{i,j,k,\ldots}[u,v,w, \ldots]$$

$$= \sum_{i=0}^{\infty} \sum_{j=0}^{\infty} \sum_{k=0}^{\infty} \ldots \int_{\infty} \cdots \int h_{i,j,k, \ldots}(\tau_1,\tau_2, \ldots)$$

$$u(t - \tau_1) \ldots u(t - \tau_i)\, v(t - \tau_{i+1}) \ldots v(t - \tau_{i+j})\, w(t - \tau_{i+j+1}) \ldots$$

$$w(t - \tau_{i+j+k}) \ldots d\tau_1\, d\tau_2 \ldots \quad . \tag{62}$$

Here, it must be understood (as a convention) that a zero subscript obviates the corresponding integrations.

III. VOLTERRA SERIES SOLUTIONS OF NONLINEAR DIFFERENTIAL EQUATIONS

Extending the results summarized in Section II, we shall show which differential equations characterize analytic systems, and present an inspection technique for finding the Volterra series solutions to those differential (or for that matter, integral or integro-differential) equations that characterize analytic systems. This technique's rationale may be stated: (i) If a differential equation characterizes an analytic system, then there is a Volterra series satisfying that differential equation. (ii) Because the system combination theorems show that the addition, multiplication, or analytic operation (the cascade) upon a Volterra series yields a Volterra series, then its substitution in the differential equation yields a Volterra series. (iii) If two Volterra series are equal, then the symmetrization of their like order kernels must be equal.

The justification of the last statement follows: Consider two Volterra series that are equal for all inputs. That is,

$$F[x] = G[x], \text{ all } x. \tag{63}$$

Equation 47 shows that

$$H_k[\lambda x] = \lambda^k H_k[x] \tag{64}$$

for any constant λ. Then by (63), (64), and (43), we see that

$$\sum_{n=0}^{\infty} \lambda^n F_n[x] = \sum_{m=0}^{\infty} \lambda^m G_m[x] \tag{65}$$

for any constant λ.

Equation 65 equates two power series in λ. For two power series to be equal, their like-order coefficients must be equal. That is,

$$F_k[x] = G_k[x], \text{ all } x. \tag{66}$$

But Eq. 45 shows that the kernels of both of these k-order functionals, when symmetrized, equal the same k-order functional derivative.[40] Thus

$$\underset{(s_1, \ldots, s_k)}{\text{Sym}} \left\{ F_k(s_1, \ldots, s_k) \right\} = \underset{(s_1, \ldots, s_k)}{\text{Sym}} \left\{ G_k(s_1, \ldots, s_k) \right\} . \tag{67}$$

The application of this technique will be illustrated by examples.

Example 1

Consider a system whose input is x and whose output y obeys the differential equation

$$\frac{dy}{dx} = 1 + \frac{dx}{dt} , \tag{68}$$

and the boundary condition of initial rest. That is,

$$y(t) = 0 \text{ until } x(t) \neq 0. \tag{69}$$

Because the system characterized by Eqs. 68 - 69 is an analytic system (we shall postpone the question of how we know that it is an analytic system), then there is some Volterra series H such that

$$y(t) = H[x] = \sum_{k=0}^{\infty} H_k[x], \text{ any } x. \tag{70}$$

The term dy/dx in (68) is not the result of an analytic operation upon y (Eq. 70) so Eq. 68 is not yet in the form whereby we can exploit the system combination theorems. Since

$$\frac{dy}{dt} = \frac{dy}{dx} \cdot \frac{dx}{dt} , \tag{71}$$

Eq. 68 can be rewritten

$$\frac{dy}{dt} = \left[1 + \frac{dx}{dt} \right] \frac{dx}{dt} . \tag{72}$$

All terms in Eq. 72 are the result of analytic operations upon either x or y. Specifically, dy/dt is the result of a cascade of system H with a linear system whose 1-order (its sole term) kernel's transform is s. (See Fig. 10.) The two other terms in (72) are trivial Volterra series in x. (See Figs. 11 and 12.)

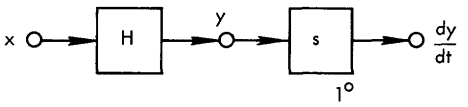

Fig. 10. Cascade synthesis of dv/dt.

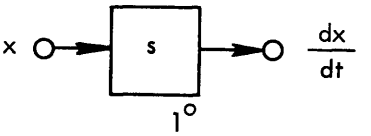

Fig. 11. Synthesis of dx/dt.

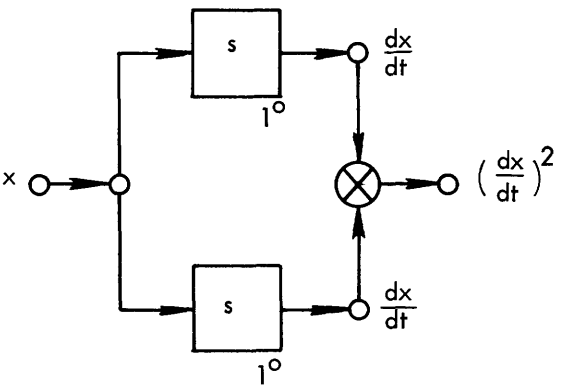

Fig. 12. Synthesis of the square of dx/dt.

Thus, with the aid of the system combination theorems of Section II and Eq. 67, we may write from (72) by inspection

$$s_1 H_1(s_1) = s_1 \tag{73}$$

$$\underset{(s_1, s_2)}{\text{Sym}} \left\{ (s_1 + s_2)\ H_2(s_1, s_2) \right\} = s_1\, s_2 \tag{74}$$

$$\underset{(s_1, \ldots, s_k)}{\text{Sym}} \left\{ (s_1 + \ldots + s_k)\, H_k(s_1, \ldots, s_k) \right\} = 0;\ k = 3, 4, \ldots . \tag{75}$$

By considering the boundary condition (69) when x = 0, we can add that

$$H_0[x] = 0. \tag{76}$$

For solutions to Eqs. 73 - 75, let us choose* the remaining kernels to be

$$H_1(s_1) = 1 \tag{77}$$

$$H_2(s_1, s_2) = \frac{s_1 s_2}{s_1 + s_2} \tag{78}$$

$$H_k(s_1, \ldots, s_k) = 0;\ k = 3, 4, \ldots . \tag{79}$$

These solutions are amenable to synthesis by another application of the system combination theorems. (See Fig. 13.) The time-domain expression for y can be written by inspection of this synthesis (Fig. 13). It is

$$y(t) = u_0(t)\ (*)x(t) + u_{-1}(t)\ (*)\ (u_{+1}(t)\ (*)x(t))^2$$

$$= x(t) + \int_{-\infty}^{t} \left(\frac{dx}{dt}\right)^2 dt. \tag{80}$$

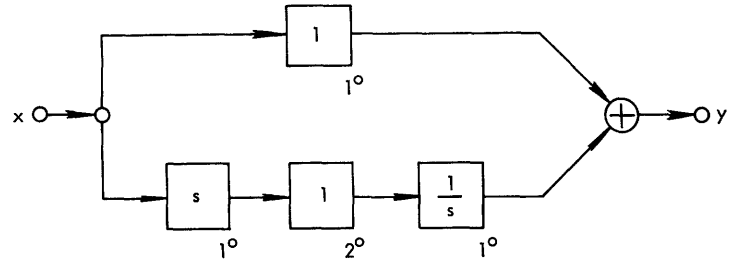

Fig. 13. Synthesis of H.

The observation that (80) is indeed the solution to (68) and (69) is trivial. Example 1 was not chosen to show the solution of a difficult differential equation, rather it was chosen to be an easy illustration of the solution technique. An example in which a less trivial differential equation is used follows.

*The "choice" of kernels for solving Eqs. 73 - 75 is irrelevant. Any kernel that satisfies these equations will, when substituted in Eq. 70, yield the same value for y. The only difference in the answers will be the way in which the integration over the dummy variables takes place.[40]

Example 2

Consider a system whose input is x and whose output is y which obeys the differential equation

$$x\left[1+\frac{d}{dt}\right]^3 y - \frac{dx}{dt}\left[1+\frac{d}{dt}\right]^2 y = 2x^3 \tag{81}$$

and the boundary condition of initial rest. That is,

$$y(t) = 0 \text{ until } x(t) \neq 0. \tag{82}$$

Because the system characterized by Eqs. 81 - 82 is an analytic system (we shall postpone the question of how we know that it is an analytic system), there is some Volterra series F such that

$$y(t) = F[x] = \sum_{k=0}^{\infty} F_k[x], \text{ all } x. \tag{83}$$

Equation 81 is already written in a form such that all terms are the results of analytic operations upon either x or y. Hence, by inspection, we write

$$1\,[1+0]^3 F_0 - s_1\,[1+0]^2 F_0 = 0 \tag{84}$$

$$\underset{(s_1, s_2)}{\text{Sym}} \left\{ 1\,[1+s_2]^3 F_1(s_2) - s_1\,[1+s_2]^2 F_1(s_2) \right\} = 0 \tag{85}$$

$$\underset{(s_1, s_2, s_3)}{\text{Sym}} \left\{ 1\,[1+s_2+s_3]^3 F_2(s_2, s_3) - s_1\,[1+s_2+s_3]^2 F_2(s_2, s_3) \right\} = 2 \tag{86}$$

$$\underset{(s_1, \ldots, s_{k+1})}{\text{Sym}} \left\{ 1\,[1+s_2+\ldots+s_{k+1}]^3 F_k(s_2, \ldots, s_{k+1}) \right.$$

$$\left. - s_1\,[1+s_2+\ldots+s_{k+1}]^2 F_k(s_2, \ldots, s_{k+1}) \right\} = 0; \; k = 3, 4, \ldots . \tag{87}$$

For Eqs. 84, 85, and 87 we choose the solutions

$$0 = F_0 = F_1 = F_3 = F_4 = \ldots . \tag{88}$$

But for (86) we must choose an F_2 such that

$$\underset{(s_1, s_2, s_3)}{\text{Sym}} \left\{ (1 + s_2 + s_3)^2 \, (1 - s_1 + s_2 + s_3) \; F_2 \, (s_2, s_3) \right\} = 2. \tag{89}$$

An F_2 that satisfies Eq. 89 can be found quickly if we restrict our choice of F_2 to those that are symmetrical. That is,

$$F_2 \, (s_a, s_b) = F_2 \, (s_b, s_a), \text{ all } s_a, s_b. \tag{90}$$

When we evaluate Eq. 89 at $(s_1, s_2, s_3) = (0, 0, 0)$, the result is

$$F_2 \, (0, 0) = 2. \tag{91}$$

When we evaluate Eq. 89 at $(s_1, s_2, s_3) = (s, 0, 0)$, the result is

$$\frac{1}{3} \Big\{ [1]^2 \, [1 - s] \, F_2 \, (0, 0) + [1 + s]^2 \, [1 + s] \, F_2 \, (s, 0) + [1 + s]^2 \, [1 + s] \, F_2 \, (0, s) \Big\} = 2. \tag{92}$$

When Eqs. 90 and 91 are substituted in Eq. 92, then the result is

$$F_2 \, (0, s) = F_2 \, (s, 0) = \frac{s + 2}{(s + 1)^3} \tag{93}$$

When we evaluate Eq. 89 at $(s_1, s_2, s_3) = (s_1, s_2, 0)$, the result is

$$\frac{1}{6}\Big\{(1+s_2)^2\,(1-s_1+s_2)\,F_2(s_2,0)+(1+s_1)^2\,(1-s_1+s_2)\,F_2(0,s_2)$$

$$+(1+s_2)^2\,(1-s_1+s_2)\,F_2(0,s_2)+(1+s_1)^2\,(1-s_2+s_1)\,F_2(0,s_1)$$

$$+(1+s_1+s_2)^2\,(1+s_1+s_2)\,F_2(s_1,s_2)$$

$$+(1+s_1+s_2)^2\,(1+s_1+s_2)\,F_2(s_2,s_1)\Big\}=2. \tag{94}$$

When Eqs. 90 and 93 are substituted in Eq. 94, then the result is

$$F_2(s_1,s_2)=\frac{s_1+s_2+2}{(s_1+1)\,(s_2+1)\,(s_1+s_2+1)^2}. \tag{95}$$

It should be clear that the method that we have just used to get Eq. 95 from Eq. 89 is general. That is, whenever a k-order kernel transform is in a constraint equation with more than k frequencies, then that kernel's transform can be found in k + 1 steps; namely by evaluating that equation at $(0,0,0,\ldots)$, $(s_1,0,0,\ldots)$, $(s_1,s_2,0,\ldots)$, $\ldots$, and $(s_1,s_2,\ldots s_k,0,\ldots)$.

The Inverse transform of Eq. 95 is

$$f_2(\tau_1,\tau_2)=u_{-1}(\tau_1)\,u_{-1}(\tau_2)\,\underline{m}(\tau_1,\tau_2)\exp\left(-\overline{m}(\tau_1,\tau_2)\right), \tag{96}$$

where $\underline{m}$ and $\overline{m}$ are the minimum and maximum functions. They are

$$\underline{m}(\tau_1,\tau_2)=\begin{cases}\tau_1, & \tau_1\le\tau_2\\ \tau_2, & \tau_1\ge\tau_2\end{cases} \tag{97}$$

$$\overline{m}(\tau_1,\tau_2)=\begin{cases}\tau_2, & \tau_1\le\tau_2\\ \tau_1, & \tau_1\ge\tau_2\end{cases}. \tag{98}$$

When the expression for f_2 (the only nonzero kernel) is substituted in Eq. 83, the result (the solution to Eqs. 81 - 82) is

$$y(t) = \int_{-\infty}^{\infty}\int f_2(\tau_1, \tau_2)\ x(t - \tau_1)\ x(t - \tau_2)\, d\tau_1\, d\tau_2$$

$$= 2\int_{0}^{\infty}\int_{0}^{\tau_2} \tau_1 \exp(-\tau_2)\ x(t - \tau_1)\ x(t - \tau_2)\, d\tau_1\, d\tau_2. \qquad (99)$$

A frequency-domain synthesis of this system (from Eq. 95) is shown in Fig. 14. Upon examination of Fig. 14, two qualitative observations about the system's behavior may be made by inspection:

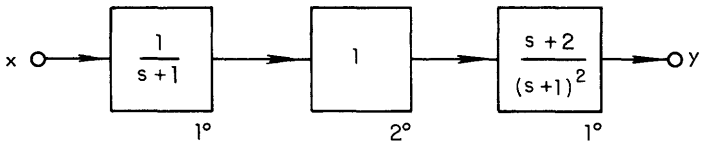

Fig. 14. Synthesis of F.

(i) If x is a low-frequency signal ($|s| << 1$), then $y \approx 2x^2$.

(ii) If x is a high-frequency signal ($|s| >> 1$) of narrow bandwidth (small compared with 1), then y is approximately twice the low-frequency component of the square of the integral of x.

Both of these observations are simple by-products of the Volterra series solution of the system characterized by Eqs. 81 - 82. These equations completely describe this system but neither observation (i) nor (ii) were, a priori, obvious from them. Thus we see that the Volterra series description of a system may well provide more insight into the behavior of that system than its differential equation description.

In the two examples considered thus far, the extraction of like order terms in the kernel transforms from the system's characteristic equation gave equations that were independent. This is not usually the case. The usual result is a set of simultaneous equations in the kernels. In this event, solution for the kernel transforms involves the formulation of a recursive formula for the kernel transforms. An example follows.

Example 3

Consider a system whose input is x and whose output is y which obeys the differential equation

$$y + \frac{dy}{dt} - [2y + 1]\, x = y^2\, [x - 1] \tag{100}$$

and the boundary condition of initial rest. That is,

$$y(t) = 0 \text{ until } x(t) \neq 0. \tag{101}$$

Because the system characterized by (100) and (101) is analytic, for a certain class of input signals (we shall postpone the questions of which class of input signals and how we know that it is an analytic system for them), there is some Volterra series G such that

$$y(t) = G[x] = \sum_{k=0}^{\infty} G_k[x], \text{ all } x \text{ in a class.} \tag{102}$$

Equation 100 is already in such a form that all terms are the results of analytic operations upon either x or y. Hence, by inspection, we may write

$$G_0 + 0 - 0 = 0 - G_0^2 \tag{103}$$

$$G_1(s_1) + s_1 G_1(s_1) - (2G_0 + 1)\, 1 = G_0^2 - 2\, G_0 G_1(s_1) \tag{104}$$

$$\begin{aligned} &\underset{(s_1, \ldots, s_k)}{\text{Sym}} \left\{ G_k(s_1, \ldots, s_k) + (s_1 + \ldots + s_k) G_k(s_1, \ldots, s_k) - 2G_{k-1}(s_1, \ldots, s_{k-1}) \right\} \\ &= \underset{(s_1, \ldots, s_k)}{\text{Sym}} \left\{ \sum_{n=0}^{k-1} G_n(s_1, \ldots, s_n)\, G_{k-n-1}(s_{n+1}, \ldots, s_{k-1}) \right. \\ &\left. - \sum_{m=0}^{k} G_m(s_1, \ldots, s_m) \cdot G_{k-m}(s_{m+1}, \ldots, s_k) \right\}; \quad k = 2, 3, \ldots . \end{aligned} \tag{105}$$

Equation 103 can be rewritten as

$$(G_0 + 1)\, G_0 = 0. \tag{106}$$

Equation 104 can be solved for G_1. The result is

$$G_1(s_1) = \frac{(G_0 + 1)^2}{s_1 + 2G_0 + 1}. \tag{107}$$

The highest order term in (105) can be isolated and solved for. The result is

$$\underset{(s_1, \ldots, s_k)}{\text{Sym}} \left\{ G_k(s_1, \ldots, s_k) \right\} = \underset{(s_1, \ldots, s_k)}{\text{Sym}}$$

$$\left\{ \frac{G_{k-1}(s_1, \ldots, s_{k-1})(G_0 + 2) + \sum_{n=1}^{k-1} G_n(s_1, \ldots, s_n) \left[G_{k-n-1}(s_{n+1}, \ldots, s_{k-1}) - G_{k-n}(s_{n+1}, \ldots, s_k) \right]}{s_1 + \ldots + s_k + 2G_0 + 1} \right\}$$

$$k = 2, 3, 4, \ldots . \tag{108}$$

Equation 108 is a recursive formula for G_k. That is, given G_0 and G_1, it constrains G_2; given G_0, G_1, and G_2, it constrains G_3; and so on.

Equation 106 allows us two choices of values for G_0, 0 and -1. These two distinct values of G_0 correspond to the two distinct states possessed by that system which obeys Eq. 100. They are the ' -1 State ' (denoted by a single prime (')), and the "0 State" (denoted by a double prime (")).

' -1 State '.

If, for solution to Eq. 106 we choose

$$G'_0 = -1, \tag{109}$$

then the solution to Eq. 107 is

$$G'_1(s_1) = 0 \tag{110}$$

and, for Eq. 108, we may choose the solutions

$$G'_k (s_1, \ldots, s_k) = 0; \; k = 2, 3, \ldots . \tag{111}$$

The substitution of the kernels whose transforms are given by Eqs. 109 - 111 in Eq. 102 yields the Volterra series G' for the system's -1 state. It is

$$y(t) = G' [x] = -1. \tag{112}$$

That is, in its -1 state, this system's output is y = - 1, regardless of the input x.

For input signals x such that

$$\lim_{t \to -\infty} [x(t)] \neq 0, \tag{113}$$

the output signal y(t) = - 1, all t, is indeed a solution to the system's characteristic equations (Eq. 100 - 101). For inputs that do not begin until time T, that is, if

$$x(t) = u_{-1} (t - T) \, x(t) \, , \text{ all t,} \tag{114}$$

the boundary condition of initial rest, Eq. 101, requires that

$$y(t) = u_{-1} (t - T) \;\; y(t), \text{ all t.} \tag{115}$$

In order to satisfy (115) , we must choose $G_0 = 0$. Thus, for input signals that do not begin until time T, the system must be in its 0 state for at least the time interval $(-\infty, T)$.

" 0 State ".

If, for solution to Eq. 106, we choose

$$G''_0 = 0, \tag{116}$$

then the solution to Eq. 107 is

$$G''_1 (s_1) = \frac{1}{s_1 + 1} \tag{117}$$

and, for Eq. 108, we may choose the solutions

$$G''_k(s_1, \ldots, s_k) = \frac{1}{(s_1 + 1) \ldots (s_k + 1)}; \quad k = 2, 3, \ldots . \tag{118}$$

The substitution of the kernels whose transforms are given by Eqs. 116 - 118 in Eq. 102 yields the Volterra series G'' for the system's 0 state. A frequency-domain synthesis of this state of the system is shown in Fig. 15. A closed form of that synthesis is shown in Figs. 16 and 17. Figure 16 uses feedback, Fig. 18 uses one linear but memoried system and one nonlinear no-memory system. Inspection of any of these syntheses yields

$$y(t) = G''[x] = \frac{\int_0^\infty \exp(-\tau)\, x(t - \tau)\, d\tau}{1 - \int_0^\infty \exp(-\sigma)\, x(t - \sigma)\, d\sigma} \tag{119}$$

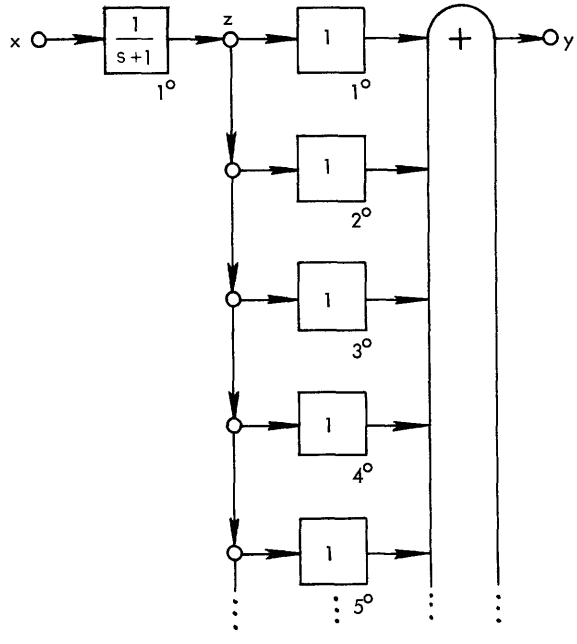

Fig. 15. Parallel synthesis of G''.

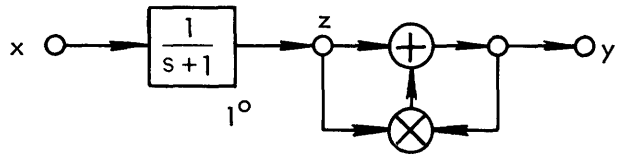

Fig. 16. Feedback synthesis of G''.

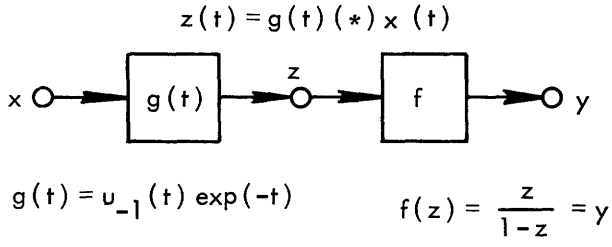

Fig. 17. Cascade synthesis of G''.

Direct substitution will verify that Eq. 119 does indeed solve the system's characteristic equations, Eqs. 100 - 101.

While inputs that do not begin until time T, as in (114), require that the system begin in its 0 state, this does not mean that the system has to stay there. For example, consider an input x_c which begins at time T but is such that later, at time $T_s > T$, it has caused an output

$$y_c = G'' [x_c] \tag{120}$$

such that

$$y_c (T_s) = -1 \tag{121}$$

and

$$\frac{d}{dt} y_c(t) \Big]_{t = T_s} = 0. \tag{122}$$

For input x_c, the system could switch states at time $t = T_s$. Having switched states, the system could then stay in its -1 state forevermore, or, at some later time, it could

decide to switch back to its 0 state – all without violating its characteristic equations (Eqs. 100 - 101). For inputs like x_c, the system has the opportunity to exercise free will. Therefore, for this class of input signals, the system is nondeterministic and not analytic.

Having raised the question of analyticity again, let us now answer it.

3.1 EQUATIONS THAT CHARACTERIZE ANALYTIC SYSTEMS

In the three examples considered, we stated that the equations considered characterized analytic systems. Any differential equation (or for that matter, any integral or integro-differential equation) that characterizes an analytic system has a Volterra series solution. But not every differential equation characterizes an analytic system. For example, the differential equation

$$\left(\frac{dy}{dt}\right)^2 = x^2 \tag{123}$$

characterizes a nondeterministic system (at any instant of time t, the system may choose either $(dy/dt) = x$ or $(dy/dt) = -x$) and, therefore, it characterizes a system that is not analytic.

On the other hand, the differential equation

$$xy + \frac{dy}{dt} + 1 = 0 \tag{124}$$

can, with an appropriate boundary condition, characterize a deterministic system, but not one that is also time-invariant (consider $x(t) = u_{-1}(t - T)$ for various T) and, therefore, it characterizes a system that is not analytic.

Otherwise, the differential equation

$$\frac{dy}{dt} = |x| \tag{125}$$

can, with an appropriate boundary condition, characterize a time-invariant deterministic system, but not one that is analytic. (It can be shown that if the input to an analytic system is infinitely differentiable, then that system's output must also be infinitely differentiable. The input $x(t) = \cos(t)$ is infinitely differentiable but the third derivative of its corresponding output does not exist.)

In Section II, an analytic system was defined to be a time-invariant deterministic system whose functional was analytic about zero input at some time. Therefore, an

equation characterizes an analytic system if and only if (i) solution pairs to the equation exist (so that the equation characterizes a system), (ii) for a given input signal the equation's output solutions are unique (so that the equation characterizes a deterministic system), (iii) the equation's input-output solution pairs must co-translate in time (so that the equation characterizes a time-invariant system), and (iv) certain limits of the equation's output solutions for small perturbations of the input signal about zero are well behaved (all the terms in Eq. 41 must exist and the series must converge absolutely in order for that functional to be analytic).

Given an equation, there is an assortment of ways in which to show that it has properties (i) - (iv), if it does, and thereby prove that it characterizes an analytic system. There are several general tests for existence (property i) but there are no general tests for uniqueness (property ii).[8] In general, a uniqueness proof must be constructed for each given equation.* Once uniqueness has been shown, then the proof of time-invariance is usually trivial (property iii). Showing that the functional is analytic about zero at some time (property iv) by a "brute-force" application of Volterra's definition is tedious and unnecessary. Instead, once existence, uniqueness, and time-invariance have been shown, then it is far easier to use our inspection technique to find a Volterra series solution to the equation (if there is one) and prove that it converges absolutely (perhaps for a certain class of inputs). If this can be done, then, on account of uniqueness, this is sufficient to prove analyticity.

3.2 MULTI-INPUT SYSTEMS

The extension of our inspection technique to multi-input systems is straightforward. The only significant change is that when two Volterra series are equal (see Eq. 62), then the symmetrization in parts of their like order terms are equal. That is, if

$$F[u, v, w, \dots] = G[u, r, w, \dots]; \text{ all } u, v, w, \dots, \tag{126}$$

then

$$\overset{\text{Sym}}{(s_1, \dots, s_i)\,(s_{i+1}, \dots, s_{i+j})\,(s_{i+j+1}, \dots, s_{i+j+k})} \left(\dots \left\{ F_{i,j,k,\dots}(s_1, s_2, \dots) - G_{i,j,k,\dots}(s_1, s_2, \dots) \right\} \right. = 0. \tag{127}$$

*The author's experience has been that if our inspection technique is used, on a trial basis, to get a Volterra series solution to the equation and if that solution implies a feedback synthesis for the system, then that feedback synthesis often suggests an approach to a uniqueness proof.

IV. THE SIMPLE PENDULUM

> "Molecules, pendulums, violin strings, structures, etc., all have oscillatory motion similar to that of a mass attached to a spring . . . . The spring-type force, F = -Kx, . . . increases linearly with x, the displacement from equilibrium position. An oscillator with a force of this type is called a linear or a harmonic oscillator, and the corresponding oscillation is called harmonic motion. If the force depends on x in any other way, the oscillator is called nonlinear. We find that although many oscillators are nonlinear, most are linear or approximately so, at sufficiently small amplitudes of oscillations."[22]

We shall now present an application of the inspection technique developed in Section III. We shall consider an actual nonlinear physical system – a simple pendulum. We choose this as our first example because (i) the reader is intuitively familiar with a pendulum's physical behavior, (ii) the reader is familiar with the standard mathematical solution of a pendulum's behavior for "small amplitudes of oscillations", (iii) the Volterra series solution of a pendulum's behavior is easily obtained by our inspection technique, and (iv) the Volterra series solution shows a new aspect of a pendulum's behavior – nonlinear resonance. We shall see that this nonlinear resonance phenomenon cannot be explained by the standard "small amplitudes" solution but that it is nontheless clearly part of a pendulum's physical behavior.

Consider the damped simple pendulum, oscillating in a plane, which is shown in Fig. 18. It is characterized by the well-known differential equation

$$mL^2 \frac{d^2\theta}{dt^2} = \tau - a \frac{d\theta}{dt} - mgL \sin \theta \tag{128}$$

and the boundary condition of initial rest

$$\theta(t) = 0 \text{ until } \tau(t) \neq 0, \tag{129}$$

where τ is the input torque to the pendulum, and θ is its output angle.*

For a certain class of input torques, this pendulum is an analytic system. Thus there exists some functional H such that

---

*A pendulum problem is not out of place in an electrical engineering report. Minorsky shows that, with appropriate identification of variables, Eq. 128 also describes the motion of a synchronous machine.[25]

$$\theta(t) = H[\tau] = \sum_{m=0}^{\infty} H_m[\tau]. \tag{130}$$

Observe that if the input τ produces the output θ, then Eq. 128 shows that the input $-\tau$ produces the output $-\theta$. The pendulum's output angle θ is thus an odd functional of its input torque τ. That is,

$$-\theta(t) = H[-\tau] = \sum_{m=0}^{\infty} (-)^m H_m[\tau], \tag{131}$$

in which we have used the result given by Eq. 64.

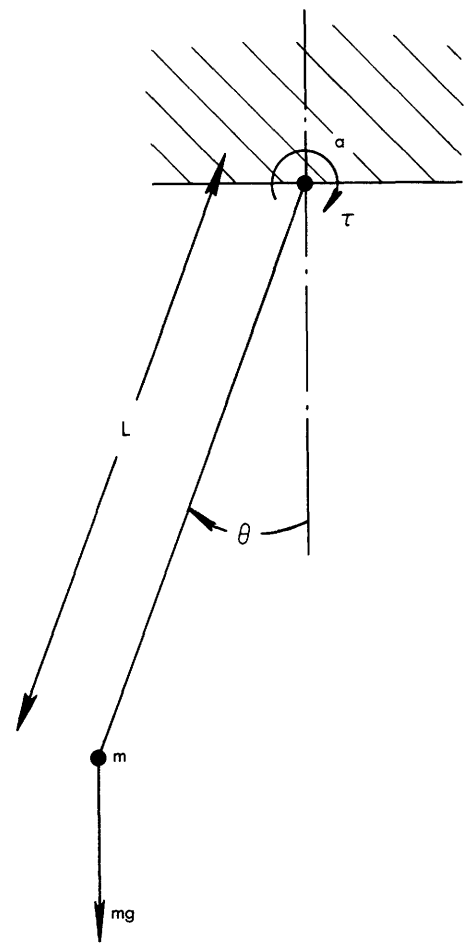

Fig. 18. Damped simple pendulum.

Equations 130 and 131 are simultaneously true. Therefore all the even-order terms must vanish. That is,

$$0 = H_0 = H_2[\tau] = \ldots = H_{2k}[\tau] = \ldots \quad . \tag{132}$$

In order to find the odd-order kernels by our inspection technique, we shall substitute a Taylor series for sin θ in (128). The result is

$$\tau = mL^2 \frac{d^2\theta}{dt^2} + a \frac{d\theta}{dt} + mgL \sum_{k=0}^{\infty} (-)^k \frac{\theta^{2k+1}}{(2k+1)!}. \tag{133}$$

By inspection, the first-order terms in (133) give us

$$1 = mL^2 s_1^2 H_1(s_1) + a s_1 H_1(s_1) + mgL H_1(s_1). \tag{134}$$

In order to write our solutions in compact form, we shall define a dimensionless linear filter whose system function is G. G(s) is

$$G(s) = \frac{mgL}{mL^2 s^2 + as + mgL}$$

$$= \frac{\omega_0^2}{(s - s_0)(s - s_0^*)}. \tag{135}$$

Here, we have used the standard notation for the filter's natural frequencies

$$s_0 = -\alpha + j\omega_D \tag{136}$$

$$\alpha = \frac{a}{2mL^2} \tag{137}$$

$$\omega_D = \sqrt{\omega_0^2 - \alpha^2} \tag{138}$$

$$\omega_0 = \sqrt{\frac{g}{L}} \quad . \tag{139}$$

The s-plane plot of G is shown in Fig. 19.

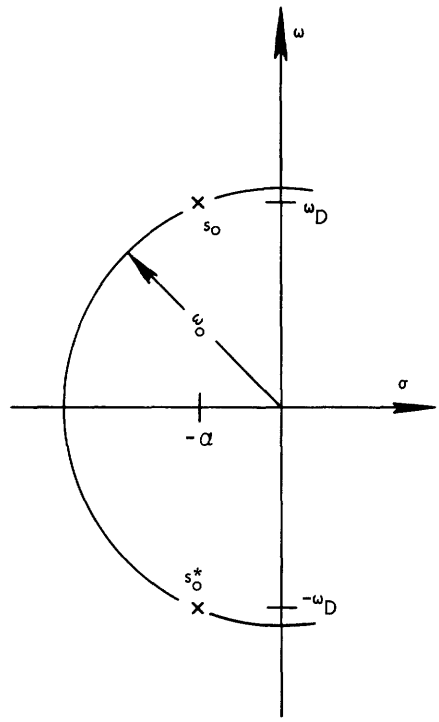

Fig. 19. s-plane plot of G(s).

The solution to Eq. 134 can now be written

$$H_1(s_1) = \frac{1}{mgL}\, G(s_1). \tag{140}$$

By inspection, the third-order terms in (133) give us

$$0 = \underset{(s_1,s_2,s_3)}{\text{Sym}} \left\{ \left[mL^2(s_1 + s_2 + s_3)^2 + a(s_1 + s_2 + s_3) + mgL \right] H_3(s_1,s_2,s_3) \right.$$

$$\left. - \frac{mgL}{3!}\, H_1(s_1)\, H_1(s_2)\, H_1(s_3) \right\} . \tag{141}$$

The symmetrical solution* to (141) is

$$H_3(s_1,s_2,s_3) = \frac{1}{3!(mgL)^3}\, G(s_1)\, G(s_2)\, G(s_3)\, G(s_1 + s_2 + s_3) \tag{142}$$

---

*We could have chosen any kernel that satisfied Eq. 141. It makes no difference in the final answer for θ.[40] Throughout, however, we shall always choose a symmetrical kernel because it will make some of our later frequency domain arguments easier to write. (See footnote, page 42.)

By inspection, the fifth-order terms in Eq. 133 give us

$$0 = \underset{(s_1, \ldots, s_5)}{\text{Sym}} \Bigg\{ \Big[mL^2 s^2 + as + mgL \Big] H_5(s_1, \ldots, s_5) \Big|_{s = s_1 + \ldots + s_5}$$

$$- \frac{mgL}{3!} \Big[H_1(s_1)\, H_1(s_2)\, H_3(s_3, s_4, s_5)$$

$$+ H_1(s_1)\, H_3(s_2, s_3, s_4)\, H_1(s_5)$$

$$+ H_3(s_1, s_2, s_3)\, H_1(s_4)\, H_1(s_5) \Big]$$

$$+ \frac{mgL}{5!} H_1(s_1) \ldots H_1(s_5) \Bigg\} . \qquad (143)$$

The symmetrical solution to Eq. 143 is

$$H_5(s_1, \ldots, s_5) = \frac{1}{5!\,(mgL)^5} G(s_1) \ldots G(s_5)\, G(s_1 + \ldots + s_5)$$

$$\underset{(s_1, \ldots, s_5)}{\text{Sym}} \Big\{ 10\, G(s_1 + s_2 + s_3) - 1 \Big\} . \qquad (144)$$

The higher order odd kernel's transforms can be found similarly. The key to writing the (2k+1)-order terms is in finding all of the possible combinations of an odd number of positive odd integers that add to 2k + 1 (Zames' trees can aid us here[44]).

A parallel synthesis of our pendulum system (from (132), (140), (142), and (144) is shown in Fig. 20. Note that every term in the system's functional (except for the first) is the result of both a prefiltering and a postfiltering by G. This suggests the feedback synthesis of the system which is shown in Fig. 21. This feedback synthesis can be verified by first rewriting Eq. 128 as

$$\frac{L}{g} \cdot \frac{d^2\theta}{dt^2} + \frac{a}{mgL} \cdot \frac{d\theta}{dt} + \theta = \frac{\tau}{mgL} + \theta - \sin\theta, \qquad (145)$$

and then taking into account the boundary condition (129), inverting (135) to get g, and convolving g(t) with (145). The final result is

$$\theta(t) = g(t)(*) \Big[\frac{\tau(t)}{mgL} + \theta(t) - \sin\Big(\theta(t)\Big) \Big] . \qquad (146)$$

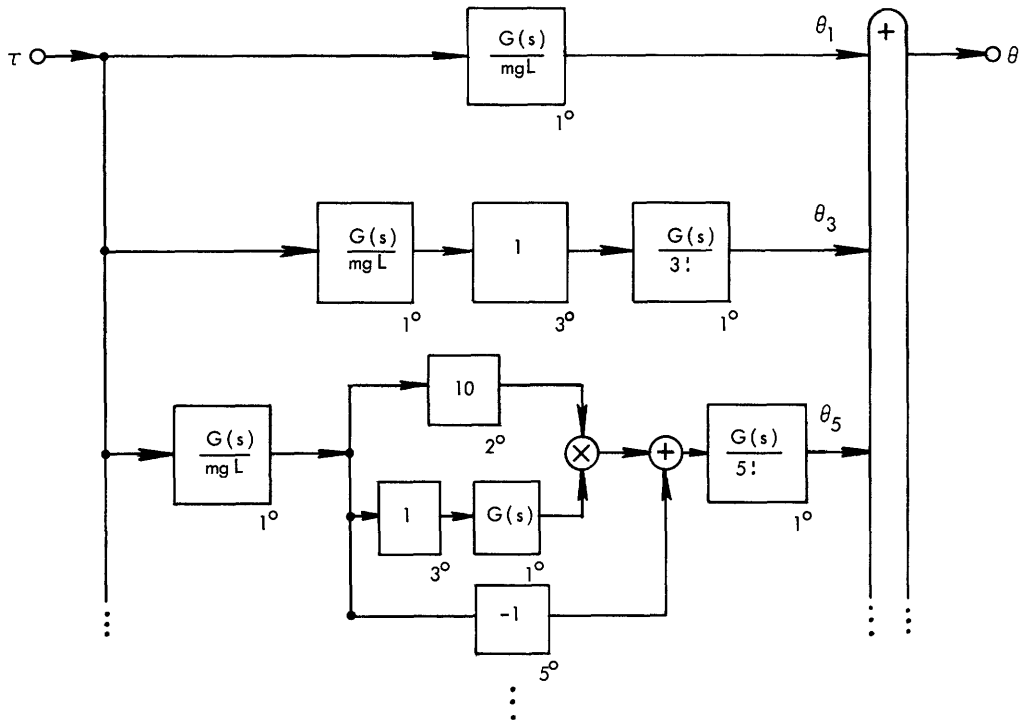

Fig. 20. Parallel synthesis of H.

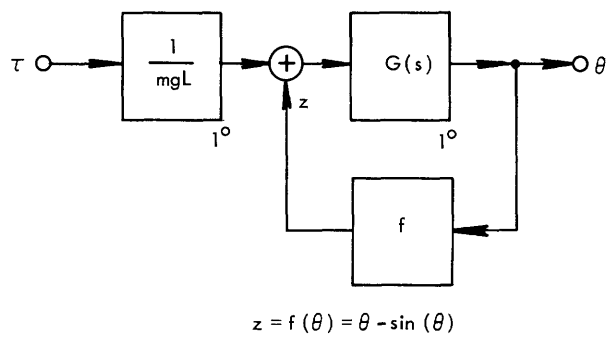

Fig. 21. Feedback synthesis of H.

Equation 146 verifies the feedback synthesis in Fig. 21 and, therefore, indirectly verifies the synthesis in Fig. 20 and our solutions for the kernels which led to it.

The feedback synthesis, Fig. 21, uses one linear memoried system, one linear no-memory system, and one nonlinear no-memory system f for feedback. The transfer curve, over the interval $(-\pi, \pi)$, of f is graphed in Fig. 22. This graph shows that the nonlinear system has a "dead band" for small θ. (For example, if $|\theta| < 45°$, then $|z| < 0.08$.) Thus we have arrived (albeit roundaboutly) at the standard mathematical

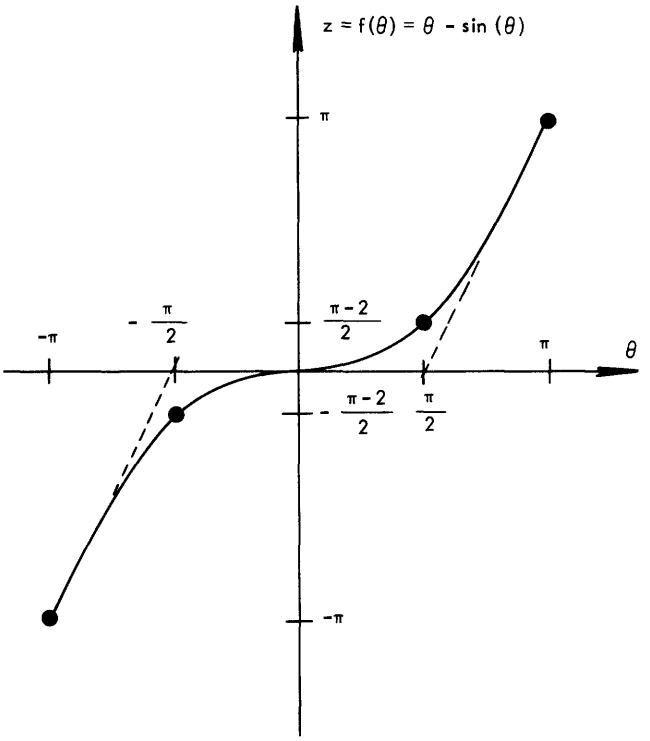

Fig. 22. Transfer curve of f.

solution to a pendulum's "small amplitudes of oscillations" behavior: If the pendulum's output angle θ is such that we can neglect θ - sin θ with respect to τ/mgL as the input to filter g, then θ is approximately equal to the convolution of the impulse response of g with τ/mgL, and the pendulum is therefore a "linear" or a "harmonic" oscillator. That is,

$$\theta(t) \approx g(t)(*) \frac{\tau(t)}{mgL} = \frac{1}{mgL} \int_0^\infty g(\sigma)\, \tau(t - \sigma)\, d\sigma. \tag{147}$$

It is not true, however, that Eq. 147 follows if "θ is small enough" or if "θ is small compared with τ/mgL". Indeed, we shall show that there are cases in which θ can be as small as we might wish and yet it is still not valid to neglect θ - sin θ with respect to τ/mgL. This we shall see, is because when filter g is highly resonant, then the critical consideration will not be "what are the relative magnitudes of θ and τ" but rather "what are the frequency components of θ and τ".

As an illustration of the critical dependence of a pendulum's behavior upon frequency, consider the single-frequency input torque signal

$$\tau(t) = T_0 \exp(st). \tag{148}$$

Equations 47, 130, 132, 140, 142, and 144 then give us

$$\theta(t) = H\left[T_0 \exp(st) \right]$$

$$= \sum_{k=0}^{\infty} T_0^{2k+1} H_{2k+1}(s, \ldots, s) \exp\left([2k+1]\, st \right)$$

$$= \frac{T_0}{mgL} G(s) \exp(st) + \frac{T_0^3}{3!(mgL)^3} G^3(s)\, G(3s) \exp(3st)$$

$$+ \frac{T_0^5}{5!(mgL)^5} G^5(s)\, G(5s) \left[10G(3s) - 1 \right] \exp(5st)$$

$$+ \ldots \quad . \tag{149}$$

Note that the (2k+1)-order term in Eq. 149 is multiplied by $G\left([2k+1]s\right)$. (It comes from the postfiltering by g.) Since the frequencies s_0 and s_0^* are the natural frequencies (poles) of G(s) (see Eq. 135), then Eq. 149 shows that θ fails to exist at the frequencies $s_0/2k+1$ and $s_0^*/2k+1$ (k = 0, 1, 2, ...).

We shall call these frequencies the nonlinear natural frequencies of the pendulum. They are shown in Fig. 23.

4.1 NONLINEAR RESONANCES OF A PENDULUM

To illustrate the nonlinear resonances of a pendulum, in the vicinity of its nonlinear natural frequencies, consider the sinusoidal input torque signal

$$\tau(t) = \mathrm{Re}\left[T_0 \exp(j\omega t) \right] . \tag{150}$$

Equations 47, 130, 132, 140, 142, and 144 then give us*

*Cf. Eq. 149. Equation 151 came out in this simple form because we made the kernels symmetric. (See footnote, page 38.)

$$\theta(t) = H\left[\text{Re } T_0 \exp(j\omega t)\right]$$

$$= \text{Re}\left[\sum_{m=0}^{\infty}\sum_{k=m}^{\infty} \frac{(2k+1)!\ T_0^{k+m+1}\ (T_0^*)^{k-m}}{(k+m+1)!\ (k-m)!\ 2^{2k}}\right.$$

$$\left. H_{2k+1}(\overbrace{j\omega, \ldots, j\omega}^{k+m+1}, \overbrace{-j\omega, \ldots, -j\omega}^{k-m}) \exp\left(j[2m+1]\,\omega t\right)\right]$$

$$= \text{Re}\left[\left(\frac{T_0}{mgL} G(j\omega) + \frac{T_0^2\, T_0^*}{8(mgL)^3} G^3(j\omega)\, G(-j\omega)\right.\right.$$

$$+ \frac{T_0^3\,(T_0^*)^2}{192(mgL)^5} G^3(j\omega)\, G^2(-j\omega)\left[G(3j\omega) + 6G(j\omega)\right.$$

$$\left.\left. + 3G(-j\omega) - 1\right] + \ldots\right) \exp(j\omega t)$$

$$+ \left(\frac{T_0^3}{24(mgL)^3} G^3(j\omega)\, G(3j\omega)\right.$$

$$+ \frac{T_0^4\, T_0^*}{384(mgL)^5} G^4(j\omega)\, G(-j\omega)\, G(3j\omega)\left[6G(j\omega) + 4G(3j\omega) - 1\right]$$

$$\left. + \ldots\right) \exp(3j\omega t) + \left(\frac{T_0^5}{1920(mgL)^5} G^5(j\omega)G(5j\omega) \left[10G(3j\omega) - 1\right]\right.$$

$$\left. + \ldots\right) \exp(5j\omega) + \ldots\Big]. \tag{151}$$

Note the presence of terms like $G\left([2k+1]j\omega\right)$ in Eq. 151. Since filter g is resonant, for sinusoidal frequencies in the vicinity of ω_D (see Fig. 19), then Eq. 151 shows that the pendulum is resonant for sinusoidal frequencies in the vicinity of $\omega_D/2k+1$ (k = 0, 1, 2, . . .). To be specific, let us consider sinusoidal inputs at the first odd subharmonic of ω_D (k = 1). That is,

$$\omega = \frac{\omega_D}{3}. \tag{152}$$

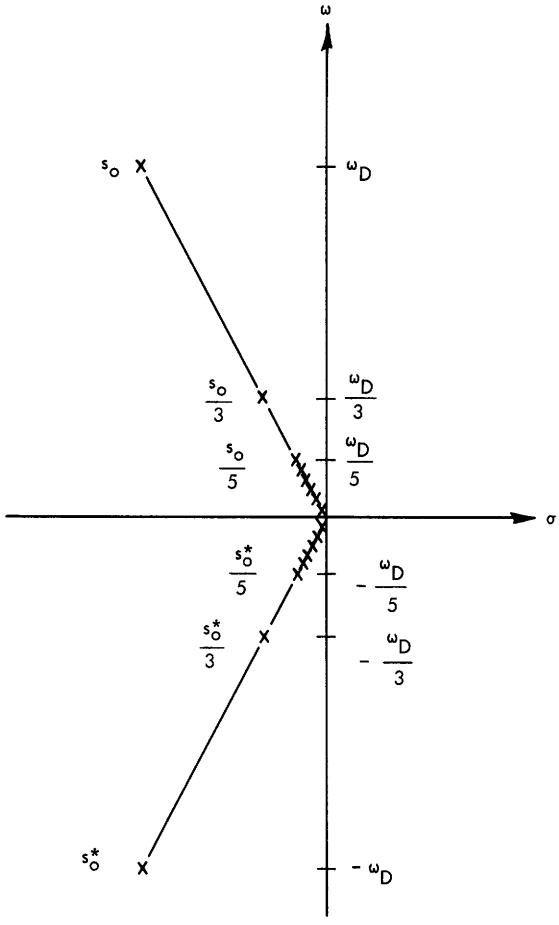

Fig. 23. s-plane plot of a pendulum's natural frequencies.

Let us assume that the pendulum is very lightly damped, that is,

$$\alpha << \omega_0. \tag{153}$$

Then Eq. 138 gives us

$$\omega_D \approx \omega_0, \tag{154}$$

and Eq. 135 gives us

$$G\left(\frac{j\omega_D}{3}\right) \approx \frac{9}{8} \tag{155}$$

$$G(j\omega_D) \approx -\frac{j\omega_0}{2\alpha} \tag{156}$$

$$G\left(\frac{5j\omega_D}{3}\right) \approx -\frac{9}{16}. \tag{157}$$

If we define two real constants, A and B and a phase angle ϕ such that

$$\frac{9T_0}{8mgL} = A \exp(j\phi) \tag{158}$$

$$\frac{\omega_0}{48a} = B, \tag{159}$$

then (151) – (159) gives us

$$\theta(t) \approx R_e \left[\left(A + \frac{9}{64}A^3 - \frac{j}{8}A^5B + \ldots\right) \exp\left(j\left[\frac{\omega_0 t}{3} + \phi\right]\right)\right.$$
$$+ \left(-jA^3B - 6A^5B^2 + \ldots\right) \exp\left(j[\omega_0 t + 3\phi]\right)$$
$$+ \left(\frac{j9}{128}A^5B + \ldots\right) \exp\left(j\left[\frac{5\omega_0 t}{3} + 5\phi\right]\right)$$
$$\left. + \ldots\right]. \tag{160}$$

Equation 160 shows us that if we choose B large enough (make the damping a small enough compared with ω_0), then the major component of the output will not be at the same frequency as the input. An examination of (147) shows that this aspect of a pendulum's behavior cannot be predicted or explained on the basis of the standard "small amplitudes of oscillations" solution for a pendulum. Yet it is not true that this phenomenon does not take place at "small amplitudes of oscillations". Equation 160 also shows that if we choose A small enough (make T_0 small enough compared with mgL), then this phenomenon can take place at arbitrarily small amplitudes of oscillation.

4.2 PHYSICAL EXPLANATION OF A PENDULUM'S NONLINEAR RESONANCES

The pendulum's nonlinear resonance phenomena, while unexplainable by the standard mathematical solution of its behavior for "small amplitudes of oscillations", is nonetheless, easily explained physically. Consider Fig. 21. It shows that if an odd subharmonic of G's resonant frequency is present in τ, then a component at that frequency must also be present in θ. Since the feedback network's transfer curve (see Fig. 22) is an odd function of θ, then the fed-back signal z must contain a component at the filter's resonant frequency. If filter G is resonant enough, then this component can easily induce a significant sinusoidal component in θ at G's resonant frequency – even if the input τ contains no component at that frequency.

V. COMMUTATOR MACHINES

We shall now present another application to an actual nonlinear physical system of the inspection technique developed in Section III. We shall investigate one of the oldest devices known to electrical engineering, the commutator machine.

Figure 24 is a schematic diagram of a single-axis commutator machine driving a load that is both inertial and frictional. The parameters[37] of this system are

v_f, field voltage

v_a, armature voltage

i_f, field current

i_a, armature current

ω, rotation speed of the machine

R_f, field resistance

R_a, series resistance of the armature and the brushes

L_f, field's self-inductance

L_a, armature's self-inductance

G, machine's speed coefficient

A, load's coefficient of torque drag per rotation speed

J, load's moment of inertia.

We shall assume that R_f, R_a, L_f, L_a, G, A, and J are constants (that is, coil saturation and variable loading will not be considered). With this restriction, the system's equations of motion[38] are

$$\left(R_f + L_f \frac{d}{dt}\right) i_f = v_f \tag{161}$$

$$G\omega i_f + \left(R_a + L_a \frac{d}{dt}\right) i_a = v_a \tag{162}$$

$$\left(A + J \frac{d}{dt}\right)\omega = G\, i_a\, i_f \tag{163}$$

with the boundary condition of initial rest

$$i_f(t),\ i_a(t),\ \text{and}\ \omega(t) = 0 \ \text{until}\ v_f(t),\ v_a(t) \neq 0. \tag{164}$$

When excited by a single source, the two configurations of the device are as a shunt-wound motor (Fig. 25) and as a series-wound motor (Fig. 26).

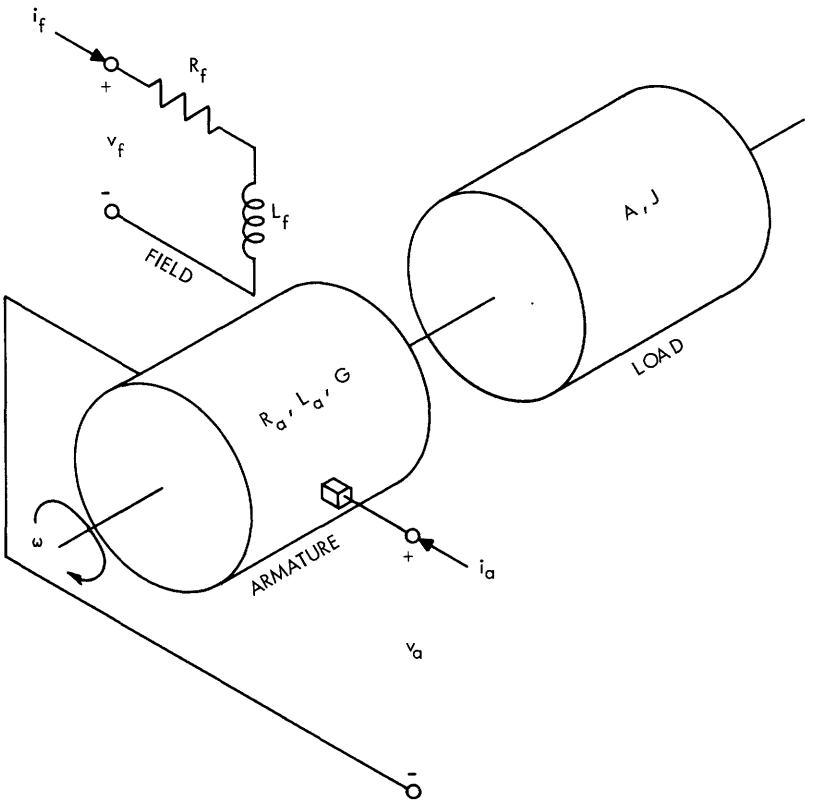

Fig. 24. Schematic diagram of a single axis commutator machine driving a load.

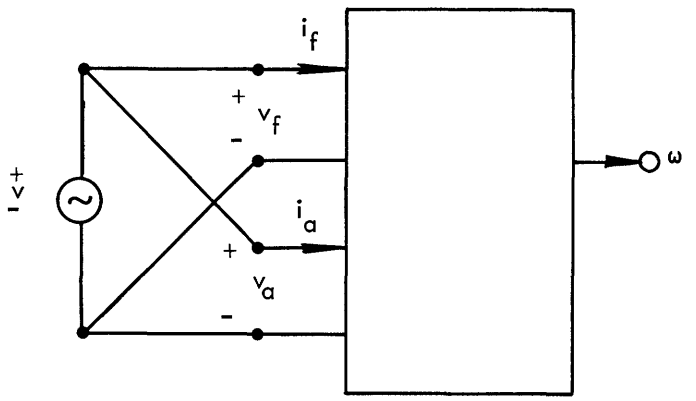

Fig. 25. Diagram of a shunt-wound motor.

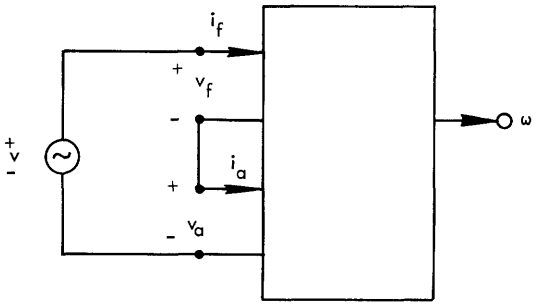

Fig. 26. Diagram of a series-wound motor.

5.1 SHUNT-WOUND

When wired as a shunt-wound commutator machine, the system has two additional constraints. They are

$$v_f = v_a = v \tag{165}$$

$$i_f + i_a = i. \tag{166}$$

The author has shown elsewhere that Eqs. 161 – 166 characterize an analytic system for a certain class of inputs.[26,28] Therefore, there are three functionals, F, I, and W, such that

$$i_f(t) = F[v] \tag{167}$$

$$i_a(t) = I[v] \tag{168}$$

$$\omega(t) = W[v]. \tag{169}$$

Observe from the characterizing equations (Eqs. 161–166) that if input v yields outputs i_f, i_a, and ω, then input -v yields outputs $-i_f$, $-i_a$, and $+\omega$. Thus F and I are odd functionals, and W is an even functional. Observe also that if input v yields output i_f, then input λ v yields output λi_f, where λ is any constant. Thus F is a linear functional of v. Also, observe that the boundary condition (164) gives that W_0 is zero (we already know that F_0 and I_0 were zero because F and I are odd). These observations allow us to rewrite (167) – (169) as

$$i_f(t) = F_1[v] \tag{170}$$

$$i_a(t) = \sum_{m=0}^{\infty} I_{2m+1}[v] \tag{171}$$

$$\omega(t) = \sum_{m=1}^{\infty} W_{2m}[v]. \tag{172}$$

By inspection of Eqs. 161 and 165, we get

$$(R_f + s_1 L_f)\, F_1(s_1) = 1. \tag{173}$$

By inspection of Eqs. 162 and 165 for first-order terms, we get

$$0 + (R_a + s_1 L_a)\, I_1(s_1) = 1. \tag{174}$$

For (2k+1)-order terms (k = 1, 2, 3, . . . ,), we get

$$\underset{(s_1, \ldots, s_{2k+1})}{\text{Sym}} \left\{ GW_{2k}(s_1, \ldots, s_{2k})\, F_1(s_{2k+1}) + (R_a + sL_a) \right] I_{2k+1}(s_1, \ldots, s_{2k+1}) \Big\}_{s = s_1 + \ldots + s_{2k+1}} = 0. \tag{175}$$

By inspection for (2k)-order terms (k = 1, 2, 3, . . . ,), Eqs. 163 and 165 give us

$$\underset{(s_1, \ldots, s_{2k})}{\text{Sym}} \left\{ (A + sJ) \right] W_{2k}(s_1, \ldots, s_{2k}) \Big\}_{s = s_1 + \ldots + s_{2k}} = \underset{(s_1, \ldots, s_{2k})}{\text{Sym}} \left\{ GI_{2k-1}(s_1, \ldots, s_{2k-1})\, F_1(s_{2k}) \right\} . \tag{176}$$

For solutions to Eqs. 173 – 176 we shall choose

$$F_1(s_1) = \frac{1}{R_f + s_1 L_f} \tag{177}$$

$$I_1(s_1) = \frac{1}{R_a + s_1 L_a} \tag{178}$$

$$I_{2k+1}(s_1, \ldots, s_{2k+1}) = \frac{-G\, W_{2k}(s_1, \ldots, s_{2k})}{(R_f + s_{2k+1} L_f)(R_a + [s_1 + \ldots + s_{2k+1}]L_a)};$$

$$k = 1, 2, 3, \ldots \tag{179}$$

$$W_{2k}(s_1, \ldots, s_{2k}) = \frac{G\, I_{2k-1}(s_1, \ldots, s_{2k-1})}{(R_f + s_{2k} L_f)(A + [s_1 + \ldots s_{2k}]J)};$$

$$k = 1, 2, 3, \ldots \quad . \tag{180}$$

Syntheses of these solutions are shown in Figs. 27, 28, and 29. Taken together, these syntheses imply the feedback synthesis shown in Fig. 30. This feedback synthesis is directly verified by Eqs. 161 – 163, and 165. Thus Eqs. 177 – 180 are also verified.

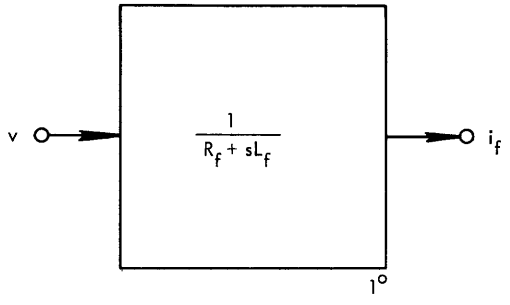

Fig. 27. Synthesis of i_f.

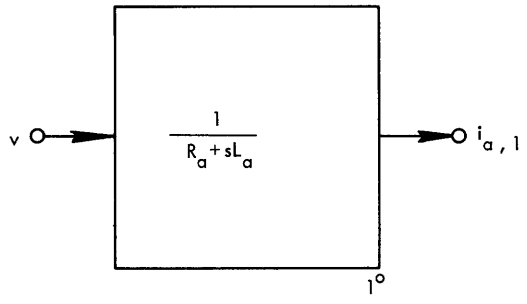

Fig. 28. Synthesis of $i_{a,1}$.

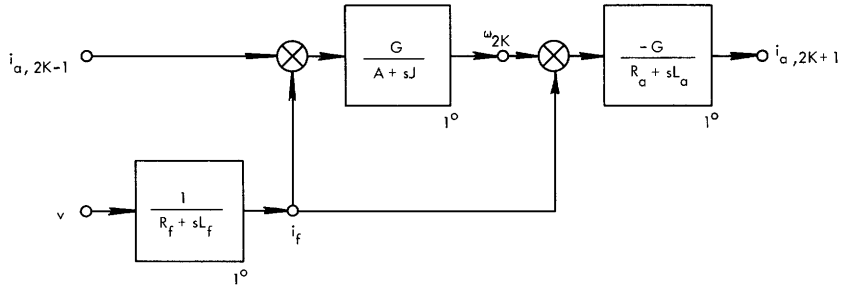

Fig. 29. Synthesis of ω_{2k} and $i_{a,2k+1}$.

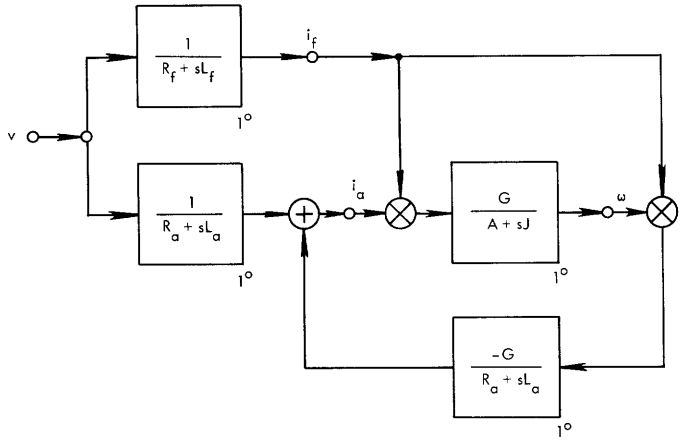

Fig. 30. Feedback synthesis i_f, i_a, and ω.

Equations 179 and 180 make up a two-step recursive formula for I_{2k+1} and W_{2k} (cf. Eq. 108). They result in the following closed forms:

$$I_{2k+1}(s_1, \ldots, s_{2k+1}) = \frac{(-)^k G^{2k}}{(R_a + s_1 L_a)} \prod_{m=1}^{k} \frac{1}{(R_f+s_{2m}L_f)(R_f+s_{2m+1}L_f)(A+[s_1+\ldots+s_{2m}]J)(R_a+[s_1+\ldots+s_{2m+1}]L_a)};$$

$$k = 1, 2, 3, \ldots \tag{181}$$

$$W_2(s_1,s_2) = \frac{G}{(R_a + s_1 L_a)(R_f + s_2 L_f)(A + [s_1 + s_2] J)} \tag{182}$$

$$W_{2k}(s_1, \ldots, s_{2k}) = \frac{-(-)^k G^{2k-1}}{(R_a + s_1 L_a)(R_f + s_{2k} L_f)(A + [s_1 + \ldots + s_{2k}] J)} \prod_{n=1}^{k-1} \frac{1}{(R_f+s_{2n}L_f)(R_f+s_{2n+1}L_f)(A+[s_1+\ldots+s_{2n}]J)(R_a+[s_1+\ldots+s_{2n+1}]L_a)};$$

$$k = 2, 3, 4, \ldots \quad . \tag{183}$$

5.2 TWO CASES OF INPUTS

For a quick check on our results, let us consider the trivial case for which $v(t) = V_0$, a constant. Equations 170 – 172 then give us

$$i_f(t) = F[V_0] = V_0 F_1(0) \tag{184}$$

$$i_a(t) = I[V_0] = \sum_{n=0}^{\infty} V_0^{2n+1} I_{2n+1}(0, \ldots, 0) \tag{185}$$

$$\omega(t) = W[V_0] = \sum_{m=1}^{\infty} V_0^{2m} W_{2m}(0, \ldots, 0). \tag{186}$$

Equations 177, 178, and 181 – 183 give us

$$F_1(0) = \frac{1}{R_f} \tag{187}$$

$$I_{2k+1}(0, \ldots, 0) = \frac{1}{R_a}\left(\frac{-G^2}{A R_a R_f^2}\right)^k ; \quad k = 0, 1, 2, \ldots \tag{188}$$

$$W_{2k}(0, \ldots, 0) = \frac{-R_f}{G}\left(\frac{-G^2}{A R_a R_f^2}\right)^k ; \quad k = 1, 2, 3, \ldots \quad . \tag{189}$$

If $|V_0| < (R_f/G)\sqrt{A R_a}$, then the substitution of Eqs. 187 – 189 in Eqs. 184 – 186 gives

$$i_f(t) = \frac{V_0}{R_f} \tag{190}$$

$$i_a(t) = \frac{\frac{V_0}{R_a}}{1 + \frac{G^2 V_0^2}{A R_a R_f^2}} \tag{191}$$

$$\omega(t) = \frac{\dfrac{G\,V_0^2}{A\,R_a R_f}}{1 + \dfrac{G^2 V_0^2}{A\,R_a R_f^2}} \quad . \tag{192}$$

The substitution of Eqs. 190 – 192 in Eqs. 161 – 163 will show that they are indeed the correct DC solutions for the shunt-wound motor.

Let us next consider the nontrivial case in which v is g, stationary white Gaussian noise of power density P. The statistical expectation (ensemble average) of the product of an odd number of g's is zero.[20,30]

$$E\left[\prod_{k=1}^{2n+1} g\,(t - \tau_k)\right] = 0. \tag{193}$$

The statistical expectation of an even number of g's is the sum of the products of their expectations taken in pairs.[20,30]

$$E\left[\prod_{k=1}^{2m} g(t - \tau_k)\right] = \sum_{\text{pairs}} \prod_{i,j,} E\left[g(t - \tau_i)\, g(t - \tau_j)\right]. \tag{194}$$

For example,[20]

$$E[g(t - \tau_1)\, g(t - \tau_2)] = P u_0(\tau_1 - \tau_2) \tag{195}$$

$$E[g(t - \tau_1)\, g(t - \tau_2)\, g(t - \tau_3)\, g(t - \tau_4)] = P^2 \left[u_0(\tau_1 - \tau_2)u_0(\tau_3 - \tau_4) + u_0(\tau_1 - \tau_3)u_0(\tau_2 - \tau_4) + u_0(\tau_1 - \tau_4)u_0(\tau_2 - \tau_3)\right]. \tag{196}$$

Since F and I are odd, then the substitution of Eq. 193 in the expectations of the expressions given by Eqs. 170 – 171 shows that when v = g the statistical expectations of i_f and i_a are zero. That is,

$$\begin{aligned} E\left[i_f(t)\right] &= E\left[F[g]\right] \\ &= E\left[F_1[g]\right] \\ &= 0 \end{aligned} \tag{197}$$

$$E\left[i_a(t)\right] = E\left[I[g]\right]$$

$$= \sum_{n=0}^{\infty} E\left[I_{2n+1}[g]\right]$$

$$= 0. \tag{198}$$

But W is an even functional of v, hence its statistical expectation need not vanish. It is

$$E\left[\omega(t)\right] = E\left[W[g]\right]$$

$$= \sum_{m=1}^{\infty} E\left[W_{2m}[g]\right] . \tag{199}$$

For example, the first two terms in (199) are

$$E\left[\omega_2(t)\right] = E\left[W_2[g]\right]$$

$$= \int_{-\infty}^{\infty}\int w_2(\tau_1, \tau_2)\, Pu_0(\tau_1 - \tau_2)\, d\tau_1\, d\tau_2$$

$$= P \int_{-\infty}^{\infty} w_2(\tau_1, \tau_1)\, d\tau_1 \tag{200}$$

$$E\left[\omega_4(t)\right] = E\left[W_4[g]\right]$$

$$= \int_{-\infty}^{\infty}\int\int\int w_4(\tau_1, \tau_2, t_3, \tau_4)\, P^2 \left[u_0(\tau_1 - \tau_2)\, u_0(\tau_3 - \tau_4)\right.$$

$$\left. + u_0(\tau_1 - \tau_3)\, u_0(\tau_2 - \tau_4) + u_0(\tau_1 - \tau_4)\, u_0(\tau_2 - \tau_3)\right]$$

$$d\tau_1\, d\tau_2\, d\tau_3\, d\tau_4 \tag{201}$$

$$= P^2 \int_{-\infty}^{\infty}\int \Big[w_4(\tau_1, \tau_1, \tau_2, \tau_2) + w_4(\tau_1, \tau_2, \tau_1, \tau_2) + w_4(\tau_1, \tau_2, \tau_2, \tau_1) \Big] d\tau_1, d\tau_2.$$

(201 Cont.)

These terms can be evaluated, in a few steps, with the aid of George's association theorem.[19,20] Consider the particular input $\tilde{v}$

$$\tilde{v}(t) = \sqrt{P}\, u_0(t) \tag{202}$$

which yields the particular output $\tilde{\omega}$. Then

$$\tilde{\omega}_2(t) = W_2[\tilde{v}]$$

$$= \int_{-\infty}^{\infty}\int w_2(\tau_1, \tau_2)\, P u_0(t - \tau_1)\, u_0(t - \tau_2)\, d\tau_1\, d\tau_2$$

$$= P w_2(t, t). \tag{203}$$

Equations 200 and 203 show that the expectation of ω_2 is equal to the bilateral Laplace transform of $\tilde{\omega}_2$ at s = 0. That is,

$$\tilde{\Omega}_2(0) = \left[\int_{-\infty}^{\infty} \tilde{\omega}_2(t) \exp(-st)\, dt \right]_{s=0}$$

$$= P \int_{-\infty}^{\infty} w_2(t,t)\, dt$$

$$= E\left[\omega_2(t)\right]. \tag{204}$$

The value of $\tilde{\Omega}_2(s)$ is easily found by considering the multilinear correspondent of $\tilde{\omega}_2$ (Eq. 56). It is[18]

$$\tilde{\omega}_{(2)}(t_1, t_2) = \int_{-\infty}^{\infty}\int w_2(\tau_1, \tau_2)\, Pu_0\,(t_1 - \tau_1)\, u_0\,(t_2 - \tau_2)\, d\tau_1\, d\tau_2$$

$$= P\, w_2(t_1, t_2) \tag{205}$$

whose bilateral Laplace transform, by Eq. 182, is

$$\tilde{\Omega}_{(2)}(s_1, s_2) = P\, W_2(s_1, s_2)$$

$$= \frac{PG}{L_a L_f J \left(s_1 + \frac{R_a}{L_a}\right)\left(s_2 + \frac{R_f}{L_f}\right)\left(s_1 + s_2 + \frac{A}{J}\right)} . \tag{206}$$

The application of George's association theorem to (206) shows[19] by inspection that

$$\tilde{\Omega}_2(s) = \frac{PG}{L_a L_f J \left(s + \frac{R_a}{L_a} + \frac{R_f}{L_f}\right)\left(s + \frac{A}{J}\right)} . \tag{207}$$

When (207) is evaluated at s = 0 and that value is substituted in (204), then the result is

$$E\left[\omega_2(t)\right] = \frac{PG}{A(L_f R_a + L_a R_f)} . \tag{208}$$

The higher order terms in (199) are found similarly. Thus we can find the average rotation speed of a shunt-wound motor when it is excited by stationary white Gaussian noise.

The two cases of input signals just considered serve to illustrate some of the areas of usefulness for the Volterra series characterization of nonlinear systems. Namely, in addition to the straightforwardness of the computation of the output of an analytic system for a constant-input signal or a sinusoidal-input signal (e. g., the pendulum output, Section IV), the statistical moments of the system's output for stochastic inputs can also be calculated – even in those cases in which there are no known methods for executing such computations from the system's characterizing differential equation.

This is not to say that the Volterra series does not have disadvantages. One of its most serious disadvantages is that in being an infinite series, we have to decide how many terms we must compute in order to get an adequate approximation for its value. This question need not be without answer. For example, in the case of the shunt-wound motor, the author has shown elsewhere[27] that if the input voltage is everywhere bounded, then the truncation error introduced by approximating ω by its first N nonzero terms is also everywhere bounded. That is, if

$$|v(t)| \leq V < V_B = \frac{R_f \sqrt{A R_a}}{G} \; ; \text{ for all } t, \tag{209}$$

then

$$\left| \omega(t) - \sum_{m=1}^{N} W_{2m}[v] \right| < \frac{R_f}{G} \cdot \frac{\left(\frac{V}{V_B}\right)^{2N+2}}{1 - \left(\frac{V}{V_B}\right)^2} \; ; \text{ all } t. \tag{210}$$

5.3 SERIES MOTOR

When wired as a series-wound commutator machine (see Fig. 26 and Eqs. 161 – 163), then the single-axis commutator machine's characteristic differential equations are

$$\left(R + L \frac{d}{dt}\right) i + G \omega i = v \tag{211}$$

$$\left(A + J \frac{d}{dt}\right) \omega = G i^2, \tag{212}$$

where

$$v = v_f + v_a \tag{213}$$

$$i = i_f + i_a \tag{214}$$

$$R = R_f + R_a \tag{215}$$

$$L = L_f + L_a. \tag{216}$$

Equations 211 and 212 show that i is an odd functional and ω is an even functional of v. The boundary condition (164) shows that the zero-order term of ω is zero. Thus

$$i(t) = H[v] = \sum_{n=0}^{\infty} H_{2n+1}[v] \tag{217}$$

$$\omega(t) = Q[v] = \sum_{m=1}^{\infty} Q_{2m}[v]. \tag{218}$$

The first-order terms of (211) are

$$(R + s_1 L)H_1(s_1) + 0 = 1. \tag{219}$$

The (2k)-order terms of (212) are

$$\underset{(s_1, \ldots, s_{2k})}{\text{Sym}} \left\{ (A + s J) \Big] Q_{2k}(s_1, \ldots, s_{2k}) \Big|_{s = s_1 + \ldots + s_{2k}} \right\}$$

$$= \underset{(s_1, \ldots, s_{2k})}{\text{Sym}} \left\{ G \sum_{n=0}^{k-1} H_{2n+1}(s_1, \ldots, s_{2n+1}) H_{2(k-n)-1}(s_{2n+2}, \ldots, s_{2k}) \right\};$$

$$k = 1, 2, 3, \ldots \quad . \tag{220}$$

The (2k+1)-order terms of (211) are

$$\underset{(s_1, \ldots, s_{2k+1})}{\text{Sym}} \left\{ (R + sL) \Big] H_{2k+1}(s_1, \ldots, s_{2k+1}) \Big|_{s = s_1 + \ldots + s_{2k+1}} \right.$$

$$\left. + G \sum_{m=1}^{k} Q_{2m}(s_1, \ldots, s_{2m}) H_{2(k-m)+1}(s_{2m+1}, \ldots, s_{2k+1}) \right\} = 0;$$

$$k = 1, 2, 3, \ldots \quad . \tag{221}$$

Equation 219 gives us

$$H_1(s_1) = \frac{1}{R + s_1 L}. \tag{222}$$

Equations 220 and 221 give us two-step recursive formulas for all of the Q's and all of the remaining H's. We shall choose the solutions

$$Q_{2k}(s_1, \ldots, s_{2k}) = \frac{G \sum_{n=0}^{k-1} H_{2n+1}(s_1, \ldots, s_{2n+1}) H_{2(k-n)-1}(s_{2n+2}, \ldots, s_{2k})}{A + [s_1 + \ldots + s_{2k}]J};$$

$$k = 1, 2, 3, \ldots \tag{223}$$

and

$$H_{2k+1}(s_1, \ldots, s_{2k+1})$$

$$= \frac{-G \sum_{m=1}^{k} Q_{2m}(s_1, \ldots, s_{2m})\, H_{2(k-m)+1}(s_{2m+1}, \ldots, s_{2k+1})}{R + [s_1 + \ldots + s_{2k+1}]L};$$

$$k = 1, 2, 3, \ldots \quad . \tag{224}$$

VI. THE VARACTOR

When a semiconductor diode is operated backbiased, then it behaves like a nonlinear capacitor and displays variable reactance – hence the name varactor. We shall present an application of the inspection technique, developed in Section III, to a varactor circuit.

6.1 MODEL OF A VARACTOR

The abrupt junction semiconductor diode, shown in Fig. 31, stores a charge +q in the N-type region of its depletion layer, and a charge -q in the P-type region of its depletion layer. The voltage across the depletion layer is kq^2, where k is a positive constant.[29] The diode has a bulk resistance R, and a Fermi contact potential ϕ (because of the two leads attached to it). We shall assume that both R and ϕ are positive constants. The diode's voltage v_D can then be modeled by the usual equation for an abrupt junction varactor.

$$v_D = R\frac{dq}{dt} + kq^2 - \phi. \tag{225}$$

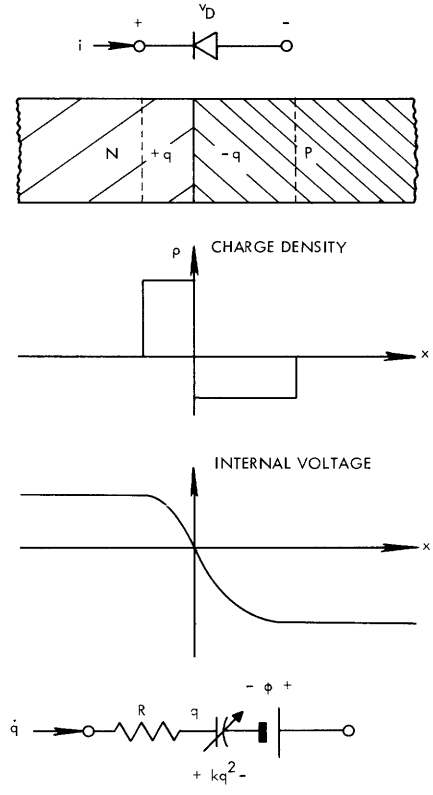

Fig. 31. Abrupt-junction semiconductor diode.

Equation 225 is a model, rather than a characterization, because it fails to match all of the varactor's nuances. Some of its defects are: (i) negative values of q are physically unobtainable; (ii) when v_D is a positive constant, then Eq. 225 predicts that $i = (dq/dt) = 0$. (In reality, there is a small, but nonzero, leakage current.) (iii) In an actual diode, the bulk resistance R changes slightly with the width of the depletion layer (which depends upon q). Nonetheless, we shall use (225) as our characteristic differential equation for an abrupt junction varactor but we must bear in mind that our analysis will be subject to its defects.

6.2 ONE VARACTOR IMBEDDED IN A LINEAR NETWORK

Consider a system composed of one abrupt-junction varactor imbedded in a linear network. If we form the Thévenin equivalent of the linear network, then Fig. 32 shows a circuit model for that system. Here Z is the Thévenin equivalent output impedance of the linear network, as seen by the varactor. We have divided the Thévenin equivalent open-circuit voltage into two parts: E_0. the varactor's bias voltage (a constant), and e, a variable. By inspection of Fig. 32 and Eq. 225, the circuits characteristic equations are

$$E_0 + e - R\frac{dq}{dt} - kq^2 + \phi - v = 0 \tag{226}$$

and

$$V(s) = Z(s)sQ(s). \tag{227}$$

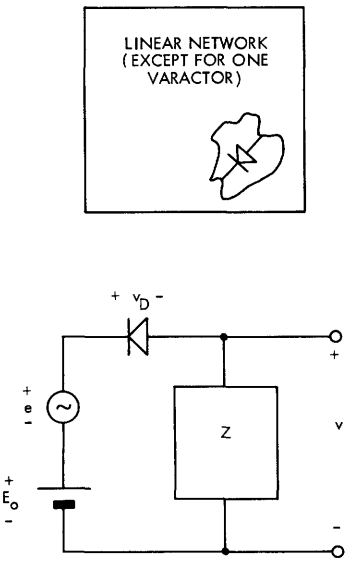

Fig. 32. Thévenin equivalent of one varactor imbedded in a linear network.

We shall assume that Z has no series capacitor.* That is,

$$\lim_{s \to 0} \left[sZ(s) \right] = 0. \tag{228}$$

Then there are two DC solutions to (226). They are

$$q_0 = \pm \sqrt{\frac{E_0 + \phi}{k}}. \tag{229}$$

Depending on which of these two values we choose as the zero-order term of a functional solution for q, we get two different functional power series (cf. Eq. 106). We might eliminate the negative value on physical grounds (the charge stored in the N-type region of the depletion layer must be positive), but there is a more interesting reason for not choosing the negative value – it is unstable. To show this, consider Eq. 226 when both e and v are zero. We may then rewrite it

$$\frac{dq}{dt} = \frac{E_0 + \phi}{R} - \frac{k}{R} q^2$$

$$= \frac{k}{R} (q_0^2 - q^2). \tag{230}$$

The phase-plane graph of (230) is shown in Fig. 33. It shows that the positive DC solution is stable but that the negative DC solution is not. The significant fact is that had we chosen the negative value as the zero-order term of a functional for q, then the Volterra series that we get by our inspection technique has natural frequencies in the right half-plane. This example serves to remind us that, given a differential equation, we cannot rashly assume that it characterizes an analytic system.

Having extablished which DC solution is tenable, we see that the boundary condition of initial rest for this varactor system is

$$v(t) = 0, q(t) = \sqrt{\frac{E_0 + \phi}{k}} \text{ until } e(t) \neq 0. \tag{231}$$

*In a practical circuit, this is true. If there were a series capacitor, then it would keep the bias E_0 from the varactor.

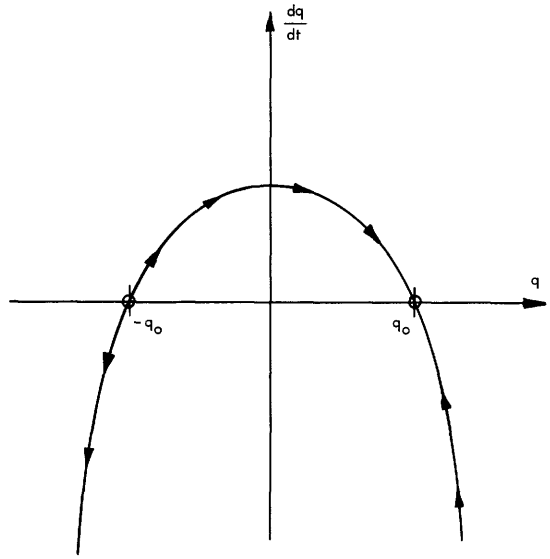

Fig. 33. Phase-plane graph of Eq. 230.

It can be shown that, for a class of inputs about zero, Eqs. 226, 227, and 231 characterize an analytic system. Hence

$$q(t) = G[e] \tag{232}$$

$$v(t) = H[e]. \tag{233}$$

From the boundary condition, (231), the zero-order terms of G and H are

$$G_0 = \sqrt{\frac{E_0 + \phi}{k}} \tag{234}$$

$$H_0 = 0. \tag{235}$$

The first-order terms of (226) are

$$1 - s_1 R G_1(s_1) - 2k\, G_0\, G_1(s_1) - H_1(s_1) = 0. \tag{236}$$

The n-order terms of (226) are

$$\underset{(s_1,\ldots,s_n)}{\text{Sym}} \left\{ -[s_1+\ldots+s_n]\, RG_n(s_1,\ldots,s_n) \right.$$

$$- k\left[\sum_{m=0}^{n} G_m(s_1,\ldots,s_m) \cdot G_{n-m}(s_{m+1},\ldots,s_n) \right]$$

$$\left. - H_n(s_1,\ldots,s_n) \right\} = 0;\ n = 2, 3, 4, \ldots . \tag{237}$$

The m-order terms of (227) are

$$\underset{(s_1,\ldots,s_m)}{\text{Sym}} \left\{ H_m(s_1,\ldots,s_m) \right\}$$

$$= \underset{(s_1,\ldots,s_m)}{\text{Sym}} \left\{ [s_1+\ldots+s_m]\, Z(s_1+\ldots+s_m)\, G_m(s_1,\ldots,s_m) \right\} ;$$

$$m = 1, 2, 3, \ldots . \tag{238}$$

For solution to Eq. 238 we shall choose

$$H_m(s_1,\ldots,s_m) = sZ(s) \Big] G_m(s_1,\ldots,s_m) ;\ m = 1, 2, 3, \ldots .$$

$$s = s_1+\ldots+s_m \tag{239}$$

When (239) is evaluated for $m = 1$ and the resultant value for $H_1(s_1)$ is substituted in Eq. 236, then the result is

$$G_1(s_1) = \frac{1}{2kG_0 + s_1\left[R + Z(s_1)\right]} . \tag{240}$$

When the value for H_m given by (239) is substituted in (237) and the highest order term of G is isolated, then it is seen that we may choose the solution

$$G_n(s_1, \ldots, s_n) = \frac{-k \sum_{m=1}^{n-1} G_m(s_1, \ldots, s_m)\, G_{n-m}(s_{m+1}, \ldots, s_n)}{2kG_0 + s\left[R + Z(s)\right]\Big]_{s = s_1 + \ldots + s_n}} ;$$

$$n = 2, 3, 4, \ldots . \qquad (241)$$

Parallel syntheses of G and H are shown in Figs. 34 and 35. Together they imply the feedback synthesis of both G and H shown in Fig. 36. Figure 36 can be directly verified by Eqs. 226, 227, and 231 which therefore verifies Eqs. 234, 235, and 239 - 241.

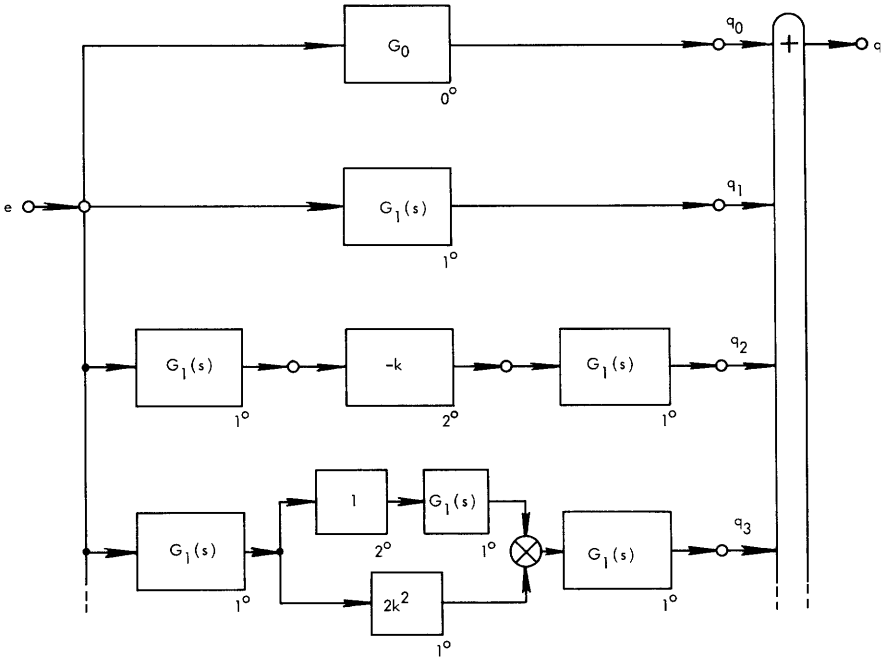

Fig. 34. Parallel synthesis of G.

6.3 TRANSIENT RESPONSE OF A VARACTOR FREQUENCY DOUBLER

As an example of the application of our solution, we shall compute a frequency doubler circuit's transient response. For simplicity, we shall let Z be an inductor,

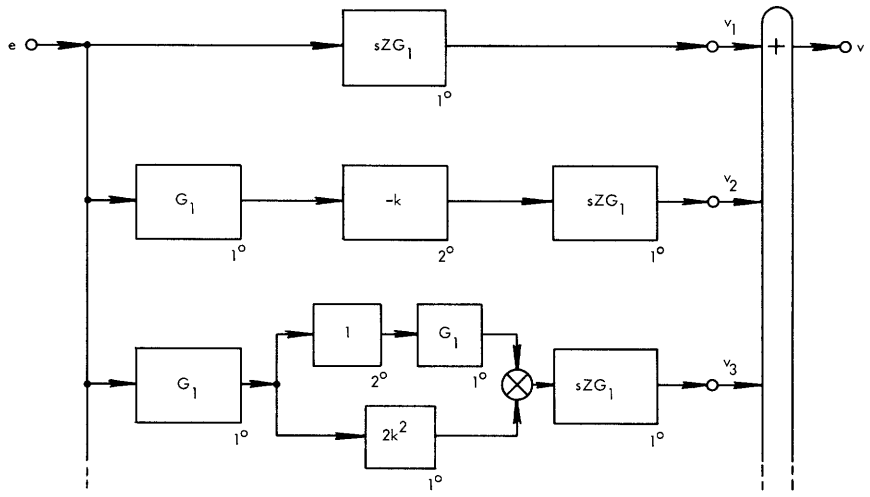

Fig. 35. Parallel synthesis of H.

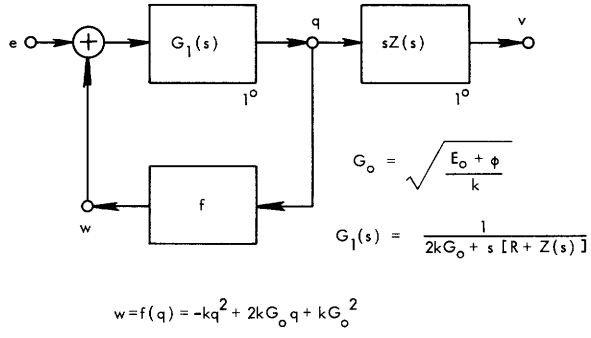

Fig. 36. Feedback synthesis of G and H.

that is,

$$Z(s) = sL, \tag{242}$$

and we shall restrict our attention to the second-order term in the output voltage.* The multilinear correspondent to the second-order term[18] is

*There is no zero-order term (see Eq. 235). There is no doubler effect from the first-order term (cf Eq. 147). If we consider small-amplitude input signals and choose our frequencies judiciously, then the doubler effect from terms higher than the second-order term can be made small as compared with it.

$$v_{(2)}(t_1, t_2) = \int_{-\infty}^{\infty}\int h_2(\tau_1, \tau_2)\, e\,(t_1 - \tau_1)\, e\,(t_2 - \tau_2)\, d\tau_1 d\tau_2. \tag{243}$$

Its multivariate bilateral Laplace transform is

$$v_{(2)}(s_1, s_2) = H_2(s_1, s_2)\, E(s_1)\, E(s_2). \tag{244}$$

The value of H_2 is found from Eqs. 234 and 239 - 242. They give us

$$H_2(s_1, s_2) = \frac{-k(s_1+s_2)\, Z(s_1+s_2)}{\left(2kG_0+s_1[R+Z(s_1)]\right)\left(2kG_0+s_2[R+Z(s_2)]\right)\left(2kG_0+[s_1+s_2]\cdot[R+Z(s_1+s_2)]\right)}$$

$$= \frac{-(s_1+s_2)^2 kL}{\left([s_1+s_2]^2 L+[s_1+s_2]R+2kG_0\right)\left(s_1^2 L+s_1 R+2kG_0\right)\left(s_2^2 L+s_2 R+2kG_0\right)}$$

$$= \frac{+F(s_1+s_2)}{(s_1-s_0)\left(s_1-s_0^*\right)(s_2-s_0)\left(s_2-s_0^*\right)}, \tag{245}$$

where

$$F(s) = \frac{-\,k\,s^2}{L^2\,(s - s_0)\,(s - s_0^*)}, \tag{246}$$

and (cf . Eqs. 136 - 139)

$$s_0 = -\alpha + j\omega_D. \tag{247}$$

$$\alpha = \frac{R}{2L} \tag{248}$$

$$\omega_D = \sqrt{\omega_0^2 - \alpha^2} \tag{249}$$

$$\omega_0 = \sqrt{\frac{2kG_0}{L}}$$

$$= \sqrt{\frac{2}{L}} \left[k(E_0 + \phi) \right]^{\frac{1}{4}}. \tag{250}$$

In preparation for application of George's association technique, we shall rewrite (245) in a partial fraction form. That is,

$$H_2(s_1, s_2) = F(s_1 + s_2) \left[\frac{A}{s_1 - s_0} + \frac{A^*}{s_1 - s_0^*} \right] \left[\frac{A}{s_2 - s_0} + \frac{A^*}{s_2 - s_0^*} \right], \tag{251}$$

where

$$A = \frac{1}{s_0 - s_0^*} = \frac{-j}{2\omega_D}. \tag{252}$$

We shall let the input-voltage signal e be a step of sinusoid. That is,

$$e(t) = \mathrm{Re} \left[E_i \exp(s_i t) \right] u_{-1}(t). \tag{253}$$

The bilateral Laplace transform of e is therefore

$$E(s) = \frac{B}{s - s_i} + \frac{B^*}{s - s_i^*}, \tag{254}$$

where

$$B = \frac{1}{2} E_i. \tag{255}$$

When Eqs. 251 and 254 are substituted in Eq. 244, we find that the transform of the multilinear correspondent to v_2 is

$$v_{(2)}(s_1, s_2) = F(s_1 + s_2)\left[\frac{A}{s_1 - s_0} + \frac{A^*}{s_1 - s_0^*}\right]\left[\frac{B}{s_1 - s_i} + \frac{B^*}{s_1 - s_i^*}\right]$$

$$\left[\frac{A}{s_2 - s_0} + \frac{A^*}{s_2 - s_0^*}\right]\left[\frac{B}{s_2 - s_i} + \frac{B^*}{s_2 - s_i^*}\right]$$

$$= F(s_1 + s_2)\left[\frac{C}{s_1 - s_0} + \frac{C^*}{s_1 - s_0^*} + \frac{D}{s_1 - s_i} + \frac{D^*}{s_1 - s_i^*}\right]$$

$$\left[\frac{C}{s_2 - s_0} + \frac{C^*}{s_2 - s_0^*} + \frac{D}{s_2 - s_i} + \frac{D^*}{s_2 - s_i^*}\right] \quad (256)$$

where

$$C = A\left[\frac{B}{s_0 - s_i} + \frac{B^*}{s_0 - s_i^*}\right] \quad (257)$$

and

$$D = B\left[\frac{A}{s_i - s_0} + \frac{A^*}{s_i - s_o^*}\right] \quad (258)$$

By using George's frequency association technique, the transform of v_2 is found from Eq. 256 by inspection[19] to be

$$V_2(s) = F(s)\left[\frac{C^2}{s - 2s_0} + \frac{(C^*)^2}{s - 2s_0^*} + \frac{D^2}{s - 2s_i} + \frac{(D^*)^2}{s - 2s_i^*} + \frac{2CC^*}{s - s_0 - s_0^*}\right.$$

$$+ \frac{2DD^*}{s - s_i - s_i^*} + \frac{2CD}{s - s_0 - s_i} + \frac{2C^*D^*}{s - s_0^* - s_i^*} + \frac{2CD^*}{s - s_0 - s_i^*}$$

$$\left. + \frac{2C^*D}{s - s_0^* - s_i}\right] \quad (259)$$

Before evaluating $v_2(t)$ from (259), let us take a moment out to study v_2 in the vicinity of t = 0. Observe from (246) that

$$\lim_{s\to\infty}\left[F(s)\right] = -\frac{k}{L^2} . \tag{260}$$

Therefore, from (259) we find

$$\lim_{s\to\infty}\left[V_2(s)\right] = 0. \tag{261}$$

That is, $v_2(t)$ has no singularities at t = 0. We also find that

$$v_2(0^+) = \lim_{s\to\infty}\left[sV_2(s)\right]$$

$$= -\frac{k}{L^2}\left[C^2 + (C^*)^2 + D^2 + (D^*)^2 + 2CC^* + 2DD^* + 2CD + 2C^*D^* + 2CD^* + 2C^*D\right]$$

$$= -\frac{k}{L^2}\,(C + C^* + D + D^*)^2 = -\frac{4k}{L^2}\left(\mathrm{Re}[C + D]\right)^2. \tag{262}$$

From (257) and (258) we find

$$C + D = \frac{AB}{s_0 - s_i} + \frac{AB}{s_i - s_0} + \frac{AB^*}{s_0 - s_i} + \frac{A^*B}{s_i - s_0}$$

$$= 2j\,\mathrm{Im}\left[\frac{AB^*}{s_0 - s_i}\right] . \tag{263}$$

Therefore

$$\mathrm{Re}[C + D] = 0 \tag{264}$$

and by Eq. 262 we have

$$v_2(0^+) = 0. \tag{265}$$

That is, $V_2(t)$ is continuous at $t = 0$. Similarly, it can be shown that the derivative of v_2 at $t = 0$ is zero. Thus we see that the transient response is a smooth build-up to the steady state.

The steady-state terms in Eq. 259 are due to the poles at $s = 2s_i$ and $s = 2s_i^*$. This shows that the circuit does actually double input frequencies. The residue of V_2 at $s = 2s_i$, by Eq. 259, is

$$\text{Res}\,(2s_i) = \lim_{s \to 2s_i} \left[(s - 2s_i)\ V_2(s)\right]$$

$$= F(2s_i)D^2$$

$$= \frac{-4ks_i^2B^2}{L^2(2s_i - s_0)(2s_i - s_0^*)} \left[\frac{A}{s_i - s_0} + \frac{A^*}{s_i - s_0^*}\right]^2 \qquad (266)$$

Here we have used Eqs. 246 and 258 to evaluate F and D.

Equations 266 show that if we wish to maximize the amplitude of the doubler's steady-state output, then we should choose s_i in the vicinity of s_0. This may be somewhat of a surprise. The natural frequency of the linear incremental model of the doubler's circuit is s_0. By "physical insight", we might have guessed a priori that the doubler's output would have been maximized when the input's frequency was at half the resonant frequency of the linear incremental model. Our reasoning would be: "If s_i is near $1/2\ s_0$, then when s_i is doubled it resonates the incremental circuit and, therefore, gives the largest possible output." Equation 266 shows that such reasoning is false. The residue of the doubled term does have a relative maximum near $s_i = (j\omega_D/2)$ (when $2s_i - s_0 = a$) but its absolute maximum is near $s_i = j\omega_D$. A posteriori, we can explain this result physically: When the input frequency is near the linear incremental circuit's resonant frequency, then the voltage source's input current is maximized. When the maximum current is "doubled", it produces the maximum double-frequency output. Thus we choose

$$s_i = j\omega_D. \qquad (267)$$

The distinct frequencies present in Eq. 259 are then*

*Frequencies $s_{0,3}$ and $s_{0,3}^*$ came from F(s) in Eq. 259. Equation 259 looks as if there is also a frequency at $s = s_i + s_i^* = 0$ but Eq. 246 shows that it has a residue of zero.

$$s_{0,1} = s_0 + s_i^*$$

$$= -\alpha \tag{268}$$

$$s_{0,2} = s_0 + s_0^*$$

$$= -2\alpha \tag{269}$$

$$s_{0,3} = s_0$$

$$= -\alpha + j\omega_D \qquad (\text{and } s_{0,3}^*) \tag{270}$$

$$s_{0,4} = 2s_0$$

$$= -2\alpha + 2j\omega_D \qquad (\text{and } s_{0,4}^*) \tag{271}$$

$$s_{0,5} = s_0 + s_i$$

$$= -\alpha + 2j\omega_D \qquad (\text{and } s_{0,5}^*) \tag{272}$$

$$s_{0,6} = 2s_i$$

$$= 2j\omega_D \qquad (\text{and } s_{0,6}^*) \tag{273}$$

An s-plane plot of these frequencies is shown in Fig. 37. It shows that $v_2(t)$ consists of two dying exponentials, ($s_{0,1}$ and $s_{0,2}$), one exponentially damped sinusoid at half the frequency of the steady state ($s_{0,3}$), two exponentially damped sinusoids at the same frequency as the steady state ($s_{0,4}$ and $s_{0,5}$), and the steady state ($s_{0,6}$). The value of $v_2(t)$ is found by rewriting (259) as

$$V_2(s) = \frac{\text{Res}(s_{0,1})}{s - s_{0,1}} + \frac{\text{Res}(s_{0,2})}{s - s_{0,2}} + \sum_{n=3}^{6} \left[\frac{\text{Res}(s_{0,n})}{s - s_{0,n}} + \frac{\left[\text{Res}(s_{0,n})\right]^*}{s - s_{0,n}^*} \right] \tag{274}$$

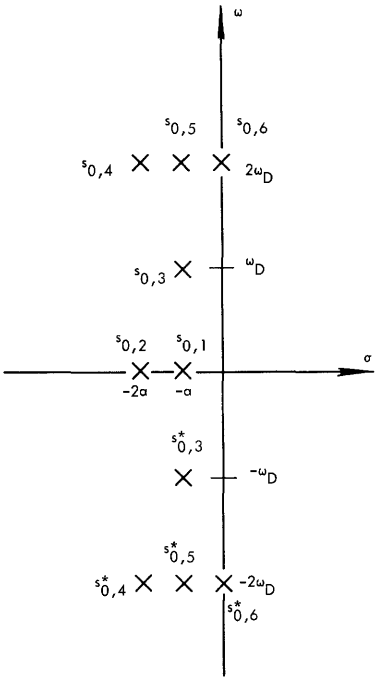

Fig. 37. s-plane plot of the frequencies in v_2.

Then it is seen that

$$v_2(t) = \left\{ \text{Res}\,(s_{0,1}) \ \exp\,(s_{0,1}t) + \text{Res}\,(s_{0,2}) \ \exp\,(s_{0,2}t) \right.$$

$$\left. + 2 \sum_{n=3}^{6} \text{Re}\left[\text{Res}\,(s_{0,n}) \exp\,(_{0,n}t)\right] \right\} u_{-1}(t). \qquad (275)$$

For the sake of illustration, we shall compute the double frequency terms in (275) in the case of small damping. That is,

$$\alpha << \omega_D. \qquad (276)$$

So that Eq. 249 shows that

$$\omega_D \approx \omega_0, \qquad (277)$$

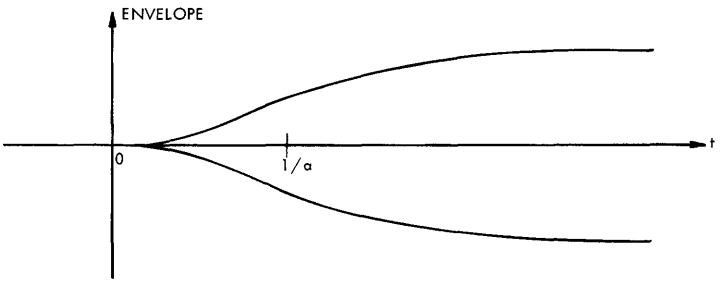

Fig. 38. Envelope on the double frequency components in v_2.

then

$$\text{Res}\,(s_{0,4}) \approx \frac{k E_i^2}{3(\omega_0 R)^2} \tag{278}$$

$$\text{Res}\,(s_{0,5}) \approx \frac{-2 k E_i^2}{3(\omega_0 R)^2} \tag{279}$$

$$\text{Res}\,(s_{0,6}) \approx \frac{k E_i^2}{3(\omega_0 R)^2}. \tag{280}$$

When Eqs. 278 - 280 are substituted in Eq. 275 then the result is that the doubled-frequency terms are

$$v_2(t)_{2\omega_0} \approx \frac{2k}{3(\omega_0 R)^2}\left[1 - 2\exp(-\alpha t) + \exp(-2\alpha t)\right]$$

$$\text{Re}\left[E_i^2 \exp(2j\omega_0 t)\right] u_{-1}(t). \tag{281}$$

Figure 38 is a graph of the envelope on the transient build-up to the steady state of the doubled-frequency terms that we have just computed.

VII. ANALYSIS OF A MAGNETIC SUSPENSION DEVICE

The inertial guidance instruments of some of our nation's space vehicles are magnetically suspended by a device developed at the Instrumentation Laboratory, M. I. T.[9, 12, 21, 23] A single axis version of this magnetic suspension device is shown in Fig. 39. The device's principle of operation is as follows: If the suspended block is moved toward the right, then it detunes the circuit on the right but it tunes the circuit on the left. This causes the current flow on the right to decrease and the current flow on the left to increase. This imbalance in currents produce a net magnetic force to the left which restores the block to center.

We shall now present an application of our inspection technique, developed in Section III, to this single-axis version of the magnetic suspension device. Specifically, we shall use the functional characterization of this magnetic suspension device, obtained by our inspection technique, in order to (i) determine the device's static suspension stability, (ii) determine the device's dynamic suspension stability, and (iii) show that the suspension will have an oscillatory instability whenever the device has insufficient mechanical damping. (The results of an experimental verification of these predicted oscillatory instabilities are given in the appendix.)

In order to use our inspection technique to determine this magnetic suspension device's functional characterization, we shall first derive this device's characterizing differential equations by the well-known state-function, state-variables, Hamilton's principle approach.

7.1 DIFFERENTIAL EQUATIONS CHARACTERIZING THE DEVICE

In a state-function, state-variables, Hamilton's principle derivation of the equations that characterize the device shown in Fig. 39, we must first extract the device's lossless magnetic energy-storage structure, which is shown in Fig. 40. Figure 40 shows that the differential increment dw, in the structure's stored magnetic energy w, owing to differential increments in the variable pairs at the structure's one mechanical and four electrical ports, is

$$dw = - f_r\, dx + \sum_{k=1}^{4} e_k\, i_k\, dt$$

$$= - f_r\, dx + \sum_{k=1}^{4} i_k\, d\lambda_k, \qquad (282)$$

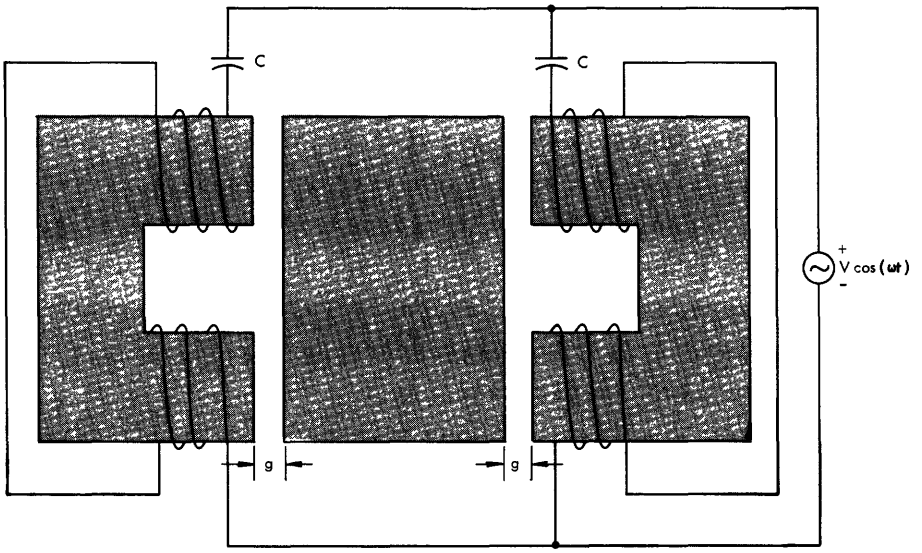

Fig. 39. Single-axis magnetic suspension device.

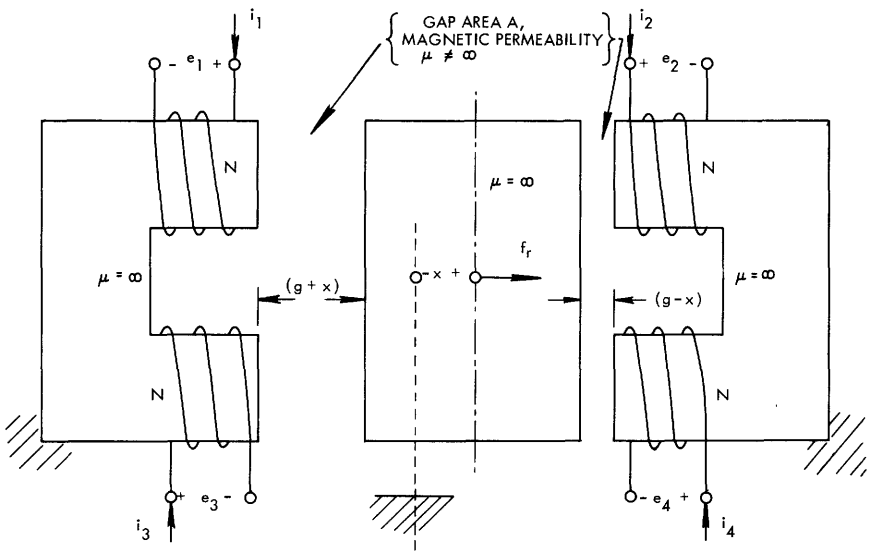

Fig. 40. Suspension device's lossless magnetic energy storage structure.

where f_r is the device's restoring force. The differential form of (282) demonstrates that w is a state function of five state variables (the four flux linkages λ_k and the block displacement x) and that their port pairs are

$$i_k = \frac{\partial}{\partial \lambda_k} w(\lambda_1, \lambda_2, \lambda_3, \lambda_4, x); \quad k = 1, 2, 3, 4 \tag{283}$$

$$- f_r = \frac{\partial}{\partial_x} w(\lambda_1, \lambda_2, \lambda_3, \lambda_4, x). \tag{284}$$

Although the structure's stored energy is a function of four flux linkages, if we neglect leakage, then there are only two independent flux linkages in the entire structure. We shall choose the structure's mean flux linkage.

$$\lambda = \frac{\lambda_1 + \lambda_2 + \lambda_3 + \lambda_4}{4} \tag{285}$$

and its mean-difference flux linkage

$$\delta = \frac{- \lambda_1 + \lambda_2 - \lambda_3 + \lambda_4}{4} \tag{286}$$

to be the two independent flux linkages. The structure's other flux linkages are, then,

$$\lambda_k = (-)^k \delta + \lambda; \quad k = 1, 2, 3, 4. \tag{287}$$

If we neglect fringing in the gaps, then the structure's stored magnetic energy is

$$w = \frac{2 g (\lambda^2 + \delta^2) - 4 x \lambda \delta}{\mu A N^2} \tag{288}$$

When the expression for w, given by (288), is substituted in Eq. 284, then the result is

$$f_r = \frac{4 \lambda \delta}{\mu A N^2}. \tag{289}$$

The partials of Eq. 288 with respect to λ and δ, with the aid of Eqs. 283 and 284, yield two additional equations. They are

$$4\,\frac{g\lambda - x\delta}{\mu A N^2} = \frac{\partial w}{\partial \lambda} = \sum_{k=1}^{4} \frac{\partial w}{\partial \lambda_k} \cdot \frac{\partial \lambda_k}{\partial \lambda} = \sum_{k=1}^{4} i_k \tag{290}$$

$$4\,\frac{g\lambda - x\lambda}{\mu A N^2} = \frac{\partial w}{\partial \delta} = \sum_{k=1}^{4} \frac{\partial w}{\partial \lambda_k} \cdot \frac{\partial \lambda_k}{\partial \delta} = \sum_{k=1}^{4} (-)^k i_k. \tag{291}$$

Figure 41 shows the connections external to the lossless magnetic energy-storage structure, shown in Fig. 40, which completes the formation of the device shown in Fig. 39, except that the capacitors have been generalized to any linear impedance Z. These external connections impose seven independent constraints. They are

$$v_1(t) = z(t)\ (*)\ i_1(t) \tag{292}$$

$$v_2(t) = z(t)\ (*)\ i_2(t) \tag{293}$$

$$i_1 = i_3 \tag{294}$$

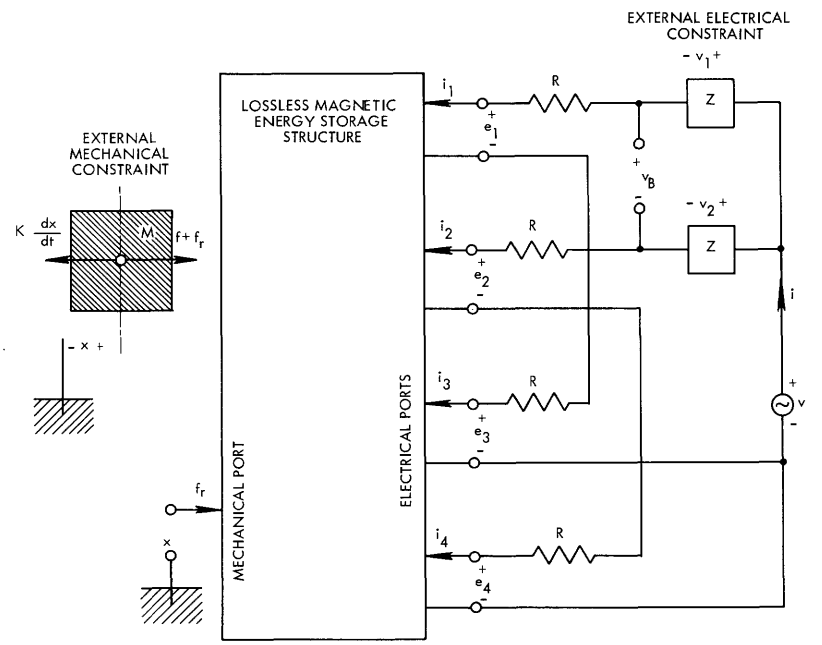

Fig. 41. Diagram for the suspension device.

$$i_2 = i_4 \tag{295}$$

$$v = v_1 + i_1 R + e_1 + i_3 R + e_3 \tag{296}$$

$$v = v_2 + i_2 R + e_2 + i_4 R + e_4 \tag{297}$$

$$f + f_r - K \frac{dx}{dt} = M \frac{d^2 x}{dt^2} . \tag{298}$$

There are seven external constraints (Eqs. 292 - 298), seven internal constraints (Eq. 287 four times, Eqs. 289 - 291), and four definitions ($e_k\, dt = d\lambda_k$ (Eq. 282)) for a total of eighteen equations in twenty-one variables. When we eliminate the 15 internal variables i_k, e_k, λ_k, v_1, v_2, and f_r, then we are left with three equations in the remaining 6 variables t, λ, δ, v, x, and f. Together with the boundary condition of initial rest, these three equations characterize the device. They are

$$\mu A N^2 v = \left[z(t) + 2Ru_0(t) \right] (*) \left[(g + x)\ (\lambda - \delta) \right] + 2\mu A N^2 \frac{d}{dt} (\lambda - \delta) \tag{299}$$

$$\mu A N^2 v = \left[z(t) + 2Ru_0(t) \right] (*) \left[(g - x)\ (\lambda + \delta) \right] + 2\mu A N^2 \frac{d}{dt} (\lambda + \delta) \tag{300}$$

$$f = \frac{d}{dt} \left(M \frac{d}{dt} + K \right) x - \frac{4 \lambda \delta}{\mu A N^2} . \tag{301}$$

7.2 FUNCTIONAL SOLUTIONS OF THE SYSTEM'S CHARACTERISTIC EQUATIONS

These three equations (Eqs. 299 - 301) in six variables, t, λ, δ, v, x, and f, together with the boundary condition of initial rest, characterize a system with two input signals (two functions of t = three variables) and three output signals. As is shown in Fig. 42, we shall choose v and x, rather than v and f, as the input signals to this multi-input system. We do so because the functional characterization that we shall then obtain for the system is simpler and is analytic for the stability demonstrations that we wish to show.

If the signals v, x, λ, and δ are solutions of Eqs. 299 and 300,* then for any constant c, the signals cv, x, $c\lambda$, and $c\delta$, are also solutions. Therefore λ and δ are

*We have assumed the boundary condition of initial rest. Namely f, λ, and δ are zero until either v or x is not zero.

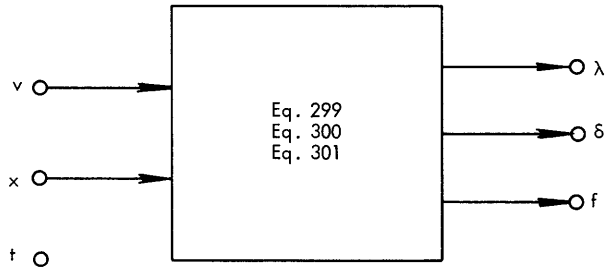

Fig. 42. System of five signals characterized by three equations.

linear functionals of v. If the signals v, x, λ, δ, and f are solutions of Eqs. 299 -301, then the signals v, -x, λ, -δ, and -f are also solutions. Therefore λ is an even functional of x, δ and f are odd functionals of x. Thus, by Eq. 62, we may write

$$\lambda = L[v, x] = \sum_{n=0}^{\infty} L_{1, 2n}[v, x] \tag{302}$$

$$\delta = D[v, x] \sum_{m=0}^{\infty} D_{1, 2m+1}[v, x] \tag{303}$$

$$f = F[v, x] = F_{0, 1}[v, x] + \sum_{p=0}^{\infty} F_{2, 2p+1}[v, x]. \tag{304}$$

The (1, 0)-order terms of either Eq. 299 or Eq. 300 are

$$\mu AN^2 \cdot 1 = \left[gZ(s_1) + 2Rg \cdot 1 + 2 \mu AN^2 s_1 \right] L_{1, 0}(s_1). \tag{305}$$

The (1, 2n)-order terms ($n \neq 0$) of either Eq. 299 or Eq. 300 are (see Eq. 127)

$$0 = \underset{(s_1)\,(s_2,\ldots,s_{2n+1})}{\text{Sym}} \Big\{ \Big[gZ(s_1+\ldots+s_{2n+1}) + 2Rg + 2\mu AN^2(s_1+\ldots+s_{2n+1}) \Big]$$

$$L_{1,\,2n}(s_1,\ldots,s_{2n+1}) - \Big[Z(s_1+\ldots+s_{2n+1}) + 2R \Big]$$

$$D_{1,\,2n-1}(s_1,\ldots,s_{2n}) \Big\} \; ; \; n = 1, 2, 3, \ldots \; . \tag{306}$$

The (1, 2m+1)-order terms of either Eq. 299 or Eq. 300 are

$$0 = \underset{(s_1)\,(s_2,\ldots,s_{2m+2})}{\text{Sym}} \Big\{ \Big[gZ(s_1+\ldots+s_{2m+2}) + 2Rg + 2\mu AN^2(s_1+\ldots+s_{2m+2}) \Big]$$

$$D_{1,\,2m+1}(s_1,\ldots,s_{2m+2}) - \Big[Z(s_1+\ldots+s_{2m+2}) + 2R \Big]$$

$$L_{1,\,2m}(s_1,\ldots,s_{2m+1}) \Big\} \; ; \; m = 0, 1, 2, \ldots \; . \tag{307}$$

Let us define two dimensionless linear filters, G and H, whose system functions are

$$G(s) = \frac{2R}{Z(s) + 2R + sL} \tag{308}$$

$$H(s) = \frac{Z(s) + 2R}{Z(s) + 2R + sL}, \tag{309}$$

where

$$L = \frac{2\mu AN^2}{g} \; . \tag{310}$$

The syntheses of G and H are shown in Fig. 43. We can now write the solution to (305) as

$$L_{1,\,0}(s_1) = \frac{L}{4R} G(s_1). \tag{311}$$

For solutions to Eqs. 306 - 307 we shall choose

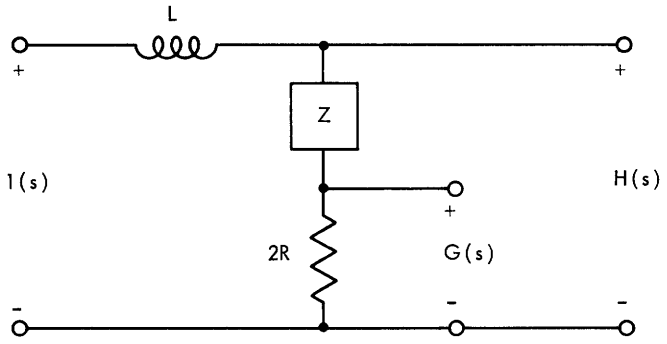

Fig. 43. Syntheses of two filters.

$$L_{1,\,2n}(s_1,\ldots,s_{2n+1}) = \frac{L}{4Rg^{2n}}\,G(s_1)\prod_{k=2}^{2n+1} H(s_1+\ldots+s_k);\ n = 1, 2, 3, \ldots \tag{312}$$

$$D_{1,\,2m+1}(s_1,\ldots,s_{2m+2}) = \frac{L}{4Rg^{2m+1}}\,G(s_1)\prod_{k=2}^{2m+2} H(s_1+\ldots+s_k);$$

$$m = 0, 1, 2, \ldots \quad . \tag{313}$$

The products in (312) and (313) imply the feedback synthesis of λ and δ which is shown in Fig. 44. It can be directly verified by Eqs. 299 - 300.

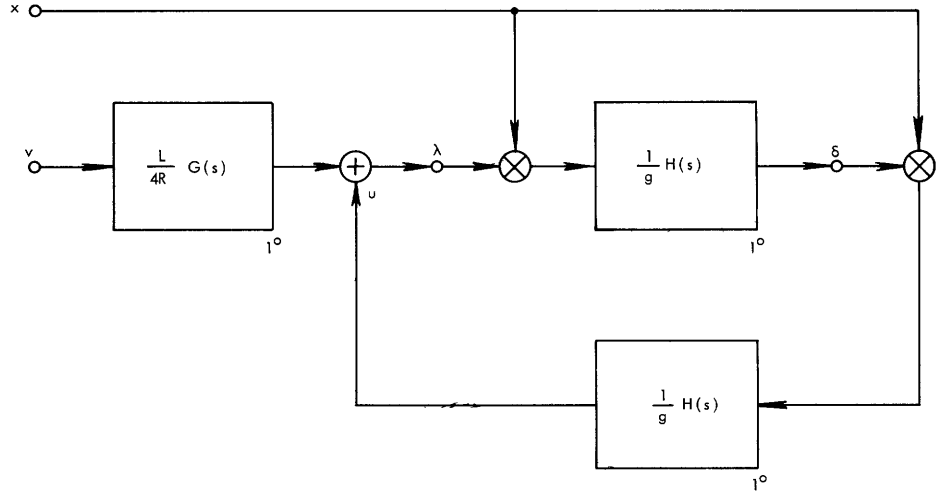

Fig. 44. Feedback synthesis of λ and δ.

The kernels of the functional for f are found from (301). Its (0, 1)-order term is

$$F_{0,1}(s_1) = s_1(s_1 M + K). \tag{314}$$

The (2, 2p+1)-order terms of Eq. 301 gives us

$$\underset{(s_1, s_2)}{\text{Sym}} \left\{ F_{2,2p+1}(s_1, \ldots, s_{2p+3}) \right\} = \underset{(s_1, s_2)}{\text{Sym}} \left\{ -\frac{8}{gL} \sum_{k=0}^{p} I_{1,2p-2k}(s_1, s_{2k+4}, \ldots, s_{2p+3})\, D_{1,2k+1}(s_2, s_3, \ldots, s_{2k+3}) \right\};$$

$$p = 0, 1, 2, \ldots . \tag{315}$$

We shall now use these solutions to study the system's stability.

7.3 D-C STABILITY

Let us first consider DC block displacement signals (that is, $x(t) = X_0$, a constant). For this case, (298) gives us

$$f = F[v, X_0] = -f_r. \tag{316}$$

That is, in order to hold the block displaced from center by X_0, we have to apply a force $f = F[v, X_0]$ to balance the device's restoring force f_r. If this device has achieved stable DC suspension, then f_r must, on the average, act so as to restore the block to center ($x = 0$). Thus a necessary condition for stable DC suspension is that the time average of the applied force, $< F[v, X_0] >$, must be such that

$$< F[v, X_0] > \begin{cases} > 0, & \text{if } X_0 > 0 \\ = 0, & \text{if } X_0 = 0 \\ < 0, & \text{if } X_0 < 0 \end{cases} \tag{317}$$

In the vicinity of the center, the slope of the curve of the time average force vs X_0

$$S = \left[\frac{\partial}{\partial X_0} < F\ [v, X_0] > \right]_{X_0=0} \tag{318}$$

is called the stiffness coefficient of the device (by analogy between the device's restorative action and that of a spring).[13] For DC stability, Eq. 317 shows that the device's stiffness coefficient must be positive. That is,

$$\text{DC stability} \longrightarrow S > 0. \tag{319}$$

Equation 304 shows us that the time average of the force, which must be applied to the block in order to make $x = X_0$, a constant, is

$$< f > = < F\ [v, X_0] >$$

$$= X_0\ F_{0,\,1}\ [v, 1] + \sum_{p=0}^{\infty} X_0^{2p+1} < F_{2,\,2p+1}\ [v, 1] >$$

$$= X_0\ F_{0,\,1}(0) + \sum_{p=0}^{\infty} X_0^{2p+1} \iint_{-\infty}^{\infty} F_{2,\,2p+1}(\tau_1, \tau_2, 0, \ldots, 0)$$

$$\phi_v(\tau_1 - \tau_2)\ d\tau_1\ d\tau_2, \tag{320}$$

where by $F_{2,\,2p+1}(\tau_1, \tau_2, 0, \ldots, 0)$ we mean the inverse transform of $F_{2,\,2p+1}$ $(s_1, s_2, 0, \ldots, 0)$, and ϕ_v is the autocorrelation function of v.

When (314) is evaluated at $s_1 = 0$, then it shows us that the $f_{0,\,1}$ term of (320) is zero. When the inverse Fourier transform of the spectral function of v is substituted for the autocorrelation function of v in Eq. 320, then the result is

$$< f > = < F\ [v, X_0] >$$

$$= \sum_{p=0}^{\infty} X_0^{2p+1} \int_{-\infty}^{\infty} F_{2,\,2p+1}(-j\omega, +j\omega, 0, \ldots, 0)\Phi_v(j\omega)\ \frac{d\omega}{2\pi}, \tag{321}$$

Where $F_{2,\,2p+1}$ has regained its usual meaning. When Eqs. 311 - 313 and 315 are evaluated at the appropriate frequencies, then the result is

$$F_{2,\,2p+1}(-j\omega, +j\omega, 0, \ldots 0) = -\frac{L}{2R^2 g^{2p+2}} \left| G(j\omega) \right|^2 \sum_{k=0}^{p} \left[H(j\omega) \right]^{2k+1} \left[H(-j\omega) \right]^{2p-2k}. \qquad (322)$$

When the expression for $F_{2,\,2p+1}$ given by (322) is substituted in (321) and appropriate reorderings of summation are made, then the result is

$$< f > = < F\,[v, X_0] >$$

$$= -\frac{L}{4\pi R^2 g} \int_{-\infty}^{\infty} \Phi_v(j\omega) \left| G(j\omega) \right|^2 \cdot \sum_{k=0}^{\infty} \sum_{n=0}^{\infty} \left[\frac{X_0}{g} H(j\omega) \right]^{2k+1} \left[\frac{X_0}{g} H(-j\omega) \right]^{2n} d\omega$$

$$= -\frac{X_0 L}{2\pi R^2 g^2} \int_0^{\infty} \left\{ \frac{\Phi_v(j\omega) \left| G(j\omega) \right|^2 Re\left[H(j\omega) \right]}{\left| 1 - \left(\frac{X_0}{g} \right)^2 \left[H(j\omega) \right]^2 \right|^2} \right\} d\omega. \qquad (323)$$

The stiffness coefficient of the device, Eq. 318, is thus

$$S = -\frac{L}{2\pi R^2 g^2} \int_0^{\infty} \Phi_v(j\omega) \left| G(j\omega) \right|^2 Re\left[H(j\omega) \right] d\omega. \qquad (324)$$

By inspection of either Eq. 323 or 324, it is evident that if the device is to achieve stable DC suspension (see Eq. 319), then the real part of the system function of the filter H must be negative over some frequency range. With reference to Fig. 43, it is then clear that the impedance Z must contain at least one capacitor. In order to maximize the stiffness of the device, the power of the input v should be concentrated at that frequency ω where $\left| G(j\omega) \right|^2 Re\left[H(j\omega) \right]$ is a minimum. Since G and H have

the same poles, this frequency is higher than the frequency that maximizes $|G(j\omega)|^2$ but lower than the frequency that minimizes $\mathrm{Re}\left[H(j\omega)\right]$. This forces us to "trade-off" between G and H in order to maximize S.

We shall next study the device's dynamic stability.

7.4 A-C STABILITY

Let us next consider AC block displacement signals (that is, x is a sum of sinusoids). For this case, when we apply the force f = F[v, x] then we are doing mechanical work. The rate at which we are doing work is our mechanical input power

$$p = f \frac{dx}{dt}. \tag{325}$$

If this device has achieved stable AC suspension, then p must, on the average, be positive. That is, we must have to work against the device's efforts to keep the block from moving.

Equations 304 and 325 show that p is a functional of v and x. That is,

$$p = R\,[v, x] = R_{0,\,2}\,[v, x] + \sum_{q=1}^{\infty} R_{2,\,2q}\,[v, x], \tag{326}$$

where we shall choose

$$R_{0,\,2}(s_1, s_2) = F_{0,\,2}(s_1)\, s_2 \tag{327}$$

and

$$R_{2,\,2q}(s_1, \ldots, s_{2q+2}) = F_{2,\,2q-1}(s_1, \ldots, s_{2q+1})\, s_{2q+2}. \tag{328}$$

The (0, 2)-order term of p always has a non-negative average.

$$\begin{aligned} \langle P_{0,\,2} \rangle &= \langle R_{0,\,2}[v, x] \rangle \\ &= \int_{-\infty}^{\infty}\int r_{0,\,2}(\tau_1, \tau_2)\, \phi_x(\tau_1 - \tau_2)\, d\tau_1\, d\tau_2 \\ &= \frac{K}{\pi} \int_{0}^{\infty} \omega^2\, \Phi_x(j\omega)\, d\omega. \end{aligned} \tag{329}$$

That is, as long as there is some viscous mechanical damping ($K \neq 0$), then it aids the AC suspension stability.

For some applications of this device, the presence of viscous mechanical damping might seem undesirable (e.g., when the suspended block is the rotor of a gyro). In order to achieve stable AC suspension when $K = 0$, the terms of p other than $p_{0,2}$ would have to have positive averages.

If v and x are independent, then the time average of $p_{2,2}$ is

$$< p_{2,2} > = < R_{2,2}[v, x] >$$

$$= \int_{-\infty}^{\infty}\int\int\int\int r_{2,2}(\tau_1, \tau_2, \tau_3, \tau_4)\, \phi_v(\tau_1 - \tau_2)\, \phi_x(\tau_3 - \tau_4)\, d\tau_1 \ldots d\tau_4$$

$$= \int_{-\infty}^{\infty}\int\int R_{2,2}(-j\omega, j\omega, -j\nu, j\nu)\, \Phi_v(j\omega)\, \Phi_x(j\nu)\, \frac{d\omega}{2\pi}\, \frac{d\nu}{2\pi}$$

$$= \frac{-j\,L}{8\pi^2 R^2 g^2} \int_{-\infty}^{\infty}\int \nu \Phi_x(j\nu)\, \Phi_v(j\omega)\, |G(j\omega)|^2\, H(j[\omega - \nu])\, d\omega\, d\nu$$

$$= \frac{L}{4\pi^2 R^2 g^2} \int_{0}^{\infty}\int \nu \Phi_x(j\nu)\, \Phi_v(j\omega)\, |G(j\omega)|^2$$

$$\mathrm{Im}\left[H(j[\omega - \nu]) - H(j[\omega + \nu])\right] d\nu\, d\omega. \quad (330)$$

Consider a particular input x whose spectral function* is

*Integrated white Gaussian noise (a random walk) has such a spectral function. Strictly speaking, this function does not exist, but this mathematical flaw can be bypassed by deletion of the singular point at $\omega = 0$.

$$\Phi_x(j\omega) = \frac{2 X_1^2 \omega_0}{\omega^2}, \tag{331}$$

where X_1 and ω_0 are any two positive constants with the dimensions of displacement and frequency, respectively. When (331) is substituted in (330) and the Hilbert transform

$$\mathrm{Re}\left[H(j\omega)\right] = \int_0^\infty \frac{\mathrm{Im}\left[H(j[\omega - \nu]) - H(j[\omega + \nu])\right]}{\pi\nu} d\nu \tag{332}$$

is used to relate the imaginary part of filter H's system function to its real part, then the result is

$$<p_{2,2}> = -\omega_0 X_1^2 S, \tag{333}$$

where S is the device's stiffness coefficient (see Eq. 324).

Equation 333 is highly significant. If the device is DC stable, then S is positive. If S is positive, then (333) shows that there is at least one x (Eq. 331) such that $< p_{2,2} >$ is negative. If K = 0, then there is some $X_1 > 0$ which is small enough so that $< p >$ is negative. If $< p >$ is negative for some x, then the device is AC unstable (because the power to sustain the block's movement is flowing out of the device rather than into it). Thus (333) shows that: <u>If viscous mechanical damping is not present in the device, then its magnetic suspension is unstable.</u>

Since the device has now been shown to be either AC or DC unstable whenever viscous mechanical damping is absent, then let us next determine just how much damping is needed in order for the device to be both AC and DC stable.

Under normal operating conditions, the input voltage v is a simple sinusoid.

$$v = \mathrm{Re}\left[V_1 \exp(j\omega_e t)\right]. \tag{334}$$

Then the voltage spectrum consists of a pair of impulses

$$\Phi_v(j\omega) = \frac{\pi |V_1|^2}{2} \left[u_0(\omega - \omega_e) + u_0(\omega + \omega_e)\right], \tag{335}$$

and the evaluation of (323) yields the fact that the time average force necessary to displace the device's block by X_0, a constant, is

$$< F[v, X_0] > = - \frac{L |V_1|^2 X_0 |G(j\omega_e)|^2 Re\left[H(j\omega_e)\right]}{4R^2 g^2 \left| 1 - \left[\frac{X_0 H(j\omega_e)}{g} \right] \right|^2} . \tag{336}$$

By substituting Eq. 335 in Eq. 324, we find that the stiffness coefficient is

$$S = - \frac{L|V_1|^2}{4R^2 g^2} |G(j\omega_e)|^2 Re\left[H(j\omega_e)\right] . \tag{337}$$

The necessary condition for DC stability is then simply

$$Re\left[H(j\omega_e)\right] < 0. \tag{338}$$

If the impedance Z is simply a capacitor C, as in Fig. 39, then Eq. 309 yields

$$Re\left[H(j\omega)\right] = \frac{1 - \omega^2 (LC - 4R^2C^2)}{(LC\omega^2 - 1)^2 + (2RC\omega)^2} . \tag{339}$$

Thus the device achieves DC stability whenever both

$$C < \frac{L}{4R^2} \tag{340}$$

and

$$\omega_e^2 > \frac{1}{LC - 4R^2C^2} . \tag{341}$$

(incidentally, the conditions given by Eqs. 340 - 341 are strong enough so that the denominator of Eq. 336 (the time average force) can never go to zero).

After (308) is solved for $|G(j\omega_e)|^2$ then the stiffness coefficient can be found from (337) and (339). It is[13]

$$S = \frac{L|V_1|^2\left[\omega_e^2(LC - 4R^2C^2) - 1\right]}{16\,\omega_e^2 g^2 R^4 C^2 \left[\left[\frac{LC\,\omega_e^2 - 1}{2\omega_e RC}\right]^2 + 1\right]^2}. \tag{342}$$

Curves for Eqs. 336 and 342 have been plotted in Frazier and Kingsley. Frazier and Kingsley's notation[14] is

$$Q_0 = \frac{\omega_e L}{2R}, \quad Q = \frac{\omega_e^2\,LC - 1}{2\omega_e RC}, \quad S = -\frac{F_0 K_{n0}}{g} = -\frac{4F_0 f(Q)}{g}.$$

In order to determine how much viscous mechanical camping is necessary to achieve both AC and DC stability when the input voltage is a simple sinusoid (see Eqs. 334 - 335), we shall consider displacement signals that are also simple sinusoids.

$$x = \mathrm{Re}\left[X_1 \exp(j\omega_m t)\right] \tag{343}$$

$$\Phi_x(j\omega) = \frac{\pi|X_1|^2}{2}\left[u_0(\omega - \omega_m) + u_0(\omega + \omega_m)\right]. \tag{344}$$

Equation 329 evaluates to

$$< p_{0,2} > = \frac{K\omega_m^2|X_1|^2}{2}. \tag{345}$$

If $\omega_e^2 \neq \omega_m^2$, then (329) evaluates to

$$< p_{2,2} > = \frac{L|X_1V_1|^2}{16R^2g^2}\,\omega_m|G(j\omega_e)|^2\,\mathrm{Im}\left[H(j[\omega_e - \omega_m]) - H(j[\omega_e + \omega_m])\right]. \tag{346}$$

If the device is to be AC stable, then Eqs. 345 - 346 show that as a necessary condition, for all ω_m, K must be such that

$$K > \frac{L|V_1|^2 |G(j\omega_e)|^2}{8R^2 g^2} \text{Im}\left[\frac{H(j[\omega_e + \omega_m]) - H(j[\omega_e - \omega_m])}{\omega_m}\right] . \qquad (347)$$

The Hilbert transform, Eq. 332, may be used to demonstrate that the expression on the right of (347) is indeed positive as long as the device is DC stable (see Eq. 338).

Thus, Eq. 347 is the lower bound to the viscous mechanical damping which must be present in the device in order for the magnetic suspension to be stable.

If the damping is less than the bound given by (347), then the suspension is unstable.

7.5 FREE OSCILLATIONS

Whenever K fails Eq. 347, then the device can exhibit self-sustained free oscillations. If these oscillations are periodic

$$x = \text{Re}\left[\sum_{n=0}^{\infty} X_n \exp(jn\omega_m t)\right] , \qquad (348)$$

and the input voltage v is a simple sinusoid (Eq. 334), then Eq. 304 shows that ω_e and ω_m must be commensurate,

$$2\omega_0 = k\omega_m ; \text{ k an integer,} \qquad (349)$$

in order for these oscillations to be force free (if the frequencies do not satisfy Eq. 349, then the frequency components present in Eq. 304 could not balance so as to sum to zero force for all time). The power to drive these oscillations is being provided by $p_{2,2}$ (and the higher order terms) which involves Im [H(jω)]. When the impedance Z is simply a capacitor C, as in Fig. 39, then Eq. 309 yields

$$\text{Im}\left[H(j\omega)\right] = \frac{-2\omega^3 RLC^2}{(LC\omega^2 - 1)^2 + (2RC\omega)^2} . \qquad (350)$$

If the first harmonic of x dominates, then (346) and (350) show that $p_{2,2}$ will contribute power to the oscillations most strongly whenever

$$\omega_e - \omega_m = \omega_\delta \cong \frac{1}{\sqrt{LC}} = \omega_0 \,. \tag{351}$$

Equations 349 and 351 then show that

$$k = \frac{2\omega_e}{\omega_e - \omega_\delta} \cong \frac{2\omega_e}{\omega_e - \omega_0} \tag{352}$$

$$\omega_e = \frac{\omega_\delta k}{k - 2} \cong \frac{\omega_0 k}{k - 2} \tag{353}$$

$$\omega_m = \frac{2\omega_\delta}{k - 2} \cong \frac{2\omega_0}{k - 2} \,. \tag{354}$$

If the third harmonic of x dominates, then instead of Eq. 351, we must write

$$\omega_e - 3\omega_m = \omega_\delta \cong \frac{1}{\sqrt{LC}} = \omega_0, \tag{355}$$

and then

$$k = \frac{6\omega_e}{\omega_e - \omega_\delta} \cong \frac{6\omega_e}{\omega_e - \omega_0} \tag{356}$$

$$\omega_e = \frac{\omega_\delta k}{k - 6} \cong \frac{\omega_0 k}{k - 6} \tag{357}$$

$$\omega_m = \frac{2\omega_\delta}{k - 6} \cong \frac{2\omega_0}{k - 6} \,. \tag{358}$$

Equations 349 - 358 predict certain properties of the magnetic suspension device's self-sustained periodic oscillatory instabilities. These predictions have been verified experimentally. The results of these experimental confirmations of Eqs. 349 - 358 are presented in Appendix A. The device's self-sustained oscillations can also be explained physically.

7.6 PHYSICAL EXPLANATION OF THE FREE OSCILLATIONS

The magnetic suspension device's self-sustained oscillations can be explained physically by the phase shift of filter H. The frequency response of filter H is

$$H(j\omega) = \text{Re}\,[H(j\omega)] + j\,\text{Im}\,[H(j\omega)]$$

$$= |H(j\omega)|\exp(j\theta(\omega)), \tag{359}$$

where $\text{Re}\left[H(j\omega)\right]$ and $\text{Im}\left[H(j\omega)\right]$ are given by Eqs. 339 and 350, and $|H(j\omega)|$ and $\theta(\omega)$ are graphed in Fig. 45.

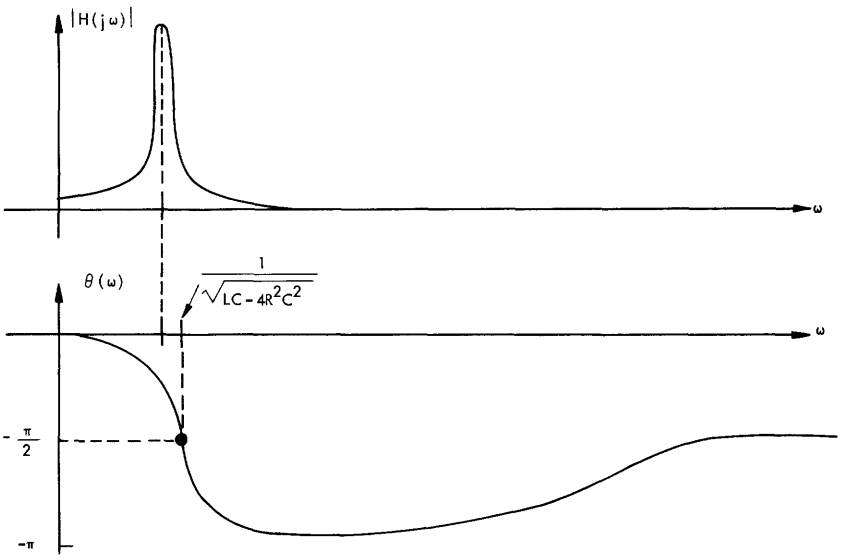

Fig. 45. Frequency response of H(jω).

By Eq. 341, the condition for DC stability is

$$\omega_e > \frac{1}{\sqrt{LC - 4R^2C^2}} \tag{360}$$

which, by Fig. 45, is equivalent to

$$-\pi < \theta(\omega_e) < -\frac{\pi}{2}\,. \tag{361}$$

Note from Fig 45 that ω_e must be past the resonant peak of $|H(j\omega)|$.

When ω_e satisfies (360) or (361) and x is either a simple sinusoid (Eq. 343) or a periodic function (Eq. 348) whose first harmonic dominates, then the line spectrums of v, x, λ, δ, and u, given by Fig. 46, follows from Fig. 44. That is, the input v (Eq. 334) gives λ a dominant component at ω_e.

$$\lambda \approx \mathrm{Re}\left[\wedge \exp (j\omega_e t)\right]. \tag{362}$$

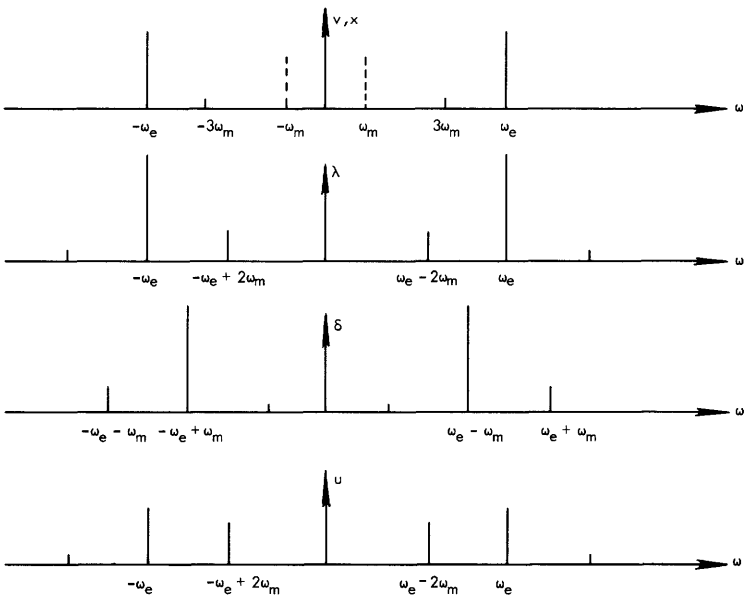

Fig. 46. Line spectrum of free oscillations.

The product $x\lambda$, therefore, has dominant components at $\omega_e + \omega_m$ and $\omega_e - \omega_m$. The component of $x\lambda$ at $\omega_e + \omega_m$ is farther past the resonent peak of $|H(j\omega)|$ than ω_e was, but the component at $\omega_e - \omega_m = \omega_\delta$ can be near the peak of $|H(j\omega)|$. (That is, $\omega_\delta \approx \omega_0$, see Eq. 351). Thus when $x\lambda$ passes through $(1/g)H$ to form δ (see Fig. 44), then the dominant component of δ is at $\omega_e - \omega_m = \omega_\delta$.*

$$\delta \approx \mathrm{Re}\left[\frac{\wedge X_1^*}{2g} \; H(j\omega_\delta) \exp (j\omega_\delta t) \right]. \tag{363}$$

The product $x\delta$, therefore, has dominant components at ω_e and $\omega_e - 2\omega_m$. These two components are nearly centered about the peak of $|H(j\omega)|$. Thus when $x\delta$ passes

*In those cases in which x is periodic and its k^{th} harmonic dominates, $\omega_e - k\omega_m$ is near the peak of $|H(j\omega)|$. (See Eq. 355.)

through $(1/g)H$ to form u, the fed-back signal, then u contributes one component which reinforces the dominant component of λ at ω_e and one subsidiary component of λ at $\omega_e - 2\omega_m$.

By Eqs. 289, 362, and 363, the device's restoring force, f_r, is

$$f_r \approx \mathrm{Re}\left[\frac{|\wedge|^2 X_1}{\mu A N^2 g} H^*(j\omega_\delta) \exp(j\omega_m t) + \frac{\wedge^2 X_{1^*}}{\mu A N^2 g} H(j\omega_\delta) \exp\left(j[2\omega_e - \omega_m]t\right)\right]. \tag{364}$$

Equation 364 shows that the component of the device's restoring force at ω_m has a phase shift, relative to x, of $-\theta(\omega_\delta)$. With reference to Fig. 45 and Eq. 361, the range of this phase shift is

$$0 < -\theta(\omega_\delta) < -\theta(\omega_e) < \pi \tag{365}$$

which is shown in Fig. 47.

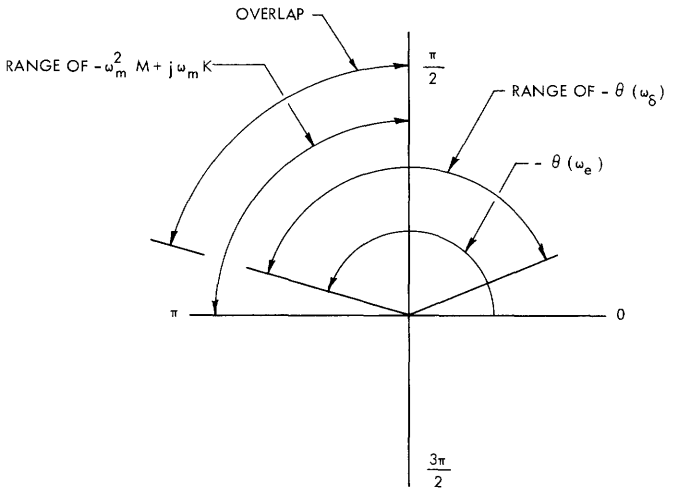

Fig. 47. Phase angles of $-\lambda\delta$ and $j\omega(j\omega M+K)$.

If we rewrite Eq. 298 as

$$f + f_r = M\frac{d^2x}{dt^2} + K\frac{dx}{dt}, \tag{366}$$

then we see that the phase shift, relative to x, because of the block's mass and the viscous mechanical damping K, is given by the polynominal $-\omega_m^2 M + j\omega_m K$ and has a

range from $\pi/2$ to π, as is also shown in Fig. 47. Figure 47 shows that these two ranges overlap. Thus it is possible for the ω_m component of f_r to balance $M\,(d^2x/dt^2) + k\,(dx/dt)$ in Eq. 366 when

$$-\pi < \theta(\omega_e) < \theta(\omega_\delta) < -\frac{\pi}{2}\,. \tag{367}$$

That is, when ω_m is such that

$$0 < \omega_m < \omega_e - \frac{1}{\sqrt{IC - 4R^2C^2}} \tag{368}$$

then the device's restoring force can balance the block's mechanical forces, even though $f = 0$ (see Eq. 366). This is the physical basis of the device's free oscillations when the damping is insufficient. The bound upon the damping which will inhibit these oscillations is given by Eq. 347. The physical basis for that bound (which is not due to the phase-angle argument that we have just completed) is in the fact that Fig. 47 tells only half of the story. That is, even when there is a phase-angle balance between the device's restoring force and the block's mechanical forces, this does not prove that f can be zero (force-free oscillations) unless their amplitudes also balance. If K is large enough to satisfy (347) for all ω_m in the range of (368), then this amplitude balance is prevented and the device's oscillatory instabilities are overcome.

VIII. CONCLUSION

If a system's behavior can be characterized by a differential, integral, or integro-differential equation, and if solutions to that equation exist, are unique (for a given input), time-invariant and "smooth" enough so that certain limits exist, then that system is an analytic system and its output can be expressed as a Volterra series of its input. If the system's characteristic equation (or equations) is (are) in the appropriate form, then that system's Volterra series can be found, in a few steps, by our inspection technique (developed here in Section III). If the characteristic equation is not in an appropriate form, it can usually be rewritten in an appropriate form by multiplying through to eliminate those terms that represent division (division is not the result of an operation by an analytic system) by one of the system's variables, (e.g., Eq. 68 rewritten as Eq. 72).

An analytic system's Volterra series is a functional characterization of that system's behavior. This functional characterization of the system is useful because (i) it can lead to interesting syntheses of that system, (ii) it is an explicit statement of that system's output for an arbitrary input (perhaps for an arbitrary input from within a class of inputs), and (iii) from it we can compute that system's output for particular inputs. Some examples of such computations that we have seen were for a DC input signal (Eqs. 184 - 192),* an AC input signal (Eqs. 150 - 160), an exponential input signal (148 - 149), an exponential-step input signal (Eqs. 243 - 281), an unknown input signal whose autocorrelation was known (Eqs. 320 - 323), and a stochastic input signal. The example of the computation of a system's output (or rather the statistical expectation of that system's output) when the input signal is stochastic, from the system's functional characterization, is of special interest because such computations may not be possible from the system's differential equation characterization.

The functional characterization of an analytic system by a Volterra series is not without disadvantages. The Volterra series is usually an infinite series. It need not always be an infinite series (e.g., Eq. 99) and even when it is an infinite series we may be able to find a closed form for its evaluation (e.g., Eq. 323), but usually we are forced to approximate it by a finite number of terms. When we approximate a Volterra series by a finite number of its terms, then we should compute a bound upon the truncation error that we have introduced (e.g., Eq. 210), but finding such a bound can be very difficult.

The extension of the work presented in this report to non-analytic systems is questionable. We suppose that, faced with a nonlinear differential equation that did

*The computation of the output for DC input signals should always be made. It is simple and it serves as a useful check on the solutions and the convergence of the series.

not characterize an analytic system (e.g., Eqs. 123 - 125), then we could use the inspection technique to get "an answer", but the meaning, if any, of such "an answer" is doubtful. This is one of the disadvantages of our inspection technique – it is too easy. That is, given a nonlinear differential equation, we may be tempted to evade the hard work of testing it to see if it characterizes an analytic system and, rashly assuming that it does, proceed to use our inspection technique to find "an answer". If the differential equation did not characterize an analytic system, then our "answer" can be grossly erroneous and misleading.

Additional research is needed on the problem of testing a differential equation in order to determine if it characterizes an analytic system. The known tests are too hard. The three major known existence theorems can be quite difficult to apply. All too often, a uniqueness proof has to be invented for each particular differential equation. The proof of time-invariance, once existence and uniqueness have been shown, is usually trivial. The proof that the system's functional is analytic at some instant of time through Volterra's definition (that is, by showing from limits of small perturbations of the input about zero that all of Volterra's functional derivatives exist at zero), is far too tedious to use. As has been said, once existence, uniqueness, and time-invariance have been established, then it is easier to use our inspection technique to find a Volterra series solution, if there is one. If we get an answer, and if we can show that it converges absolutely, then because of uniqueness, we have shown analyticity. A simpler series of tests than these would be extremely useful.

APPENDIX A

SELF-SUSTAINED OSCILLATIONS OF A MAGNETIC SUSPENSION DEVICE EXPERIMENTALLY VERIFIED

We shall present the experimental verification of the predictions in Section VII concerning the self-sustained oscillations of a magnetic suspension device.

Figure A-1 is a sketch of the suspension device upon which the measurements presented here were made.* The device consisted of a steel rotor (the suspended block) on a shaft set into a pivot bearing for the vertical suspension. Two orthogonal single-axis suspension devices provided the horizontal suspension of the device. In order to measure the device's static parameters, the current i (see Fig. A-2 and Fig. 41) was monitored with paper shims inserted in the gaps (g = 0.006") to fix the block displacement at zero. When x = 0, then it can be shown from Eqs. 290, 299, 303, and 310 that

$$2V(s) = \left[Z(s) + 2R + sL \right] I(s). \qquad \text{(A. 1)}$$

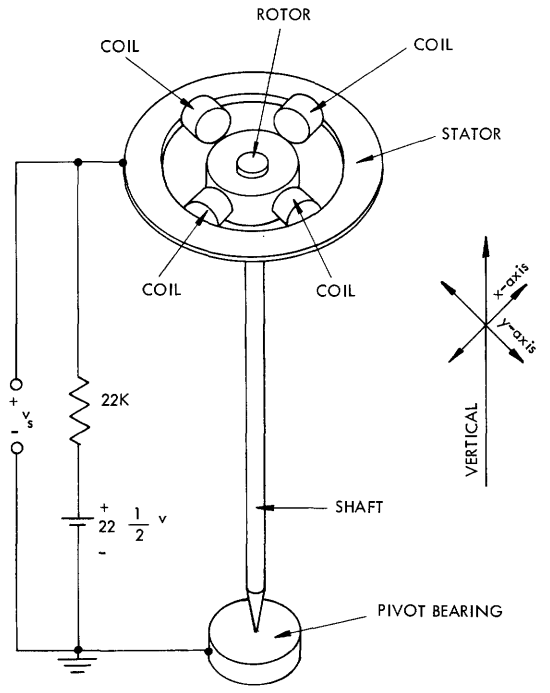

Fig. A-1. The suspension device.

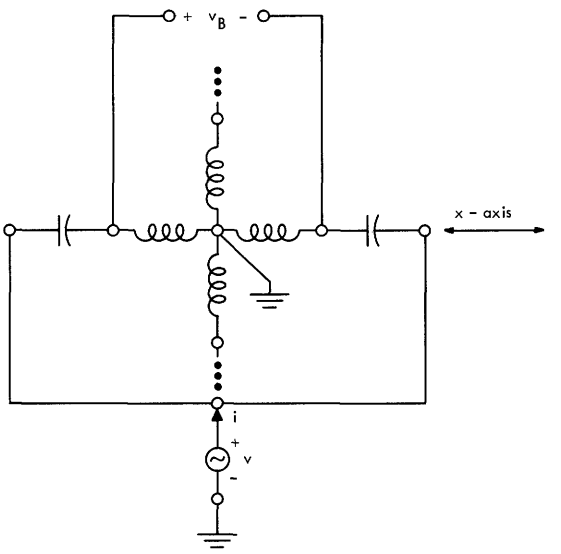

Fig. A-2. Electrical schematic diagram of the suspension device.

*Professor R. H. Frazier and Mr. P. J. Gilinson, Jr., of the Instrumentation Laboratory, M. I. T., provided the suspension device and the facilities at which the author, with the assistance of Mr. J. Scoppettuolo, conducted these experiments during the early part of June 1965.

From the tabulation of the relative phase angles between v and i, given in Table A-1, we can determine ω_0, L, and R. They are

$$\omega_0 = \frac{1}{\sqrt{L\,C}} = 6.1 \times 10^3 \ \frac{\text{radians}}{\text{sec}} \qquad \text{(A. 2)}$$

$$L = 0.273 \text{ H} \qquad \text{(A. 3)}$$

$$R = 103\ \Omega \ . \qquad \text{(A. 4)}$$

Table A-1. Measurements to determine the system parameters.

Relative Phase Angle of v and i	Frequency of v, According to Oscillator Dial	Frequency of v, According to Oscilloscope	Frequency of v, According to E-put Meter
35°	1.0	1.0	0.9994
46°	1.02	1.05	1.0212
67°	1.1	1.1	1.0971

All frequencies in kilo-cycles-per-second, $Z(s) = \frac{1}{s\,C}$, $C = 0.1\ \mu$ f.

The paper shims were then removed and v was made large enough so that self-sustained oscillations along the x-axis ensued (the y-axis v was set so that there was no oscillation along the y-axis). Three signals were then monitored: v, the input voltage to the x-axis suspension device; v_S, the stator voltage (which shows when the rotor is touching the stator (see Fig. A-1)); and v_B, the bridge voltage (shown in Figs. A-2 and 41). It is useful to monitor the bridge voltage, v_B, because it provides information about the mean-difference flux linkage δ. That is, it can be shown from Eqs. 291 – 295, and 299 – 300 that

$$V_B(s) = -\frac{4\,s\,Z(s)}{2R + Z(s)}\Delta(s). \qquad \text{(A. 5)}$$

Equation A. 5 demonstrates that the bridge voltage contains the same frequencies as δ.

Oscilloscope photographs of the three signals, v, v_S, and v_B recorded nine separate observations of the magnetic suspension device's sulf-sustained oscillations. Reproductions of the photographs of four of these observations are presented as exhibits here.

A. 1 INTERPRETATION OF EXHIBITS

If the reader will take a sheet of paper and mark an interval on its edge that is as long as the black line under the text for v(t) in Exhibit A, then he will find that that interval is as long as (i) 5 periods of v, (ii) 4 periods of v_S, (iii) 3 cycles of v_B, and (iv) one fundamental period of v_B (the interval between the two highest peaks). In this experiment, the rotor was hitting the stator twice each period of the mechanical oscillation (that is, it hit once per side). Exhibit A thus demonstrates that

$$\frac{3.0 \text{ msec}}{2\pi} = \frac{5}{\omega_e} = \frac{2}{\omega_m} = \frac{3}{\omega_\delta} = \frac{1}{\omega_{\delta 0}} , \tag{A. 6}$$

which verifies Eq. 349 and shows that k = 5 in this observation of the device's self-sustained oscillations. The verifications of Eqs. 351 – 354 by Exhibit A are tabulated on line 1 of Table A-2.

In Exhibit B, the reader will find that the length of the black line under the text for v(t) equals the length of (i) 9 periods of v, (ii) 4 periods of v_S, and (iii) 1 fundamental period of v_B. The rotor was hitting the stator once per side (twice per mechanical period). Exhibit B thus demonstrates that

$$\frac{6.5 \text{ msec}}{2\pi} = \frac{9}{\omega_e} = \frac{2}{\omega_m} = \frac{1}{\omega_{\delta 0}} , \tag{A. 7}$$

which verifies Eq. 349 and shows that k = 9 in this observation. The signal v_B is too rich in harmonics to observe ω_δ directly, but Eq. 351 can be verified indirectly by Eq. A. 7. That is,

$$\begin{aligned} \omega_\delta &= \omega_e - \omega_m \\ &= \frac{18\pi}{6.5 \text{ msec}} - \frac{4\pi}{6.5 \text{ msec}} \\ &= 6.8 \times 10^3 \frac{\text{radians}}{\text{sec}} \end{aligned} \tag{A. 8}$$

which verifies Eq. 351 (via Eq. A. 2). The verifications of Eqs. 351 – 354 by Exhibit B are tabulated on line 5 of Table A-2.

In Exhibit C, the reader will find that the length of the black line under the text for v(t) equals the length of (i) 11 periods of v, (ii) 3 intervals of v_S, and (iii) 1 fundamental period of v_B. The rotor was hitting the stator erratically (as is seen by the lack of symmetry in the waveform) and a longer sequence of pictures (not included here) shows the occasional presence of one more contact per this length. Thus the 3 intervals of v_S shown in Exhibit C really represent 2 mechanical periods. Exhibit C thus demonstrates that

Exhibit A. Self-sustained 5:2 oscillation.

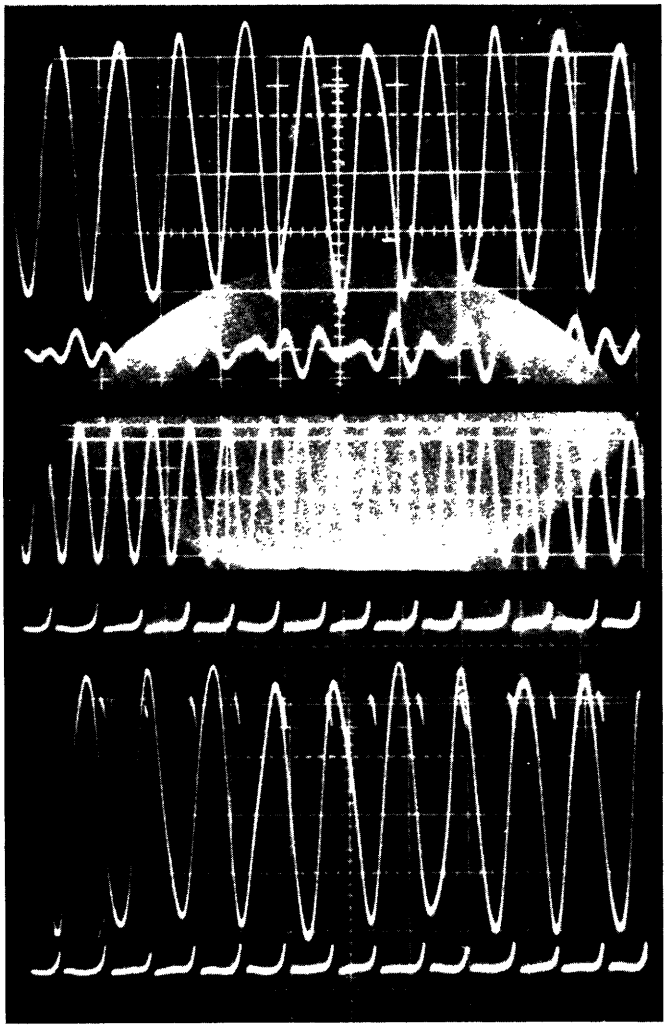

$v_B(t)$, $(10 \frac{V}{cm}) \times (1 \frac{msec}{cm})$

Y-axis bridge voltage signal,
$(10 \frac{V}{cm}) \times (1 \frac{msec}{cm})$

$v(t)$, $(20 \frac{V}{cm}) \times (1 \frac{msec}{cm})$

$v_S(t)$, $(20 \frac{V}{cm}) \times (1 \frac{msec}{cm})$

$v_B(t)$, $(10 \frac{V}{cm}) \times (1 \frac{msec}{cm})$

$v_S(t)$, $(20 \frac{V}{cm}) \times (1 \frac{msec}{cm})$

Exhibit B. Self-sustained 9:2 oscillation.

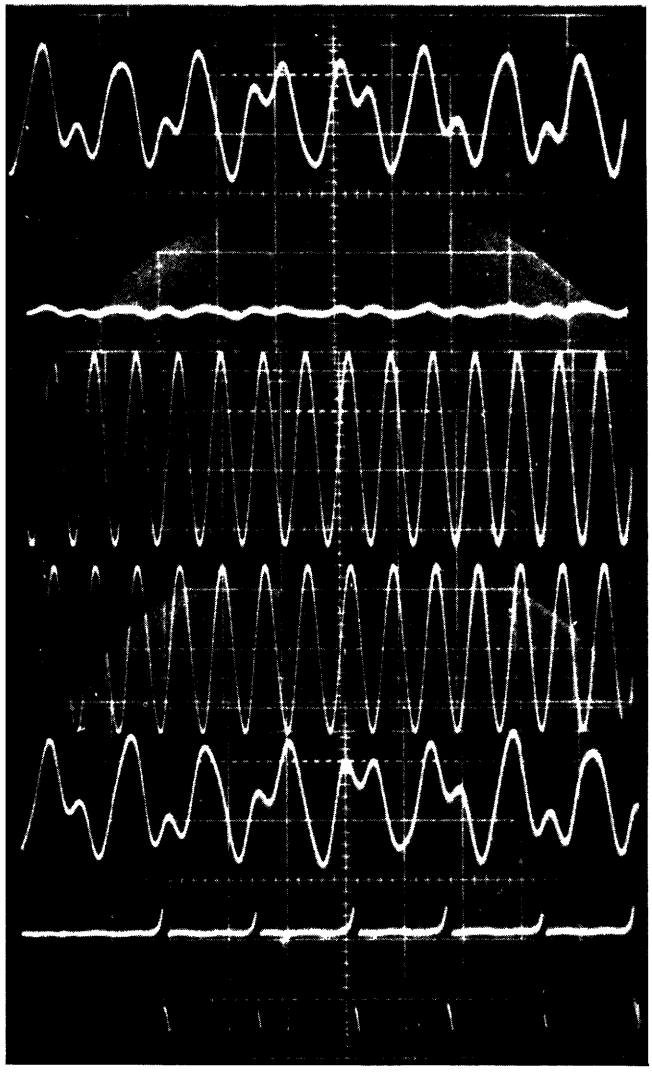

$v_B(t)$, $(10\frac{V}{cm}) \times (1\frac{msec}{cm})$

Y-axis bridge voltage signal,
$(10\frac{V}{cm}) \times (1\frac{msec}{cm})$

$v(t)$, $(20\frac{V}{cm}) \times (1\frac{msec}{cm})$

Y-axis input voltage signal,
$(20\frac{V}{cm}) \times (1\frac{msec}{cm})$

$v_B(t)$, $(10\frac{V}{cm}) \times (1\frac{msec}{cm})$

$v_S(t)$, $(20\frac{V}{cm}) \times (1\frac{msec}{cm})$

Exhibit C. Self-sustained 11:2 oscillation.

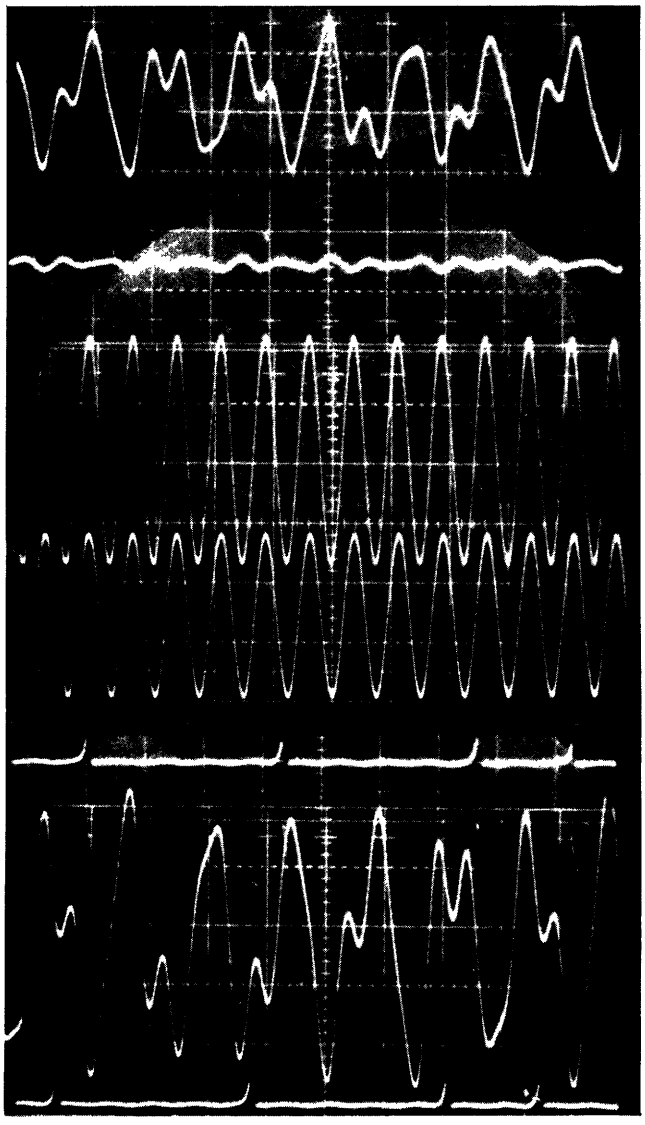

$v_B(t)$, $(10\ \frac{V}{cm}) \times (1\ \frac{msec}{cm})$

y- axis bridge voltage signal, $(10\ \frac{V}{cm}) \times (1\ \frac{msec}{cm})$

$v(t)$, $(20\ \frac{V}{cm}) \times (1\ \frac{msec}{cm})$

---

y- axis input voltage signal, $(20\ \frac{V}{cm}) \times (1\ \frac{msec}{cm})$

$v_S(t)$, $(20\ \frac{V}{cm}) \times (1\ \frac{msec}{cm})$

$v_B(t)$, $(5\ \frac{V}{cm}) \times (1\ \frac{msec}{cm})$

$v_S(t)$, $(20\ \frac{V}{cm}) \times (1\ \frac{msec}{cm})$

$$\frac{8.3 \text{ msec}}{2\pi} = \frac{11}{\omega_e} = \frac{2}{\omega_m} = \frac{1}{\omega_{\delta 0}} \tag{A.9}$$

which verifies Eq. 349 and shows that k = 11 in this observation. As before, Eq. 351 is verified indirectly by

$$\omega_\delta = \omega_e - \omega_m$$

$$= \frac{22\pi}{8.3 \text{ msec}} - \frac{4\pi}{8.3 \text{ msec}}$$

$$= 6.8 \times 10^3 \frac{\text{radians}}{\text{sec}} \tag{A.10}$$

The verifications of Eqs. 351 – 354 by Exhibit C are tabulated on line 7 of Table A-2.

Table A-2. Experimental results – first harmonic dominant.

$\omega_e \cong \frac{k\omega_0}{k-2}$		$\omega_m \cong \frac{2\omega_0}{k-2}$		$k = \frac{2\omega_e}{\omega_m} \cong \frac{2\omega_e}{\omega_e - \omega_0}$		$\omega_\delta = \omega_e - \omega_m \cong \omega_0$		Frequencies in kilo-radians per second
(meas)	(pred)	(meas)	(pred)	(meas)	(pred)	(meas)	(pred)	Remarks
10.5	10.2	4.2	4.1	5	4.8	6.3	6.1	Exhibit A
10.5	10.2	4.2	4.1	5	4.8	6.3	6.1	1/2 Voltage
10.5	10.2	4.2	4.1	5	4.8	6.3	6.1	Off center
10.2	10.2	4.1	4.1	5	5.0	6.1	6.1	Not hitting
8.7	7.9	1.9	1.7	9	6.7	6.8	6.1	Exhibit B
8.5	7.9	1.8	1.7	9	7.1	6.7	6.1	Lower frequency
8.3	7.5	1.5	1.4	11	7.6	6.8	6.1	Exhibit C

In Exhibit D, the reader will find that the length of the black line under the text for v(t) equals the length of (i) 19 periods of v, (ii) 8 periods of v_S (N. B. the change of time calibration), and (iii) 1 fundamental period of v_B. The rotor was hitting the stator 4 times each mechanical period (the third harmonic of x was dominant). Exhibit D thus demonstrates that

$$\frac{12.5 \text{ msec}}{2\pi} = \frac{19}{\omega_e} = \frac{2}{\omega_m} = \frac{1}{\omega_{\delta 0}} \tag{A.11}$$

Exhibit D. Self-sustained 19:2 oscillation.

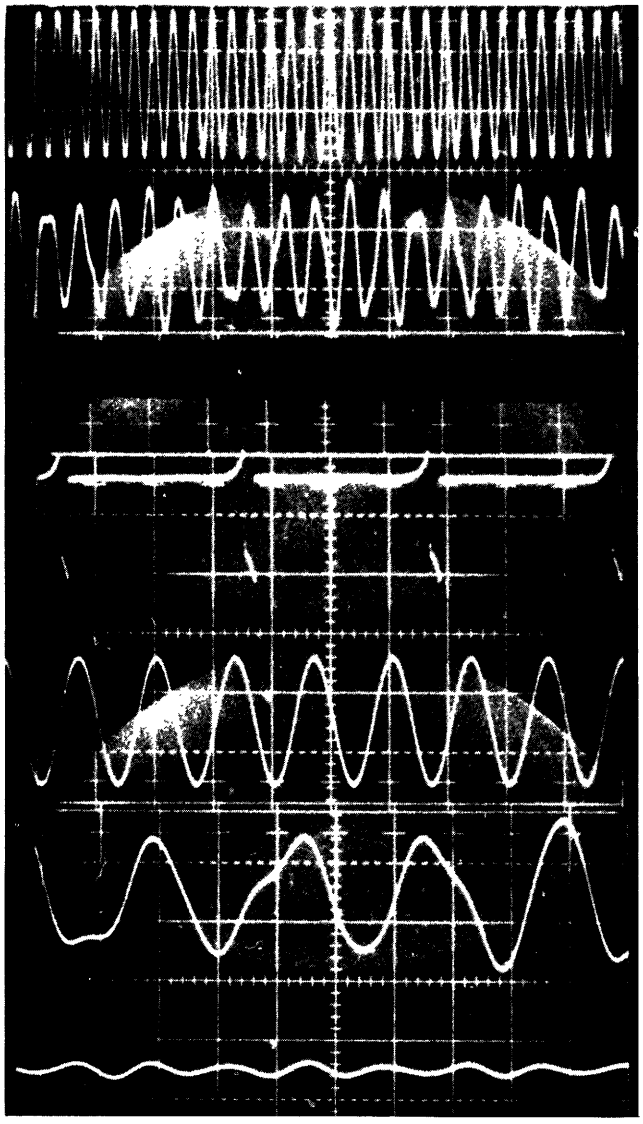

$v(t)$, $(20\ \frac{V}{cm}) \times (2\ \frac{msec}{cm})$

$v_B(t)$, $(10\ \frac{V}{cm}) \times (2\ \frac{msec}{cm})$

$v_S(t)$, $(20\ \frac{V}{cm}) \times (0.5\ \frac{msec}{cm})$

$v(t)$, $(20\ \frac{V}{cm}) \times (0.5\ \frac{msec}{cm})$

$v_B(t)$, $(10\ \frac{V}{cm}) \times (0.5\ \frac{msec}{cm})$

y-axis bridge voltage signal,
$(10\ \frac{V}{cm}) \times (0.5\ \frac{msec}{cm})$

which verifies Eq. 349 and shows that k = 19 in this observation. Unlike the preceding three exhibits, in this case the third harmonic of x dominated. Thus we can verify Eq. 355 indirectly via Eq. A. 11. That is,

$$\omega_\delta = \omega_e - 3\omega_m$$

$$= \frac{38\pi}{12.5 \text{ msec}} - \frac{12\pi}{12.5 \text{ msec}}$$

$$= 6.5 \times 10^3 \frac{\text{radians}}{\text{sec}} . \qquad \text{(A. 12)}$$

The verification of Eqs. 355 – 358 are tabulated on line 1 of Table A-3.

It will be noted in Tables A-2 and A-3 that the crudest predictions are those of k. This is so because the denominator of the formula for k is of the same order of magnitude as the approximation $\omega_\delta \approx \omega_0$.

Table A-3. Experimental results – third harmonic dominant.

$\omega_e \cong \frac{k\omega_0}{k-6}$		$\omega_m \cong \frac{2\omega_0}{k-6}$		$k = \frac{2\omega_e}{\omega_m} \cong \frac{6\omega_e}{\omega_e - \omega_0}$		$\omega_\delta = \omega_e - 3\omega_m \cong \omega_0$		
(meas)	(pred)	(meas)	(pred)	(meas)	(pred)	(meas)	(meas)	Remarks
9.5	8.9	1.0	0.94	19	16.8	6.5	6.1	Exhibit D
9.45	8.9	1.00	0.94	19	17.0	6.45	6.1	Lower frequency

(All frequencies in kilo-radians-per-second)

Acknowledgment

I wish to express my deep gratitude to Professor Yuk-Wing Lee, my thesis supervisor, who gave me all the freedom and time that I needed until I found a thesis topic that could hold my interest, and, after I had found it, became the stern taskmaster that I needed to make me complete my work.

I am also very grateful to Professor William McConway Siebert and Professor Martin Schetzen, my thesis readers, for their many helpful criticisms; to Professor Richard H. Frazier for suggesting and helping me with the magnetic suspension device presented here in Section VII (as well as serving as my thesis reader during Professor Siebert's absence); to Mr. P. J. Gilinson, Jr., for providing the facilities for the experimental work presented here in Appendix A; to Professor Carlton Everett Tucker, Executive Officer of the Department of Electrical Engineering, M. I. T., for his aid and grace in helping me to overcome problems that almost forced me to give up my thesis work before it was finished; and to Professor Henry J. Zimmermann for providing both the opportunity for and the encouragement of my work at the Research Laboratory of Electronics, M. I. T.

REFERENCES

1. J. F. Barrett, "The Use of Functionals in the Analysis of Nonlinear Physical Systems", Statistical Advisory Unit Report 1/57, Ministry of Supply, Great Britain, 1957.

2. M. B. Brilliant, "Theory of the Analysis of Nonlinear Systems", Technical Report 345, Research Laboratory of Electronics, M. I. T., Cambridge, Mass., March 3, 1958, p. 26. Equation 31 is the definition of the multivariate bilateral Laplace transform.

3. Ibid., pp. 30-44. In these four sections, Brilliant studies the combinations of analytic systems.

4. Ibid., p. 31. Equation 44 is our Eq. 52.

5. Ibid., p. 32. Equation 49 is our Eq. 53.

6. Ibid., p. 33. Equation 54 is the general cascade combination formula.

7. Ibid., pp. 37-44. In these two sections, Brilliant studies the feedback combinations of analytic systems.

8. H. T. Davis, Introduction to Nonlinear Differential and Integral Equations (United States Government Printing Office, Washington, D. C., 1960), pp. 79-93. In Chapter IV, Davis covers the three most powerful known existence theorems: The Calculus of Limits, The Method of Successive Approximations, and The Cauchy-Lipschitz Method.

9. C. S. Draper, et al., Inertial Guidance (Pergamon Press, New York, 1960), pp. 107-111. This section was written by P. J. Gilinson, Jr.

10. G. C. Evans, Functionals and Their Applications, Selected Topics, Including Integral Equations (Dover Publications, Inc., New York, reprint 1964), p. 1.

11. R. M. Fano, Transmission of Information (The M. I. T. Press, Cambridge, Mass., and John Wiley and Sons, Inc., New York, 1961), pp. 10-11.

12. R. H. Frazier and C. Kingsley, Jr., Notes for Electromechanical Components and Systems, 6.42 (Massachusetts Institute of Technology, Cambridge, Mass., 2d edition, 1964), pp. 267-273.

13. Ibid., p. 270. Equation 12-93, with appropriate identification of the variables, is our Eq. 342.

14. Ibid., Figures 12-33 to 12-35.

15. W. F. Freiberger, (ed.), The International Dictionary of Applied Mathematics, (D. Van Nostrand Company, Inc., Princeton, N. J., 1960), p. 386. The definitions of function and functional are given here.

16. D. A. George, "Continuous Nonlinear Systems", Technical Report 355, Research Laboratory of Electronics, M. I. T., Cambridge, Mass., July 24, 1959, pp. 12-27.

17. Ibid., pp. 23-27.

18. Ibid., p. 33. Here George introduces the multilinear correspondent.

19. Ibid., pp. 36-38. Here George presents his frequency association technique.

20. Ibid., pp. 60-69. Here George shows the application of his frequency association technique to systems with white noise input.

21. P. J. Gilinson, Jr., W. G. Denhard, and R. H. Frazier, "A Magnetic Support for Floated Inertial Instruments", Engineering Report R-277, Instrumentation Laboratory, M. I. T., Cambridge, Mass., April 1960; Sherman M. Fairchild Publication Fund Paper No. FF-27, Institute of the Aeronautical Sciences, New York, May 1960; Presented at the National Specialists Meeting on Guidance of Aero Space Vehicles, Boston, May 25-27, 1960.

22. U. Ingard and W. L. Kraushaar, Introduction to Mechanics, Matter, and Waves (Addison-Wesley Publishing Company, Inc., Reading, Mass., 1960), pp. 198-199.

23. S. Lees (ed.), Air, Space, and Instruments – The Draper Anniversary Volume (McGraw-Hill Book Company, Inc., New York, 1963), pp. 285-350. This chapter, entitled "Electromechanical Components" was written by P. J. Gilinson, Jr.

24. M. Liou, "Nonlinear System Analysis and Synthesis", Technical Report No. 6554-6, Systems Theory Laboratory, Stanford Electronics Laboratories, Stanford University, Stanford, Calif., October 1963, (SEL-63-095).

25. N. Minorsky, Nonlinear Oscillations (D. Van Nostrand Company, Inc., Princeton, N. J., 1962), p. 86.

26. R. B. Parente, "An Application of Volterra Functional Analysis to Shunt-Wound Commutator Machines, Part I", Quarterly Progress Report No. 76, Research Laboratory of Electronics, M. I. T., Cambridge, Mass., January 15, 1965, pp. 198-208.

27. Ibid., p. 207. The truncation error bound.

28. R. B. Parente, "An Application of Volterra Functional Analysis to Shunt-Wound Commutator Machines, Part II", Quarterly Progress Report No. 77, Research Laboratory of Electronics, M. I. T., Cambridge, Mass., April 15, 1965, pp. 274-276.

29. P. Penfield, Jr. and R. P. Rafuse, Varactor Applications (The M. I. T. Press, Cambridge, Mass., 1962), p. 65.

30. M. Schetzen, "Average of the Product of Gaussian Variables", Quarterly Progress Report No. 60, Research Laboratory of Electronics, M. I. T., Cambridge, Mass., January 15, 1961, pp. 137-141.

31. H. L. Van Trees, "Functional Techniques for the Analysis of the Nonlinear Behavior of Phase-Locked Loops", Proc. IEEE, Vol. 52, No. 8, pp. 894-911, August 1964.

32. V. Volterra, Theory of Functionals and of Integral and Integro-differential Equations (Dover Publications, Inc., New York, reprint 1959).

33. Ibid., p. 4. Volterra's definition of and notation for a functional.

34. Ibid., p. 10. The definition of a continuous functional.

35. Ibid., pp. 23-25. The derivatives of functionals.

36. Ibid., pp. 25-26. Volterra's Theorem and the definition of an analytical functional.

37. D. C. White and H. H. Woodson, Electromagnetic Energy Conversion (John Wiley and Sons, Inc., New York, 1959), p. 278, Table 4-1.

38. Ibid., p. 280, Eq. 4-57.

39. N. Wiener, "Response of a Nonlinear Device to Noise", Report 129, Radiation Laboratory, M. I. T., Cambridge, Mass., April 6, 1942.

40. N. Wiener, Nonlinear Problems in Random Theory (The Technology Press of the Massachusetts Institute of Technology, Cambridge, Mass., and John Wiley and Sons, Inc., New York, 1958), pp. 17-18. Here Wiener defines symmetrization and explains that it has no effect upon the value of the Volterra series. He writes his Volterra series in terms of Stieltjes' integral; we write ours in terms of Riemann's integral.

41. Ibid., p. 89. I interpret Wiener's comments in the last part of the penultimate paragraph and in the first part of the last paragraph as being about this result.

42. G. Zames, "Nonlinear Operators for System Analysis", Technical Report 370, Research Laboratory of Electronics, M. I. T., Cambridge, Mass., August 25, 1960, pp. 5-9.

43. Ibid., pp. 7-9. Zames' treatment of feedback.

44. Ibid., pp. 73-74. Zames' trees.

JOINT SERVICES ELECTRONICS PROGRAM
REPORTS DISTRIBUTION LIST

Department of Defense

Dr. Edward M. Reilley
Asst Director (Research)
Ofc of Defense Res & Eng
Department of Defense
Washington, D.C. 20301

Office of Deputy Director
(Research and Information Room 3D1037)
Department of Defense
The Pentagon
Washington, D.C. 20301

Director
Advanced Research Projects Agency
Department of Defense
Washington, D.C. 20301

Director for Materials Sciences
Advanced Research Projects Agency
Department of Defense
Washington, D.C. 20301

Headquarters
Defense Communications Agency (333)
The Pentagon
Washington, D.C. 20305

Defense Documentation Center
Attn: TISIA
Cameron Station, Bldg. 5
Alexandria, Virginia 22314

Director
National Security Agency
Attn: C3/TDL
Fort George G. Meade, Maryland 20755

Weapons Systems Evaluation Group
Attn: Col. Finis G. Johnson
Department of Defense
Washington, D.C. 20305

National Security Agency
Attn: R4-James Tippet
Office of Research
Fort George G. Meade, Maryland 20755

Central Intelligence Agency
Attn: OCR/DD Publications
Washington, D.C. 20505

Department of the Air Force

AUL3T-9663
Maxwell AFB, Alabama 36112

AFRSTE
Hqs. USAF
Room ID-429, The Pentagon
Washington, D.C. 20330

AFFTC (FTBPP-2)
Technical Library
Edwards AFB, Calif. 93523

Space Systems Division
Air Force Systems Command
Los Angeles Air Force Station
Los Angeles, California 90045
Attn: SSSD

SSD(SSTRT/Lt. Starbuck)
AFUPO
Los Angeles, California 90045

Det #6, OAR (LOOAR)
Air Force Unit Post Office
Los Angeles, California 90045

Systems Engineering Group (RTD)
Technical Information Reference Branch
Attn: SEPIR
Directorate of Engineering Standards
and Technical Information
Wright-Patterson AFB, Ohio 45433

ARL (ARIY)
Wright-Patterson AFB, Ohio 45433

AFAL (AVT)
Wright-Patterson AFB, Ohio 45433

AFAL (AVTE/R. D. Larson)
Wright-Patterson AFB, Ohio 45433

Commanding General
Attn: STEWS-WS-VT
White Sands Missile Range
New Mexico 88002

RADC (EMLAL-1)
Griffiss AFB, New York 13442
Attn: Documents Library

AFCRL (CRMXLR)
AFCRL Research Library, Stop 29
L. G. Hanscom Field
Bedford, Massachusetts 01731

Academy Library DFSLB)
U.S. Air Force Academy
Colorado 80840

FJSRL
USAF Academy, Colorado 80840

APGC (PGBPS-12)
Eglin AFB, Florida 32542

AFETR Technical Library
(ETV, MU-135)
Patrick AFB, Florida 32925

AFETR (ETLLG-1)
STINFO Officer (for Library)
Patrick AFB, Florida 32925

ESD (ESTI)
L. G. Hanscom Field
Bedford, Massachusetts 01731

AEDC (ARO, INC)
Attn: Library/Documents
Arnold AFS, Tennessee 37389

European Office of Aerospace Research
Shell Building
47 Rue Cantersteen
Brussels, Belgium

Lt. Col. E. P. Gaines, Jr.
Chief, Electronics Division
Directorate of Engineering Sciences
Air Force Office of Scientific Research
Washington, D.C. 20333

Department of the Army

U.S. Army Research Office
Attn: Physical Sciences Division
3045 Columbia Pike
Arlington, Virginia 22204

Research Plans Office
U.S. Army Research Office
3045 Columbia Pike
Arlington, Virginia 22204

Commanding General
U.S. Army Materiel Command
Attn: AMCRD-DE-E
Washington, D.C. 20315

Commanding General
U.S. Army Strategic Communications
Command
Washington, D.C. 20315

Commanding Officer
U.S. Army Materials Research Agency
Watertown Arsenal
Watertown, Massachusetts 02172

Commanding Officer
U.S. Army Ballistics Research Laboratory
Attn: V. W. Richards
Aberdeen Proving Ground
Aberdeen, Maryland 21005

Commandant
U.S. Army Air Defense School
Attn: Missile Sciences Division C&S Dept.
P.O. Box 9390
Fort Bliss, Texas 79916

Commanding General
Frankford Arsenal
Attn: SMFA-L6000-64-4 (Dr. Sidney Ross)
Philadelphia, Pennsylvania 19137

Commanding General
U.S. Army Missile Command
Attn: Technical Library
Redstone Arsenal, Alabama 35809

U.S. Army Munitions Command
Attn: Technical Information Branch
Picatinney Arsenal
Dover, New Jersey 07801

Commanding Officer
Harry Diamond Laboratories
Attn: Mr. Berthold Altman
Connecticut Avenue and Van Ness St. N.W.
Washington, D.C. 20438

Commanding Officer
U.S. Army Security Agency
Arlington Hall
Arlington, Virginia 22212

Commanding Officer
U.S. Army Limited War Laboratory
Attn: Technical Director
Aberdeen Proving Ground
Aberdeen, Maryland 21005

Commanding Officer
Human Engineering Laboratories
Aberdeen Proving Ground, Maryland 21005

Director
U.S. Army Engineer
Geodesy, Intelligence and Mapping
Research and Development Agency
Fort Belvoir, Virginia 22060

Commandant
U.S. Army Command and General
Staff College
Attn: Secretary
Fort Leavenworth, Kansas 66270

Dr. H. Robl, Deputy Chief Scientist
U.S. Army Research Office (Durham)
Box CM, Duke Station
Durham, North Carolina 27706

Commanding Officer
U.S. Army Research Office (Durham)
Attn: CRD-AA-IP (Richard O. Ulsh)
Box CM, Duke Station
Durham, North Carolina 27706

Superintendent
U.S. Army Military Academy
West Point, New York 10996

The Walter Reed Institute of Research
Walter Reed Medical Center
Washington, D.C. 20012

Commanding Officer
U.S. Army Engineer R&D Laboratory
Attn: STINFO Branch
Fort Belvoir, Virginia 22060

Commanding Officer
U.S. Army Electronics R&D Activity
White Sands Missile Range,
New Mexico 88002

Dr. S. Benedict Levin, Director
Institute for Exploratory Research
U.S. Army Electronics Command
Attn: Mr. Robert O. Parker, Executive
Secretary, JSTAC (AMSEL-XL-D)
Fort Monmouth, New Jersey 07703

Commanding General
U.S. Army Electronics Command
Fort Monmouth, New Jersey 07703
Attn: AMSEL-SC

AMSEL-RD-D	HL-O
RD-G	HL-R
RD-MAF-1	NL-D
RD-MAT	NL-A
RD-GF	NL-P
XL-D	NL-R
XL-E	NL-S
XL-C	KL-D
XL-S	KL-E
HL-D	KL-S
HL-L	KL-T
HL-J	VL-D
HL-P	WL-D

Department of the Navy

Chief of Naval Research
Department of the Navy
Washington, D.C. 20360
Attn: Code 427

Chief, Bureau of Ships
Department of the Navy
Washington, D.C. 20360

Chief, Bureau of Weapons
Department of the Navy
Washington, D.C. 20360

Commanding Officer
Office of Naval Research Branch Office
Box 39, Navy No 100 F.P.O.
New York, New York 09510

Commanding Officer
Office of Naval Research Branch Office
1030 East Green Street
Pasadena, California

Commanding Officer
Office of Naval Research Branch Office
219 South Dearborn Street
Chicago, Illinois 60604

Commanding Officer
Office of Naval Research Branch Office
207 West 42nd Street
New York, New York 10011

Commanding Officer
Office of Naval Research Branch Office
495 Summer Street
Boston, Massachusetts 02210

Director, Naval Research Laboratory
Technical Information Officer
Washington, D.C.
Attn: Code 2000

Commander
Naval Air Development and Material Center
Johnsville, Pennsylvania 18974

Librarian, U.S. Electronics Laboratory
San Diego, California 95152

Commanding Officer and Director
U.S. Naval Underwater Sound Laboratory
Fort Trumbull
New London, Connecticut 06840

Librarian, U.S. Naval Post Graduate School
Monterey, California

Commander
U.S. Naval Air Missile Test Center
Point Magu, California

Director
U.S. Naval Observatory
Washington, D.C.

Chief of Naval Operations
OP-07
Washington, D.C.

Director, U.S. Naval Security Group
Attn: G43
3801 Nebraska Avenue
Washington, D.C.

Commanding Officer
Naval Ordnance Laboratory
White Oak, Maryland

Commanding Officer
Naval Ordnance Laboratory
Corona, California

Commanding Officer
Naval Ordnance Test Station
China Lake, California

Commanding Officer
Naval Avionics Facility
Indianapolis, Indiana

Commanding Officer
Naval Training Device Center
Orlando, Florida

U.S. Naval Weapons Laboratory
Dahlgren, Virginia

Weapons Systems Test Division
Naval Air Test Center
Patuxtent River, Maryland
Attn: Library

Other Government Agencies

Mr. Charles F. Yost
Special Assistant to the Director
of Research
NASA
Washington, D.C. 20546

NASA Lewis Research Center
Attn: Library
21000 Brookpark Road
Cleveland, Ohio 44135

Dr. H. Harrison, Code RRE
Chief, Electrophysics Branch
NASA, Washington, D.C. 20546

Goddard Space Flight Center
NASA
Attn: Library, Documents Section Code 252
Green Belt, Maryland 20771

National Science Foundation
Attn: Dr. John R. Lehmann
Division of Engineering
1800 G Street N.W.
Washington, D.C. 20550

U.S. Atomic Energy Commission
Division of Technical Information Extension
P.O. Box 62
Oak Ridge, Tennessee 37831

Los Alamos Scientific Library
Attn: Reports Library
P.O. Box 1663
Los Alamos, New Mexico 87544

NASA Scientific & Technical Information
Facility
Attn: Acquisitions Branch (S/AK/DL)
P.O. Box 33
College Park, Maryland 20740

Non-Government Agencies

Director
Research Laboratory for Electronics
Massachusetts Institute of Technology
Cambridge, Massachusetts 02139

Polytechnic Institute of Brooklyn
55 Johnson Street
Brooklyn, New York 11201
Attn: Mr. Jerome Fox
Research Coordinator

Director
Columbia Radiation Laboratory
Columbia University
538 West 120th Street
New York, New York 10027

Director
Stanford Electronics Laboratories
Stanford University
Stanford, California

Director
Coordinated Science Laboratory
University of Illinois
Urbana, Illinois 61803

Director
Electronics Research Laboratory
University of California
Berkeley 4, California

Director
Electronics Sciences Laboratory
University of Southern California
Los Angeles, California 90007

Professor A. A. Dougal, Director
Laboratories for Electronics and
Related Sciences Research
University of Texas
Austin, Texas 78712

Division of Engineering and Applied
Physics
210 Pierce Hall
Harvard University
Cambridge, Massachusetts 02138

Aerospace Corporation
P.O. Box 95085
Los Angeles, California 90045
Attn: Library Acquisitions Group

Professor Nicholas George
California Institute of Technology
Pasadena, California

Aeronautics Library
Graduate Aeronautical Laboratories
California Institute of Technology
1201 E. California Blvd.
Pasadena, California 91109

Director, USAF Project RAND
Via: Air Force Liaison Office
The RAND Corporation
1700 Main Street
Santa Monica, California 90406
Attn: Library

The Johns Hopkins University
Applied Physics Laboratory
8621 Georgia Avenue
Silver Spring, Maryland
Attn: Boris W. Kuvshinoff
Document Librarian

School of Engineering Sciences
Arizona State University
Tempe, Arizona

Dr. Leo Young
Stanford Research Institute
Menlo Park, California

Hunt Library
Carnegie Institute of Technology
Schenley Park
Pittsburgh, Pennsylvania 15213

Mr. Henry L. Bachmann
Assistant Chief Engineer
Wheeler Laboratories
122 Cuttermill Road
Great Neck, New York

University of Liege
Electronic Institute
15, Avenue Des Tilleuls
Val-Benoit, Liege
Belgium

University of California at Los Angeles
Department of Engineering
Los Angeles, California

California Institute of Technology
Pasadena, California
Attn: Documents Library

University of California
Santa Barbara, California
Attn: Library

Carnegie Institute of Technology
Electrical Engineering Department
Pittsburgh, Pennsylvania

University of Michigan
Electrical Engineering Department
Ann Arbor, Michigan

New York University
College of Engineering
New York, New York

Syracuse University
Dept. of Electrical Engineering
Syracuse, New York

Yale University
Engineering Department
New Haven, Connecticut

Bendix Pacific Division
11600 Sherman Way
North Hollywood, California

General Electric Company
Research Laboratories
Schenectady, New York

Airborne Instruments Laboratory
Deerpark, New York

Lockheed Aircraft Corporation
P.O. Box 504
Sunnyvale, California

Raytheon Company
Bedford, Massachusetts
Attn: Librarian

UNCLASSIFIED
Security Classification

DOCUMENT CONTROL DATA - R&D

(Security classification of title, body of abstract and indexing annotation must be entered when the overall report is classified)

1. ORIGINATING ACTIVITY *(Corporate author)* Research Laboratory of Electronics Massachusetts Institute of Technology Cambridge, Massachusetts	2a. REPORT SECURITY CLASSIFICATION Unclassified 2b. GROUP None

3. REPORT TITLE
Functional Analysis of Systems Characterized by Nonlinear Differential Equations

4. DESCRIPTIVE NOTES *(Type of report and inclusive dates)*
Technical Report

5. AUTHOR(S) *(Last name, first name, initial)*
Parente, Robert Bruce

6. REPORT DATE	7a. TOTAL NO. OF PAGES	7b. NO. OF REFS
July 15, 1966	124	44

8a. CONTRACT OR GRANT NO. DA 36-039-AMC-03200(E) b. PROJECT NO. 200-14501-B31F NSF Grant GP-2495 c. NIH Grant MH-04737-05 NASA Grant NsG-496 d.	9a. ORIGINATOR'S REPORT NUMBER(S) Technical Report 444 9b. OTHER REPORT NO(S) *(Any other numbers that may be assigned this report)* None

10. AVAILABILITY/LIMITATION NOTICES
Distribution of this report is unlimited

11. SUPPLEMENTARY NOTES	12. SPONSORING MILITARY ACTIVITY
	Joint Services Electronics Program thru USAECOM, Fort Monmouth, N. J.

13. ABSTRACT An analysis, by functional calculus, of a class of nonlinear sysems is presented. The class of nonlinear systems that are analyzed includes all those analytic systems that are characterized by nonlinear differential equations. Applications of this analysis are shown for several actual nonlinear physical systems that are analytic.

The precise definition of an analytic system is given. Loosely speaking, an analytic system is any system with these three properties: (i) It is deterministic. (For a given input signal, the system can have one and only one corresponding output signal.) (ii) It is time-invariant. (iii) It is "smooth." (The system cannot introduce any abrupt or switchlike changes into its output. All such changes in the output must be caused by the input rather than the system.)

Given a nonlinear differential equation, the conditions are shown under which it characterizes an analytic system. Given an analytic system characterized by a nonlinear differential equation, it is shown how that system can be analyzed by an application of functional calculus. Specifically, an inspection technique is developed whereby a Volterra functional power series is obtained for that system's input-output transfer relationship. Applications are given for (i) the demonstration of a pendulum's nonlinear resonance phenomenon; (ii) the computation of a shunt-wound motor's response to white noise excitation; (iii) the computation of a varactor frequency doubler's transient response; and (iv) the determination of the stability of a magnetic suspension device that is now being used in space vehicles. Experimental confirmation of the last stability determination is treated in an appendix.

DD FORM 1 JAN 64 1473

UNCLASSIFIED
Security Classification

14. KEY WORDS	LINK A		LINK B		LINK C	
	ROLE	WT	ROLE	WT	ROLE	WT
Nonlinear Systems Nonlinear Differential Equations Functionals Volterra Functionals Functional Calculus System Theory, Nonlinear Stochastic Systems, Nonlinear Analytic Systems Volterra Series Pendulum, Nonlinear Shunt-wound Motor, Stochastic Excitation of a Varactor Frequency Doubler, Transient Response of a Magnetic Suspension Device, Stability of a						

INSTRUCTIONS

1. ORIGINATING ACTIVITY: Enter the name and address of the contractor, subcontractor, grantee, Department of Defense activity or other organization *(corporate author)* issuing the report.

2*a*. REPORT SECURITY CLASSIFICATION: Enter the overall security classification of the report. Indicate whether "Restricted Data" is included. Marking is to be in accordance with appropriate security regulations.

2*b*. GROUP: Automatic downgrading is specified in DoD Directive 5200.10 and Armed Forces Industrial Manual. Enter the group number. Also, when applicable, show that optional markings have been used for Group 3 and Group 4 as authorized.

3. REPORT TITLE: Enter the complete report title in all capital letters. Titles in all cases should be unclassified. If a meaningful title cannot be selected without classification, show title classification in all capitals in parenthesis immediately following the title.

4. DESCRIPTIVE NOTES: If appropriate, enter the type of report, e.g., interim, progress, summary, annual, or final. Give the inclusive dates when a specific reporting period is covered.

5. AUTHOR(S): Enter the name(s) of author(s) as shown on or in the report. Enter last name, first name, middle initial. If military, show rank and branch of service. The name of the principal author is an absolute minimum requirement.

6. REPORT DATE: Enter the date of the report as day, month, year; or month, year. If more than one date appears on the report, use date of publication.

7*a*. TOTAL NUMBER OF PAGES: The total page count should follow normal pagination procedures, i.e., enter the number of pages containing information.

7*b*. NUMBER OF REFERENCES: Enter the total number of references cited in the report.

8*a*. CONTRACT OR GRANT NUMBER: If appropriate, enter the applicable number of the contract or grant under which the report was written.

8*b*, 8*c*, & 8*d*. PROJECT NUMBER: Enter the appropriate military department identification, such as project number, subproject number, system numbers, task number, etc.

9*a*. ORIGINATOR'S REPORT NUMBER(S): Enter the official report number by which the document will be identified and controlled by the originating activity. This number must be unique to this report.

9*b*. OTHER REPORT NUMBER(S): If the report has been assigned any other report numbers *(either by the originator or by the sponsor)*, also enter this number(s).

10. AVAILABILITY/LIMITATION NOTICES: Enter any limitations on further dissemination of the report, other than those imposed by security classification, using standard statements such as:

(1) "Qualified requesters may obtain copies of this report from DDC."

(2) "Foreign announcement and dissemination of this report by DDC is not authorized."

(3) "U. S. Government agencies may obtain copies of this report directly from DDC. Other qualified DDC users shall request through _____."

(4) "U. S. military agencies may obtain copies of this report directly from DDC. Other qualified users shall request through _____."

(5) "All distribution of this report is controlled. Qualified DDC users shall request through _____."

If the report has been furnished to the Office of Technical Services, Department of Commerce, for sale to the public, indicate this fact and enter the price, if known.

11. SUPPLEMENTARY NOTES: Use for additional explanatory notes.

12. SPONSORING MILITARY ACTIVITY: Enter the name of the departmental project office or laboratory sponsoring *(paying for)* the research and development. Include address.

13. ABSTRACT: Enter an abstract giving a brief and factual summary of the document indicative of the report, even though it may also appear elsewhere in the body of the technical report. If additional space is required, a continuation sheet shall be attached.

It is highly desirable that the abstract of classified reports be unclassified. Each paragraph of the abstract shall end with an indication of the military security classification of the information in the paragraph, represented as *(TS)*, *(S)*, *(C)*, or *(U)*.

There is no limitation on the length of the abstract. However, the suggested length is from 150 to 225 words.

14. KEY WORDS: Key words are technically meaningful terms or short phrases that characterize a report and may be used as index entries for cataloging the report. Key words must be selected so that no security classification is required. Identifiers, such as equipment model designation, trade name, military project code name, geographic location, may be used as key words but will be followed by an indication of technical context. The assignment of links, rules, and weights is optional.